

**RELATIVE DEFORMATION MODEL DEVELOPMENT FOR
SEMI-DYNAMIC DATUM IMPLEMENTATION IN TRINIDAD**

A Thesis

Submitted in Partial Fulfilment of the Requirement for the Degree of
Master of Science in Geoinformatics

Of

The University of the West Indies

Jason D. Kanhai
2019

Department of Geomatics Engineering and Land Management
Faculty of Engineering
St. Augustine Campus

ABSTRACT

Relative Deformation Model Development for
Semi-Dynamic Implementation in Trinidad.

Jason D. Kanhai

Geodetic datums provide the framework within which various forms of spatial data can be correlated and managed. With the advancement of GPS-geodesy, there has been a revision of the international quality of standards that datums must meet. Traditional static datums (Naparima 1955) employed in Trinidad no longer meet these standards as their integrity and quality degrade overtime as a result of tectonic deformation. This deformation is caused by the interaction between the Caribbean and South America plates, the boundary of which lies across the island. Consequently, semi-dynamic datums are proposed as a potential new modern geodetic datum for the island nation, given their ability to continue operating in a static reference frame and incorporate deformation effects. This project investigates the nature of horizontal deformation across Trinidad through GPS observation of survey monuments across the island. These monuments were initially observed in 1990, then re-observed between 2014 and 2017 using modern GPS techniques. Updated positions estimated in ITRF2014 were compared with transformed 1990 positions to estimate relative velocities of these survey monuments. These relative velocities will contribute towards the development of a relative deformation model for Trinidad, a key component of semi-dynamic datums. Results have demonstrated that deformation is non-uniform with varying velocities ranging between 1.7 ± 1.5 mm/year and 17.4 ± 1.9 mm/year and directions ranging between 24° and 247° . There is also a general increase in velocity northward across the island signifying the increased influence of Caribbean plate motion relative to South America. These findings have proven that the Naparima 1955 datum is not resilient to non-uniform deformation and can no longer be relied upon for mapping and surveying. Relative velocities estimated for survey monuments have provided the basis for development of a relative deformation model that captures active tectonism and can be used toward semi-dynamic datum implementation.

Keywords: datum, deformation, tectonics, velocities, GPS, geodesy, ITRF, Naparima, static, semi-dynamic.

ACKNOWLEDGEMENTS

The successful execution of this project was made possible through the collaborative efforts of several individuals. Special appreciation must be given to some key individuals including my parents who have financially assisted me through this project, my classmates Ornella and Ashlyn who have encouraged me to stay strong through tough times, and my friends Vinud, Alphonsus, Jessica, Anam, Christina and Sam who have supported me through the entire research process.

Thanks must also be given to all my co-workers from the various jobs I have balanced while conducting my studies. I must thank my former supervisor JP Talma and staff at the University of Trinidad and Tobago for providing appropriate geological literature that aided in my research. I must especially thank the staff at the UWI Seismic Research Centre for providing historical earthquake data which provided much needed assistance in nominating a reference station. I am also grateful to UWI-SRC for allowing me to apply the skills learned in this research to other deformation study. I must also acknowledge the assistance provided by Kalain Hosein for plotting this historical earthquake data and providing GIS assistance throughout this project.

Appreciation must especially be given to the technical staff of the UWI Department of Geomatics Engineering and Land Management for assistance in located Haliburton sites and conducting field works. Last I must give all my thanks to my supervisor Dr. Keith Miller. He trusted and believe that I had the capability to undertake this project which combines the multiple disciplines of Geodesy, Geology and GIS. Without his guidance, patience and understanding, this project would not have been completed. I am forever indebted to his service.

Table of Contents

1	INTRODUCTION	1
1.1	PROBLEM IDENTIFICATION	1
1.2	BACKGROUND	2
1.3	PROBLEM RESOLUTION.....	4
1.4	PROJECT AIM & OBJECTIVES	5
2	SURVEY AND ANALYSIS OF EXTANT RESEARCH.....	7
2.1	GEODETIC DATUMS	8
2.2	STATIC DATUMS	9
2.2.1	<i>Static Datums of Trinidad</i>	10
2.3	FULLY-DYNAMIC DATUMS.....	12
2.3.1	<i>International Terrestrial Reference System (ITRS).....</i>	13
2.3.2	<i>International Terrestrial Reference Frame (ITRF)</i>	13
2.3.3	<i>ITRF 2014</i>	14
2.3.4	<i>WGS 84</i>	16
2.4	SEMI-DYNAMIC DATUMS	18
2.4.1	<i>New Zealand: Static NZGD1949 to Semi Dynamic NZGD2000</i>	19
2.4.2	<i>Indonesia: Static DGN1995 to Semi-Dynamic IGRS2013</i>	23
2.4.3	<i>Malaysia: Moving away from the Static GDM2000.....</i>	27
2.4.4	<i>Philippines Geodetic Datum 2016 (PGD 2016).....</i>	31
2.5	TECTONIC EVOLUTION OF TRINIDAD	34
2.6	NEOTECTONICS OF TRINIDAD	37
2.6.1	<i>Arima Fault Zone</i>	38
2.6.2	<i>Central Range Fault Zone.....</i>	39
2.6.3	<i>Los Bajos Fault Zone (LBFZ)</i>	42
2.7	HALLIBURTON GEOPHYSICAL SURVEY	43
2.8	ASSESSMENT	46
3	INVESTIGATIVE PROCEDURES	47
3.1	MONUMENT IDENTIFICATION & SELECTION	47
3.2	DATA ACQUISITION VIA STATIC GPS SURVEYING.....	51
3.3	ACQUIRING & FORMATTING CORS DATA.....	52
3.4	ESTABLISHING PRIMARY CONTROL IN ITRF 2014.....	55
3.5	ESTABLISHING SECONDARY CONTROL IN ITRF 2014.....	55
3.6	TRANSFORMATION TO ENU	56

3.7	NOMINAL REFERENCE STATION SELECTION	58
3.8	VECTOR COMPUTATION.....	59
4	PROJECT FINDINGS	61
4.1	DISPLACEMENTS & RELATIVE DEFORMATION MODEL: 1990 -2014.....	62
4.2	DISPLACEMENTS & RELATIVE DEFORMATION MODEL: 1990 – 2015	63
4.3	DISPLACEMENTS & RELATIVE DEFORMATION MODEL: 1990 -2016.....	64
4.4	DISPLACEMENTS & RELATIVE DEFORMATION MODEL: 1990 -2017.....	65
4.5	AVERAGE RELATIVE DEFORMATION MODEL	66
4.6	OBSERVED TRENDS	68
5	DISCUSSION.....	72
5.1	DISTORTION OF TRADITIONAL DATUMS	72
5.2	DEFORMATION SPEED.....	73
5.3	DEFORMATION DIRECTION	74
5.4	REGIONAL TECTONICS.....	75
5.5	NEOTECTONICS.....	75
6	CONCLUSION.....	77
6.1	KEY ACHIEVEMENTS	77
6.2	FUTURE INVESTIGATIVE NEEDS.....	79
7	REFERENCES	81
8	APPENDICES	89
8.1	APPENDIX A – HALIBURTON SITE COORDINATES (FINAL GEODETIC REPORT).....	89
8.2	APPENDIX B – DEVICE & ANTENNA METADATA.....	90
8.3	APPENDIX C – CORS ITRF2014 COORDINATES	94
8.4	APPENDIX D - HISTORICAL EARTHQUAKE MAPS	98
8.5	APPENDIX E – ADJUSTED ITRF2014 COORDINATES	105

List of Figures

Figure 1-1: Map showing transition from subduction in Eastern Caribbean to transform boundary across Trinidad (Weber, et al. 2011).....	2
Figure 1-2: Horizontal deformation model used to convert the static Taiwanese Geodetic Datum (TWD97) to a semi-dynamic datum (Ching and Chen 2015).....	5
Figure 2-1: Model of geoid is exaggerated radial variation and coloured according to variation in gravitational acceleration (Li and Gotze 2001).....	8
Figure 2-2: Local datums (left) based on ellipsoids that model a specific region of the geoid and Geocentric global datums (right) where ellipsoids attempt to model the entire geoid (ANZLIC 2016).	9
Figure 2-3: ITRF2014 network showing locations of VLBI, SLR, GNSS and DORIS sites co-located with GNSS (Altamimi, et al. 2016).	14
Figure 2-4: ITRF2014 horizontal site velocities and major plate boundaries in yellow (Altamimi, et al. 2016).....	15
Figure 2-5: ITRF2014 vertical site velocities (Altamimi, et al. 2016).	16
Figure 2-6: GPS Monitoring Stations used to realise WGS84 (Malys, Wong and True 2016).	17
Figure 2-7: Major tectonic features surrounding New Zealand (Uruski 2014).....	19
Figure 2-8: Distortion of NZGD1949 monuments (Blick and Donnelly 2016).	20
Figure 2-9:Initial relative deformation model used to complement NZGD2000 (Blick, Donnelly and Jordan 2009).....	21
Figure 2-10: Updated deformation model using PositionNZ stations and Nuvel model (Blick and Donnelly 2016).	22
Figure 2-11:Tectonic plates and blocks of Indonesia (Abidin, et al. 2015).	23
Figure 2-12: Initial velocity model generated by MORVEL (DeMets, Gordon and Argus 2010).	24
Figure 2-13:Passive geodetic monuments managed by BIG (Abidin, et al. 2015).25	
Figure 2-14: Continuous Operating Reference Stations (CORS) operated by BIG (Abidin, et al. 2015).....	25

Figure 2-15: Continuous Operating Reference Stations (CORS) operated by BPN (Abidin, et al. 2015).....	26
Figure 2-16: ITRF 2008 velocities for most BIG GPS CORS sites (Abidin, et al. 2015).....	26
Figure 2-17: Map of the Malaysia Real Time Kinetic GNSS Network (myRTKnet) (Jamill and Mohamed 2010).....	28
Figure 2-18: Secular Deformation Models showing individual North and East components (Shariff, et al. 2017)	29
Figure 2-19: Non-secular deformation models for major earthquakes (Shariff, et al. 2017).	30
Figure 2-20: Crustal Block zones and estimated velocities across the Philippines (Cayapan 2016).....	32
Figure 2-21: Existing and Proposed Active Geodetic Stations (Cayapan 2016)....	33
Figure 2-22: (a) Major geomorphic features of Trinidad, (b) Major structural features and geology of Trinidad (Arkle, Owen and Weber 2017).	34
Figure 2-23: North-south cross section of Trinidad, faults and fold & thrust belt formed during a tectonic compression (Soto, Mann and Escalona 2011).	35
Figure 2-24: Orogenic belt cross-section analogous to Miocene collision that formed Northern Range (internal core) and fold and thrust belts (external zone) (Tyson, Babb and Dyer 1991).....	36
Figure 2-25:Present tectonic regime showing transform motion across NE Venezuela and Trinidad and subduction to the east of the Lesser Antilles (Arkle, Owen and Weber 2017)	37
Figure 2-26: Map showing major geomorphic features across Trinidad transected by major fault zones (Weber 2005).	38
Figure 2-27: Shallow seismic events between 1910 and 2000 across Trinidad and NE Venezuela (Weber et al. 2011).	39
Figure 2-28: Location of Central Range Fault (bold red) and horizontal velocities estimated from GPS campaigns.....	40

Figure 2-29: Tectonic setting of Trinidad with various estimate horizontal velocities and delineated offshore seismic survey (box) conducted to explore offshore extension of CRFZ (Soto, et al. 2007).....	41
Figure 2-30: Surface trace of Los Bajos fault across topography as depicted in 2014 LIDAR campaign.....	42
Figure 2-31: Primary network of control stations used to provide survey control for seismic surveys	43
Figure 2-32: (left) Witness post and monument dimensions and (right) Aluminum cap set in concrete for TDST 0055 (Los Iros)	44
Figure 2-33: Witness diagram for TDST 0014.....	45
Figure 3-1:Geographic distribution of Haliburton geodetic monuments (red) across Trinidad relative to major fault zones (yellow).	47
Figure 3-2: Left - Monument HUBM002 likely destroyed my waterfront development in Port of Spain, Right - Monument TRG 128 located deep in forest; inaccessible and proximal to high tension power lines.	48
Figure 3-3: Geographic distribution of re-observed sites across Trinidad.	50
Figure 3-4: Leica GS14 antenna mounted atop tripod over TDST 0014 (Penal)...	52
Figure 3-5 Location of TT and UNAVCO CORS across Trinidad	53
Figure 3-6: Processed baselined in Trimble Total Control.....	56
Figure 3-7: Process flowchart for estimating dE, dN, dU.	57
Figure 3-8: Matrix Multiplication to estimate ENU (Drake 2002) where: λ - original latitude in radians, φ - original longitude in radians x _p , y _p , z _p - Present ECEF Coordinates, x _o , y _o , z _o - Original ECEF Coordinates E, N, U – displacements in Cartesian plane	58
Figure 4-1: Relative Deformation Model for 1990-2014 depicting annual relative velocities and error circles	62
Figure 4-2: Relative Deformation Model for 1990-2015 depicting annual relative velocities and error circles.....	63
Figure 4-3: Relative Deformation Model for 1990-2016 depicting annual relative velocities and error circles.....	64

Figure 4-4: Relative Deformation Model for 1990-2017 depicting annual relative velocities and error circles	65
Figure 4-5: Average Relative Deformation model depicting average annual relative velocities and error circles.....	67
Figure 4-6: Map showing location of monuments within respective fault blocks.	68
Figure 4-7: Plot of monument direction vs UTM Easting for 15 sites across Trinidad.	69
Figure 4-8: Plot of monument relative velocity vs UTM Easting for 15 sites across Trinidad.....	69
Figure 4-9: Plot of average relative displacements in Easting and North vs UTM Easting.	70
Figure 4-10: Plot of monument direction vs UTM Northing for 15 sites across Trinidad.....	70
Figure 4-11:Plot of monument relative velocity vs UTM Northing for 15 sites across Trinidad.....	71
Figure 4-12: Plot of average relative displacements in Easting and North vs Northing.....	71
Figure 8-1: Map showing distribution of earthquakes by magnitude and depth in and surrounding Trinidad relative to the Penal reference site (blue star) for the period October 1990 - September 1996.	98
Figure 8-2: Map showing distribution of earthquakes by magnitude and depth in and surrounding Trinidad relative to the Penal reference site (blue star) for the period October 1996 - September 2002.	99
Figure 8-3: Map showing distribution of earthquakes by magnitude and depth in and surrounding Trinidad relative to the Penal reference site (blue star) for the period October 2002 - September 2008.	100
Figure 8-4: Map showing distribution of earthquakes by magnitude and depth in and surrounding Trinidad relative to the Penal reference site (blue star) for the period October 2008 - September 2014.	101

Figure 8-5: Map showing distribution of earthquakes by magnitude and depth in and surrounding Trinidad relative to the Penal reference site (blue star) for the period October 2014 - September 2015.....	102
Figure 8-6: Map showing distribution of earthquakes by magnitude and depth in and surrounding Trinidad relative to the Penal reference site (blue star) for the period October 2015 - September 2016.....	103
Figure 8-7: Map showing distribution of earthquakes by magnitude and depth in and surrounding Trinidad relative to the Penal reference site (blue star) for the period October 2016 - September 2017.....	104

List of Tables

Table 3-1: List of available monuments by year from which GPS observations were conducted.....	49
Table 3-2: Observation days by year.....	51
Table 3-3: List of teqc commands used to pre-process observation and navigation files.....	54
Table 3-4: Estimating Direction from Azimuth.....	60
Table 4-1: Geodetic monument labels for Relative Deformation Models.	61
Table 4-2: Displacements and Annual Relative Velocities for 1990-2014.	62
Table 4-3: Displacements and Annual Relative Velocities for 1990 - 2015.	63
Table 4-4: Displacements and Annual Relative Velocities for 1990 - 2016.	64
Table 4-5: Displacements and Annual Relative Velocities for 1990 - 2017.	65
Table 4-6: Average relative displacements in E and N and average relative velocities (speed and direction).	66
Table 8-1: WGS84 UTM Coordinates for re-observed sites.	89
Table 8-2: Antennae height and receiver metadata for stations re-observed in 2014.	90
Table 8-3: Antennae height and receiver metadata for stations re-observed in 2015.	91
Table 8-4: Antennae height and receiver metadata for stations re-observed in 2016.	92
Table 8-5: Antennae height and receiver metadata for stations re-observed in 2017.	93
Table 8-6: ITRF2014 Coordinates for TTCORS for period October 14 th – 23 rd , 2014 (Generated by AUSPOS).....	94
Table 8-7: ITRF2014 Coordinates for TTCORS for period October 2 nd – 11 th , 2015 (Generated by AUSPOS).....	95
Table 8-8: ITRF2014 Coordinates for UNAVCO CORS for period October 9 th – 18 th , 2016 (Generated by AUSPOS).....	96

Table 8-9: ITRF2014 Coordinates for TTCORS for period October 8 th – 17 th , 2017 (Generated by AUSPOS).....	97
Table 8-11: ITRF2014 Adjusted Coordinates for re-observed sites (generated by TTC)	105
Table 8-12: ITRF2014 Adjusted Coordinates for re-observed site, continued (generated by TTC).....	106

List of Acronyms

ADM	Absolute Deformation Model
AFZ	Arima Fault Zone
ANZLIC	Australia-New Zealand Land Information Council
BDOS	British Directorate of Overseas Surveys
BIH	Bureau International de l'Heure
CORS	Continuously Operating Reference Station
CRFZ	Central Range Fault Zone
DORIS	Doppler Orbitography and Radio-positioning Integrated by Satellite
ECEF	Earth-Centred Earth-Fixed
EDM	Electronic Distance Measuring
EOP	Earth Orientation Parameters
GDM2000	Geocentric Datum of Malaysia 2000
GGRF	Global Geodetic Reference Frame
GITSA	GPS Interactive Time Series Analysis
GLONASS	Global Orbiting Navigation Satellite System
GNSS	Global Navigation Satellite System
GPS	Global Positioning System
GRS	Global Reference System
HGS	Haliburton Geophysical Services
IAU	International Astronomical Union
IERS	International Earth Rotation and Reference System
IGRS2013	Indonesia Geospatial Reference System of 2013
IGS	International GNSS Service
ITRF	International Terrestrial Reference Frame
ITRS	International Terrestrial Reference System
IUGG	International Union of Geodesy and Geophysics
LBFZ	Los Bajos Fault Zone
LINZ	Land Information New Zealand

NAMRIA	National Mapping and Resource Information Authority
NGA	National Geospatial Intelligence Agency
NZGD1949	New Zealand Geodetic Datum of 1949
NZGD2000	New Zealand Geodetic Datum of 2000
PGD2016	Philippine Geodetic Datum of 2016
PRS92	Philippines Reference System of 1992
RDM	Relative Deformation Model
SLR	Satellite Laser Ranging
TGC	Geocentric Coordinate Time
TTC	Trimble Total Control
TWD97	Taiwanese Geodetic Datum of 1996
UNAVCO	University NAVSTAR Consortium
USDoD	United States Department of Defense
UTM	Universal Transverse Mercator
VLBI	Very Long Baseline Interferometry
WGS84	World Geodetic System 1984

1 INTRODUCTION

1.1 Problem Identification

Geodetic datums are used to define the size and shape of the earth, either globally or for a specific area of the earth. They provide the basis for the development of coordinate systems; assigning coordinates to locations across an area of interest and providing a means of correlating various forms of spatial data for the purpose of decision making. Once geodetic datums are defined in static frame of reference, they will experience some degree of distortion as a direct result of tectonic deformation over the area it is applied to. Once distorted, datum quality diminishes and datasets can no longer be correlated with the accuracy needed for confident decision making.

Active tectonism is ubiquitous across the region, especially the eastern Caribbean which was formed as a direct result of the interaction between the Caribbean and South American tectonic plates. Most islands, from Grenada in the south to Saba in the north are the result of volcanism and convergent, compressive deformation, where the South American plate is subducted beneath the Caribbean plate. Trinidad, the southernmost island of this archipelago, straddles the transform boundary between these two plates and experiences predominantly shear deformation as these plates “slide” past one another.

Evidence of this tectonism includes a historical record of shallow crustal earthquakes (0 – 40 km) both onshore and offshore, active mud diapirism in southern Trinidad and various visible landforms (faults, thrusting, etc). While the existence of the plate boundary is known, it is still debated whether it is distinguished by one discreet fault zone or if it better represented by the zone of varying deformation that occurs across the island and is accommodated by multiple fault zones. Unfortunately, all datums commonly used in Trinidad are static in nature and distorted by this deformation that exists across island. This can be ameliorated by adapting international standards and developing modern datums that incorporate deformation models.

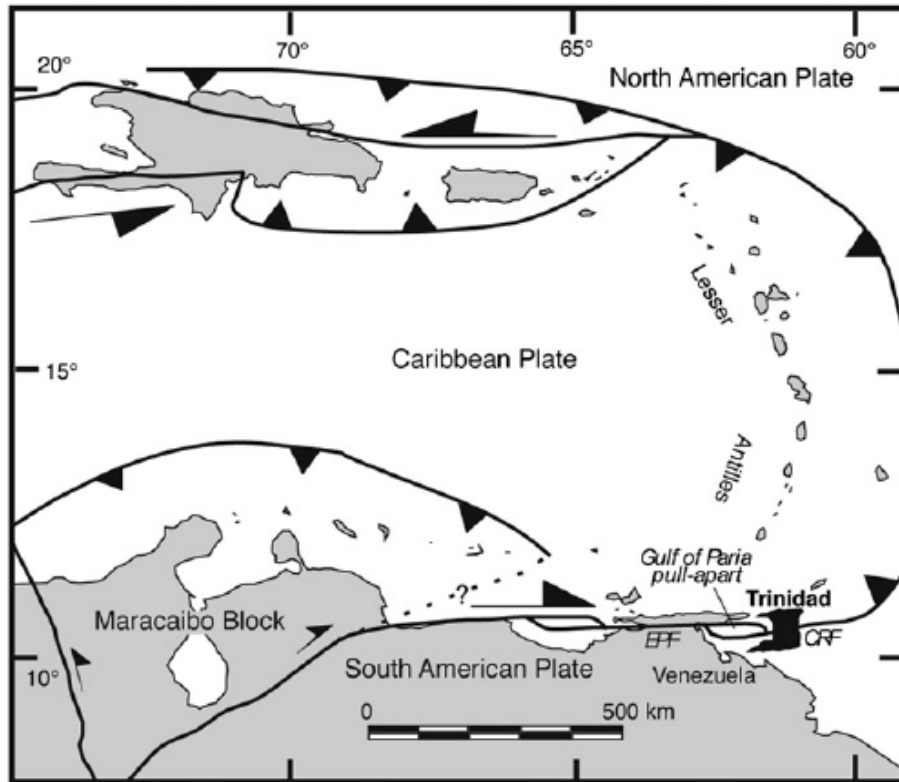


Figure 1-1: Map showing transition from subduction in Eastern Caribbean to transform boundary across Trinidad (Weber, et al. 2011).

1.2 Background

The irregular size and shape of the Earth poses problems when attempting to assign coordinates to its surface in defining locations. Its geometry is akin to that of an ellipsoid, which geodetic datums attempt to model using well defined parameters. Datums are used to define reference points on these ellipsoids, from which location specific coordinate systems are based. Historically, different ellipsoids have been generated to model specific areas of the earth's surface and only in recent times were global reference systems generated with the advent of GPS-geodesy (Chapman 2005).

Traditional, static datums provided sufficient quality and accuracy needed for the period in which they were established. This accuracy no longer meets today's demands with advent of modern satellite geodetic technologies, that have improved the accuracy of coordinate determination significantly and is currently applied in all

spheres of decision-making (Fazilova 2017). Most traditional datums also fail to incorporate ground deformation when formulated, introducing error into coordinate estimation through time. Traditional datums and coordinate systems have been used in surveying across Trinidad prior to the advent of these GPS technologies. These include the Old Trinidad datum of 1903, based on the Clarke 1858 spheroid, with its origin point defined as the Harbour Master's Flagstaff that has long been removed. The Naparima 1955 datum is also employed locally and is based on the International 1924 Ellipsoid, with an origin monument established on Naparima Hill in San Fernando, which has since been demolished by quarrying activities (Mugnier 2000).

Both historical datums used in Trinidad are static in nature, that is, the coordinates assigned to their reference points are assumed to remain infinitely constant across time. Given the consistent deformation that occurs across Trinidad, it is now known that this cannot be true and these static datums experience distortion, reducing both their quality and accuracy; introducing error into any surveys conducted using them. Datums should only be used if true and accurate coordinates of location can be estimated at any point in time; thus, they need to be resilient to tectonic and ground deformation.

Datum deterioration has drastic effects on various matters relating to national land and marine space. The national geodetic datum is referred to in legislation relating to land boundaries and is applied in the definition of maritime borders. The use of different types of datums between Papau New Guinea (dynamic) and Australia (static) in the past has made it difficult to resolve maritime boundary issues (Tregoning and Jackson 1999). While deformation is minimal within the continent, static datums produced the level of accuracy needed for survey control across most of Australia. However, this did not apply to the northern coast where the continent approaches Papau New Guinea. Dynamic datums were used in Papau New Guinea as it lies along the Pacific Ring of Fire where volcanism, earthquakes and deformation are pervasive. Transformation of coordinates between datums proved

to be inaccurate, complicating maritime boundary definition. Similar issues have been experienced in settling maritime boundary disputes between Barbados and Trinidad (United Nations 2006). Lack of proper geodetic control locally and by extension, boundary definition, resulted in Barbados winning the dispute.

1.3 Problem Resolution

The inadequacy of static datums used in Trinidad leaves the island without a valid reference frame in which confident and precise surveying and decision making can be executed. Solutions to this issue must accommodate the deformation occurring across the island as a result of the tectonic motion along the plate boundary. It must also user-friendly for those who are accustomed to working in a static frame of reference while also taking advantage of modern high precision technologies including satellite GPS-geodesy, while maintaining low-cost and technological demands.

Demands of the datum can be met through the development and implementation of a semi-dynamic datum for Trinidad. Semi-dynamic datums incorporate deformation models to monitor and incorporate changes that occur as a result of plate tectonics and deformation events (Donnelly, Blick and Stanaway 2013). Such models provide a means of operating in a static frame by allowing translation of current coordinates to the epoch the original static datum was realized. This allows correlation and compilation of datasets acquired at various periods with sufficient spatial accuracy. Semi-dynamic datums can be offered in a user-friendly environment by offering tools and utilities that eliminate the need to understand its complicated dynamics and defined using International Terrestrial Reference Frames (ITRF). Precedents exist in some of the most dynamically tectonic regions of the world such as New Zealand (Blick and Donnelly 2016) and Indonesia (Abidin, et al. 2015) and given the geological situation in Trinidad there is a need to consider a similar strategy for the small island state.

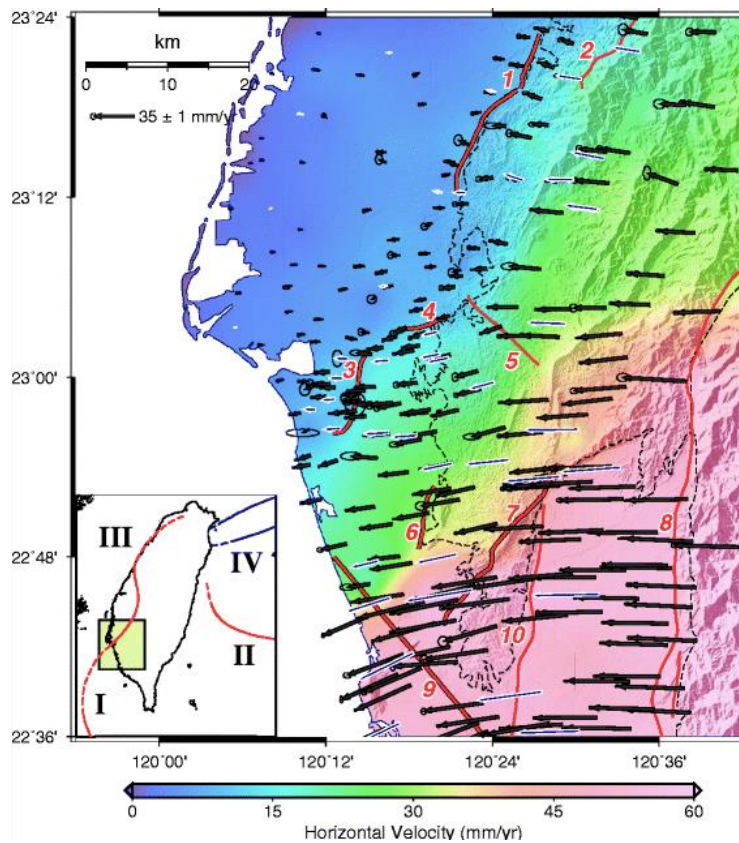


Figure 1-2: Horizontal deformation model used to convert the static Taiwanese Geodetic Datum (TWD97) to a semi-dynamic datum (Ching and Chen 2015).

1.4 Project Aim & Objectives

This research aims to investigate the nature and degree of horizontal deformation that the island of Trinidad experienced, using GPS and satellite-based geodetic methods, across a 24 to 27-year period (1990 vs 2014-2017). Horizontal deformation is estimated for the purpose of underscoring the unsuitability and inapplicability of static datums in Trinidad. Results will also provide the basis on which a local relative deformation model can be built; a key component in the development and application of semi-dynamic datums. The operation of a semi-dynamic datum across Trinidad will return much needed integrity and accuracy to coordinate determination and surveys conducted across the island. It will also better accommodate the use of satellite technologies available for precise applications in surveying, and by extension management of the national land and marine space.

As a new investigation that builds upon previous work undertaken by Saleh et al. 2004 and Weber 2011, it is enabled by the discovery of previous GPS geodetic surveys undertaken for commercial purposes by Haliburton Geophysical Services (HGS 1991).

Specific objectives are as follows:

- Review existing work on deformation across the island of Trinidad in relation to tectonic deformation across the land mass.
 - Review survey work undertaken by Haliburton in 1990, identify survey marks suitable for making GPS observations to give coverage across the island and acquire new GPS survey data at these marks.
 - Establish primary control in an international frame of reference using data acquired at local CORS sites by connection to reputable international stations.
 - Process newly acquired GPS observation data from the Haliburton marks to establish current coordinates in the international reference frame selected and quality control the new results to determine associated accuracy measures.
 - Bring older and current datasets to a common frame of reference for comparison to estimate relative displacements and velocities across a 24 to 27-year period.
 - Compare results obtained from this investigation with previous findings, align them with current understanding of local tectonics and propose a strategy for development of a semi-dynamic datum for Trinidad.
-

2 SURVEY AND ANALYSIS OF EXTANT RESEARCH

From the perspective of development in spatial science there is a need for understanding the nature of horizontal deformation ongoing across the island of Trinidad, the effects it has on currently employed geodetic frameworks and the potential means of ameliorating the fallouts. Outlined in this section is a summary and critical analysis of literature covering the relative concepts needed to provide these answers. This review covers the following spheres of research:

- I. Static datums applied across Trinidad and Tobago.
- II. Case studies that address network deformation through semi-dynamic datum implementation.
- III. Dynamic datums including the International Terrestrial Reference Frame.
- IV. Tectonic evolution and structural Geology of Trinidad.
- V. Neotectonics of Trinidad.
- VI. Review of Haliburton Geophysical Services GPS Survey.

2.1 Geodetic Datums

The main purpose of geodetic datum is to provide a reference frame within which multiple features on the Earth's surface can be related to each other. Developing such a reference frame has proven to be difficult given the geometry of the Earth; the planet itself is not a perfect sphere. A geoid offers a representation of the Earth that is defined by the physical property of gravity, but this surface is irregular in both shape and size. This irregularity is caused by variations in density distribution within the planet's interior that consequently cause gravitational variations. Mean sea-level is often used as an approximation of the geoid. (Li and Gotze 2001).

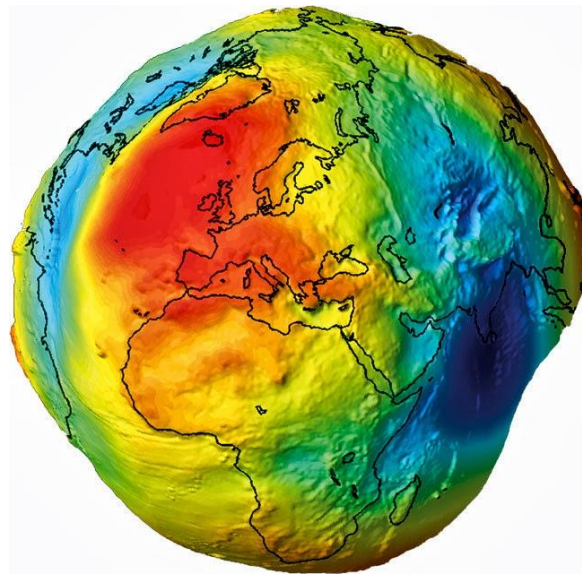


Figure 2-1: Model of geoid is exaggerated radial variation and coloured according to variation in gravitational acceleration (Li and Gotze 2001).

Given this complicated surface, horizontal positioning becomes arduous as geoids are unable to correlate between real-world locations and coordinates of latitude and longitude. Using mathematical models and parameters, ellipsoids are developed and act as first order approximations of the geoid. Ellipsoids can be used to model a specific part of the Earth's surface, where it fits best, developing geodetic datums for that specific area while others attempt to model the entire geoid and can be applied globally (see Figure 2-2), within limits (Torge and Muller 2012). Datums defined using these ellipsoids provide the means of assigning coordinates to features in three-dimensional space to the Earth's surface.

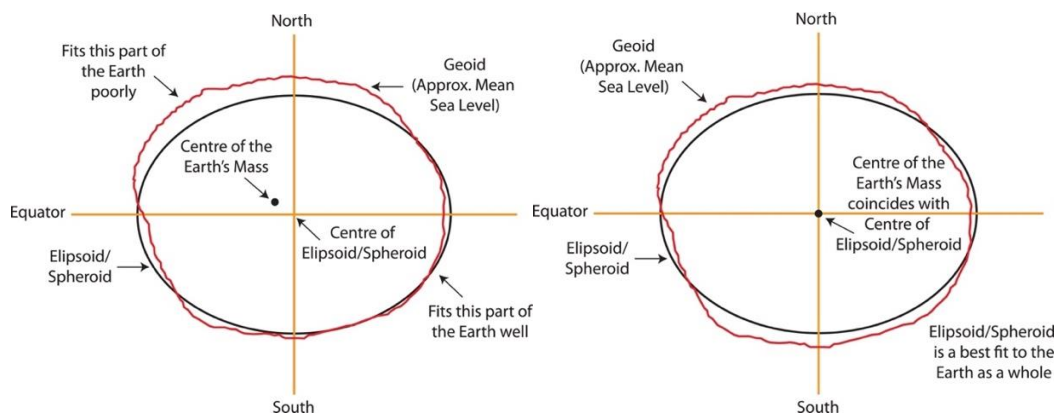


Figure 2-2: Local datums (left) based on ellipsoids that model a specific region of the geoid and Geocentric global datums (right) where ellipsoids attempt to model the entire geoid (ANZLIC 2016).

Many variations of geodetic datums exist depending on their applications, orientation (vertical vs horizontal), etc. This section focuses on datums that have varying degrees of resilience and adaptability to tectonic deformation; specifically, static, semi-dynamic and fully-dynamic datums.

2.2 Static Datums

Static geodetic datums are the simplest form of datum employed in surveying and mapping exercises. Traditionally, these datums were established through the observation and definition of a datum reference point, using outdated astronomical techniques. At this point, an ellipsoid will be adopted as a local approximation to the geoid to provide geodetic control to the required area (Chatzinikos and Kotsakis 2016). From this point, region wide observations and surveys would be conducted to develop networks via triangulation, to extend the reach of the datum locally.

Static geodetic datums are those whose coordinates are considered fixed and unchanging over time at the reference epoch; they are constantly defined by the coordinates of its geodetic monuments. They do not account for the effect of plate tectonics and other deformation inducing phenomena such as elastic rebound, plate delamination, etc (Haasdyk, et al. 2014a). Such datums do not fare well along plate boundaries where tectonism and deformation are active. Monument coordinates

change over the years, distorting these geodetic datums, adding significant error and degrading their quality over time. When employed they pose significant risk to data management where features bearing past coordinates are now in different positions, making data correlation both difficult and inaccurate.

2.2.1 Static Datums of Trinidad

The 1901-1903 triangulation network of Trinidad was the first establish reference frame employed across the island (Mugnier 2000). The network consisted on 18 primary and 600 secondary stations which were directly observed using astronomic observations. The datum adopted the 1858 Clarke ellipsoid and its plane coordinates were computed using the Cassini map projection with an origin point at the Harbour Master's Flagstaff in Port of Spain that has since been destroyed. Eventually, this triangulation network was extended the Royal Engineers in 1927 to allow 1:50000 scale mapping of the island. In 1923, Royal Engineers also commenced the development of a triangulation network for Tobago that consisted of 22 primary and 63 secondary stations, the baselines of which were also observed using astronomic techniques. It also employed the 1858 Clark ellipsoid with an origin point at Mount Dillon, fully defining the 1927 datum of Tobago.

One of the major limitations of these networks was the inability to provide and satisfy large-scale mapping of the island. Noticing this limitation, Lands & Surveys Division was tasked, in collaboration with British Directorate of Overseas Surveys (BDOS) with development of a more precise network for the island. This led to the development of the Naparima 1955 datum (Saleh, et al. 2004) which consisted of 120 old triangulations stations and 254 new stations and baseline distances estimated using Tellurometers at an accuracy of < 10 cm. The datum employed the International 1924 ellipsoid with a datum point at Naparima Hill which was observed in 1955 and estimated using astronomic techniques. Conversely, triangulation points were not observed until the mid 1960s, representing a separation between datum definition and realisation. Plane projection was done using the Universal Transverse Mercator (UTM) projection for zone 20 N.

In 1972, The Defense Mapping Agency Topographic Centre performed network adjustment of the 1955 datum using computer software, giving new coordinates for reference points within the datum. This adjustment was used to tie Tobago to survey control in Trinidad, creating the Naparima 1972 datum. It was established across Tobago using 6 traverse stations and 39 points, with direct observation measured using theodolites and distances measured using a Tellurometer. The measurements of this control network and its connection to Trinidad's by night triangulation between the two islands, started at the L&S in 1973 with the help of the United Nations and its coordinates became available in 1978-1979 (Saleh, et al. 2004). This 1972 datum was not applied by the surveying community in Trinidad which preferentially stuck to using the 1995 datum, complicating data correlation between the islands.

Of all these datums, the Naparima 1955 is the most widely used datum in Trinidad and is the default choice of most agencies including the Land & Surveys Division and the former Petroleum Company of Trinidad and Tobago (Petrotrin). Despite this, there has been a constant need to transform coordinates from the 1901-1903 datum (older datasets) to Naparima 1955 or translation between Naparima 1955 and WGS84 (modern datasets) with the advent of GPS. Crude transformation parameters and techniques have been developed within the survey community, especially before the development of the National GPS network, to execute this need. This has led to estimation of coordinates with significant error, suggesting that these datums are not ideal and do not meet the standards necessary for surveying and mapping. Compounding this is the fact that all these datums and networks have been distorted by active tectonism across Trinidad since their realisation and the “known” coordinates of reference points have since changed.

2.3 Fully-Dynamic Datums

With the increasing pace at which global positioning technologies are advancing there has been a dramatic shift in the way in which geospatial data is referenced. This shift moves away from relative estimates made in a local or regional scale to absolute positioning on a global scale. GPS, being the most widely used positioning technique and provider globally, provides positions as three-dimensional position vectors originating at the Earth's centre of mass and ending at its surface. The surface of the Earth is continuously moving due to plate tectonics, mass wasting and other phenomena, resultantly changing the position of established points. If the position of a point is consistently re-estimated, its coordinates will change as a result of this deformation. Reference frames which allow for these positions to be continuously tracked and coordinates updated are referred to as kinematic or fully-dynamic datums (Wang, Wang and Roberts 2009).

Fully-dynamic datums are those whose reference coordinates continuously change and can be estimated and known at any time within a reference frame. The International Terrestrial Reference Frame (ITRF) and all its realisations are examples of such kinematic datums. Through the use of deformation models, accountability for induce changes caused by plate tectonics is regarded by attaching velocities to reference points. Velocities are represented in the form of Absolute Deformation Models (ADM) that account for deformation in three dimensions (3D); both horizontal and vertical, as opposed to Relative Deformation Models (RDM) that are solely concerned with horizontal deformation (Stanaway, Roberts and Blick 2014). Velocities are absolute in that they are not estimated relative to a specific location or region and provide a global sense of ongoing deformation. The following section will cover the various examples of kinematic datums and assess its suitability in candidacy as a modern geodetic datum for Trinidad.

2.3.1 International Terrestrial Reference System (ITRS)

Changes at the surface of the Earth are measured through space and time using global geodesy with a given standard where these changes can be quantified and reference. Several terrestrial reference systems exist that provide a means of both positioning points on the Earth's surface while simultaneously accounting for deformation induced by plate tectonics. Despite this, a common reference system must be agreed upon internationally that would ensure global consistency when comparing spatial datasets. The International Union of Geodesy and Geophysics (IUGG) put forth the idea of an International Terrestrial Reference System (Petit and Luzum 2010), that meets the following conditions:

- I. It is geocentric, its origin being the center of mass for the whole Earth, including oceans and atmosphere.
- II. The unit of length is the meter (SI). The scale is consistent with the TCG time coordinate for a geocentric local frame, in agreement with IAU and IUGG (1991) resolutions. This is obtained by appropriate relativistic modeling.
- III. Its orientation was initially given by the BIH orientation at 1984.0.
- IV. The time evolution of the orientation is ensured by using a no-net-rotation condition with regards to horizontal tectonic motions over the whole Earth.

2.3.2 International Terrestrial Reference Frame (ITRF)

The International Terrestrial Reference Frame (ITRF) is the manifestation and realisation of the ITRS through the physical coordination of points across the Earth's surface. The International Earth Rotation and Reference System Service (IERS) is responsible for producing these realisations with a total of 13 versions of ITRF; ITRF88 being the first and ITRF2014 being the most recent (Petit and Luzum 2010). Solutions for most ITRF iterations were achieved using long-term global solution from four main techniques: Very Long Baseline Interferometry (VLBI), Satellite Laser Ranging (SLR), Doppler Orbitography and Radio-positioning Integrated by Satellite (DORIS) and GPS. As of ITRF2005, time series of station positions and

Earth Orientation Parameters (EOP), were included as additional inputs in ITRF definition (Altamimi, Collilieux, et al. 2007). The number that follow ITRF names identifies the last year of data that was used for the formation of the frame. For example, ITRF2008 designates the frame of station positions and velocities constructed in 2010 using data available until the end of 2008. While ITRF provides a model of absolute deformation speed, it does not model accelerations caused by earthquake events. This degrades the quality of each iteration with time, forcing the development of new, updated iterations.

2.3.3 ITRF 2014

ITRF2014 at Epoch 2010.0 is the thirteenth iteration and realisation of the ITRS and was formally adopted globally on February 26th, 2015. Inputs used in constructing this reference frame including DORIS, GNSS, SLR, VLBI. By combining these space geodetic techniques with time series and EOPs, this ITRF is considered to be the currently most accurate reference frame (Altamimi, et al. 2016).

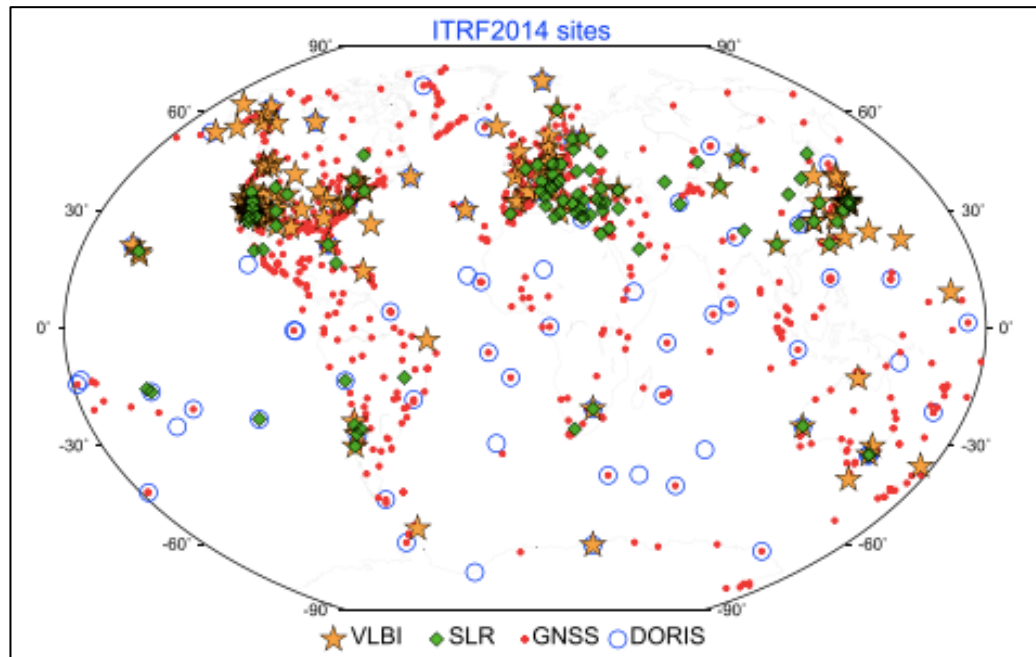


Figure 2-3: ITRF2014 network showing locations of VLBI, SLR, GNSS and DORIS sites co-located with GNSS (Altamimi, et al. 2016).

This iteration is an improved version of past realisation based on these techniques' solutions using their entire sets of historical data up to the end of 2014. It also accounts for both co-seismic and post-seismic deformation caused by major earthquakes including the 2010 M 8.8 earthquake in Chile and the 2011 M 9.0 earthquake in Japan (Altamimi, Metivier, et al. 2017) Each ITRF solution has improved accuracy when compared to its predecessors mostly as a result improved combination of ITRF inputs.

As an example of a fully-dynamic datum, ITRF2014 makes use of Absolute Deformation Models that provides velocities for sites accounting for both horizontal and vertical deformation (see Figure 2-4 and 2-5 respectively).

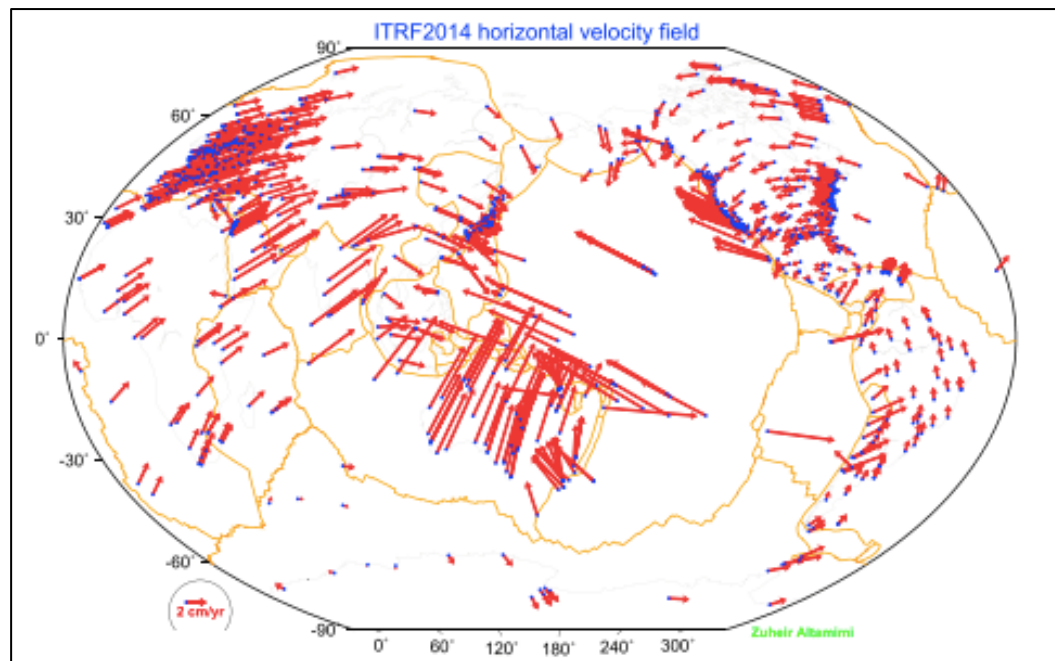


Figure 2-4: ITRF2014 horizontal site velocities and major plate boundaries in yellow (Altamimi, et al. 2016).

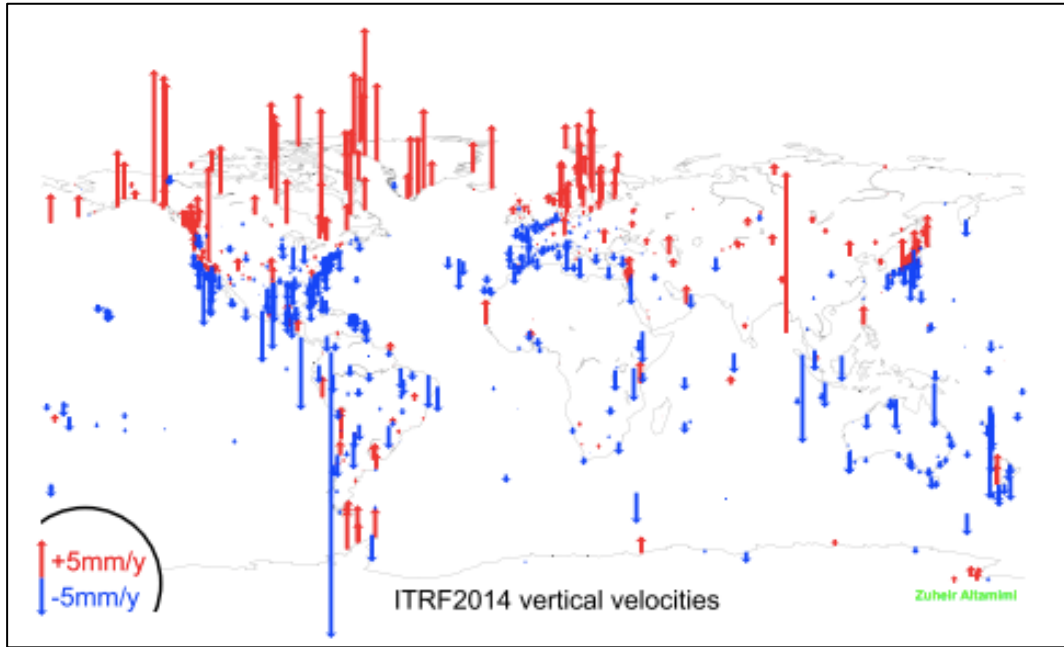


Figure 2-5: ITRF2014 vertical site velocities (Altamimi, et al. 2016).

2.3.4 WGS 84

The World Geodetic System 1984 (WGS) is another example of a terrestrial frame that is applied globally for correlating spatial data. It is the reference frame used by the Global Positioning System (GPS) that is owned and was developed by the United States Department of Defense (USDoD) and is maintained by the United States National Geospatial Intelligence Agency (NGA) (Malys, Wong and True 2016). Multiple realisations of WGS84 exist due to changes in its connection to the Earth since its initial realisation in 1987, with its most recent iteration WGS84 (G1762) being implemented in October 2013. This iteration is aligned to the International GNSS Service (IGS) realisation of ITRF2008 known as IGb08.

While realisations of WGS84 have followed similar ITRS as those employed by the IERS in realising ITRF, WGS 84 uses a much smaller array of tracking stations observed using only GPS satellites. This reference frame is realised through the global coordination of 17 DoD monitoring sites across the world. WGS84 is considered a dynamic reference frame as these station coordinates are updated at the

beginning of each year and adjusted to an epoch at the half-year mark to account for deformation caused by plate tectonics, yet it is still not suited for national geodetic control.

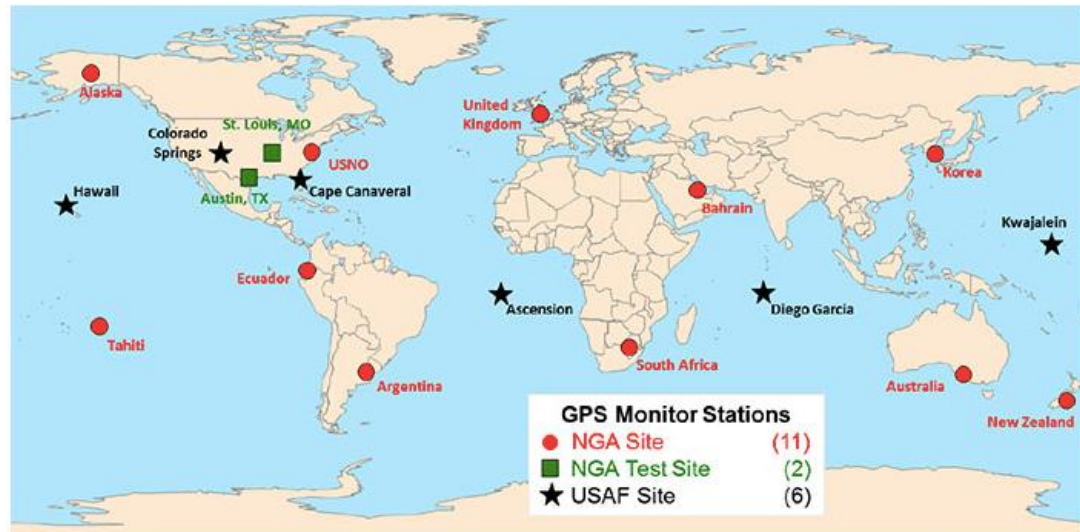


Figure 2-6: GPS Monitoring Stations used to realise WGS84 (Malys, Wong and True 2016).

2.4 Semi-Dynamic Datums

While fully-dynamic datums provide a means of consistently measuring and reporting deformation (Altamimi et al. 2016), they are not without their flaws. The need to update coordinates and spatial databases referenced to dynamic datums makes it one of the most complicated and costly datums to implement in a country (Shariff, et al. 2017). Additionally, translating all current spatial datasets to a new kinematic datum requires a significant amount of coordination and cohesion among all surveying, mapping and spatial agencies, both public and private that is severely lacking locally. Such datums may also be difficult for non-technical users to comprehend and employ, especially when choosing the right datum or epoch. Consequently, they are not suitable candidate for a modern geodetic datum locally.

Alternately, semi-dynamic datums present a compromise where users can operate in a static reference frame realised at a specific epoch while simultaneously allowing data collection in a dynamic environment (Stanaway, Roberts and Blick 2014). It represents an attempt to account for ground deformation caused by co-seismic and post-seismic displacements, tectonism and other forms of deformation. This is accomplished through the application of Relative Deformation Models (RDM) that are two dimensional and focus solely on horizontal deformation. These consist of a network of sites with attributed velocities (speed and direction) derived from time series of GPS estimated coordinates. Using these velocities, spatial datasets can be propagated towards the reference epoch accounting for any deformation that may have taken place between datum realisation and data collection (Denys, Winefield and Jordan 2007). It should be noted that RDMs consist of velocities derived from geodetic observation and estimates relative to un-modelled area adjacent to the area of interest (neighbouring plates). Resultantly, these models are only applicable to the areas they are intended and for a given time, once they produce accurate and precise coordinates according to geodetic standards. The following sections cover various case studies of the development and implementation of semi-dynamic datums for some nations and reviews the methodology employed in doing so.

2.4.1 New Zealand: Static NZGD1949 to Semi Dynamic NZGD2000

Various datums applied across local municipalities across New Zealand constituted the initial datums developed in the late 19th century. These were developed for the sole purpose of introducing some level of survey needing for mapping and settlement planning, but were created long before advancements in triangulation and survey networks that would have introduced some standard of accuracy. Eventually the national New Zealand Geodetic Datum 1949 (NZGD1949) was realised using the Hayford International ellipsoid (Lee 1978), based off a first-order triangulation network. Coordinates of these stations were considered fixed, but were not immune to crustal deformation that occurs across the twin-island state.

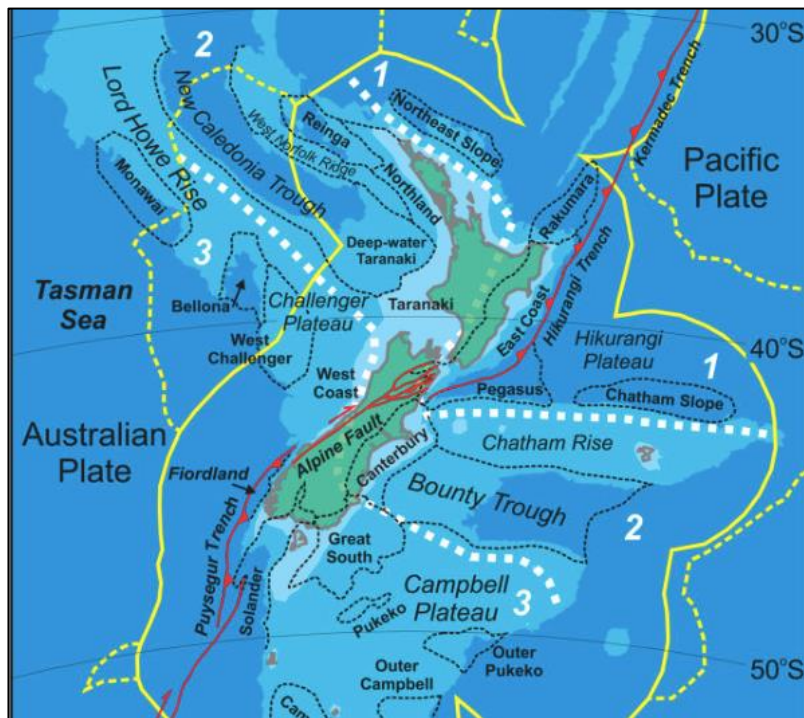


Figure 2-7: Major tectonic features surrounding New Zealand (Uruski 2014).

New Zealand lies at the boundary between the Australian and Pacific plates where the Pacific plate is subducted beneath the Australian plate to the north-east and the Australian plate is subducted beneath the Pacific in the south-west (Uruski 2014). Accompanying this is the Alpine fault, along which there is a combination of uplift (generating the Southern Alps) and strike-slip motion of 40-55 mm/year, some of the fastest motion in the world (Baratin Wachten 2018). These tectonic regimes

result in a well-recorded history of volcanism, seismicity and deformation events (landslides, uplift and subsidence). Resultantly the accuracy of the static NZGD1949 datum deteriorated with time, introducing inaccuracy over the 50-year period across all of New Zealand. This error and deformation became tangible with introduction of GPS and Electronic Distance Measurement (EDM) techniques that measured distortion of up to 25 ppm (Blick and Rowe 1997); forcing the datum to be insufficient for surveying and mapping purposes, especially with the advent of these new technologies.

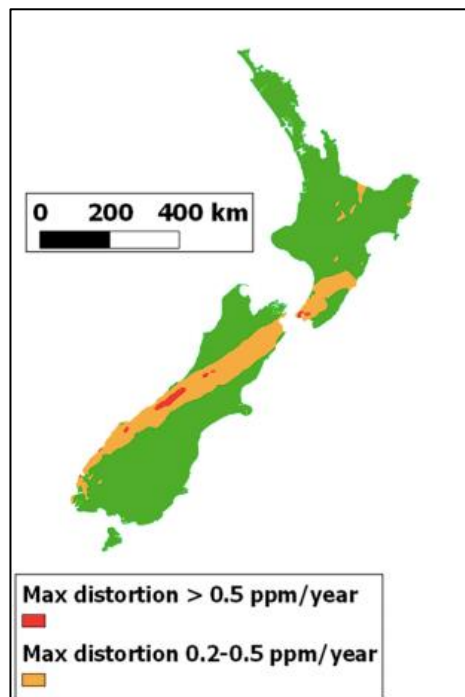


Figure 2-8: Distortion of NZGD1949 monuments (Blick and Donnelly 2016).

Deterioration in integrity of the national geodetic network led to the demand for a modern geodetic datum, one that adhered to international standards and factored in tectonic deformation. The New Zealand Geodetic Datum 2000 (NZGD2000) was then implemented using the GRS80 ellipsoid tied to ITRF96 at epoch 1st January 2000 and included a deformation model to allow propagation of coordinates backward toward the reference epoch (Blick 2003). The original deformation model used to supplant NZGD2000 was based of GPS observations at 362 monuments

across both North and South islands, between 1991 and 1998, where velocities were based relative to the Australian Plate. (Beavan and Haines 2001).

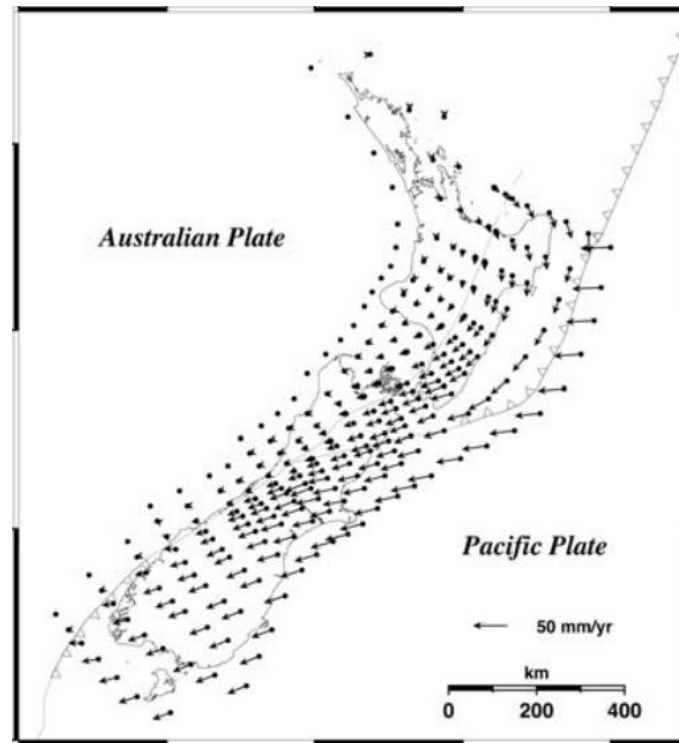


Figure 2-9:Initial relative deformation model used to complement NZGD2000 (Blick, Donnelly and Jordan 2009).

NZGD2000 has since been updated. In 2011 it was aligned with ITRF2008 and had its deformation model revised with the additional incorporation of a national network of continuously operating stations (CORS) known as the PositionNZ network (see Figure 2-6). This included 35 of these stations scattered across New Zealand, some of which also acted as IGS sites, through which NZGD2000 became tied to global datum, ensuring compatibility with international systems (Gentle, Blick and Gledhill 2016). Velocities were then combined with modeled velocities from the Nuvel 1-A no-net rotation global velocity model to provide coverage for offshore islands that required geodetic control (Crook, et al. 2016).

While deformation models exist, surveyors avoid its use and rather calibrate their surveys to monuments that have already been corrected by Land Information New Zealand (LINZ) using the deformation model (Blick and Donnelly 2016). Although

LINZ provides software that accomplishes automatic adjustment using their deformation model, it is not yet included in commercial applications.

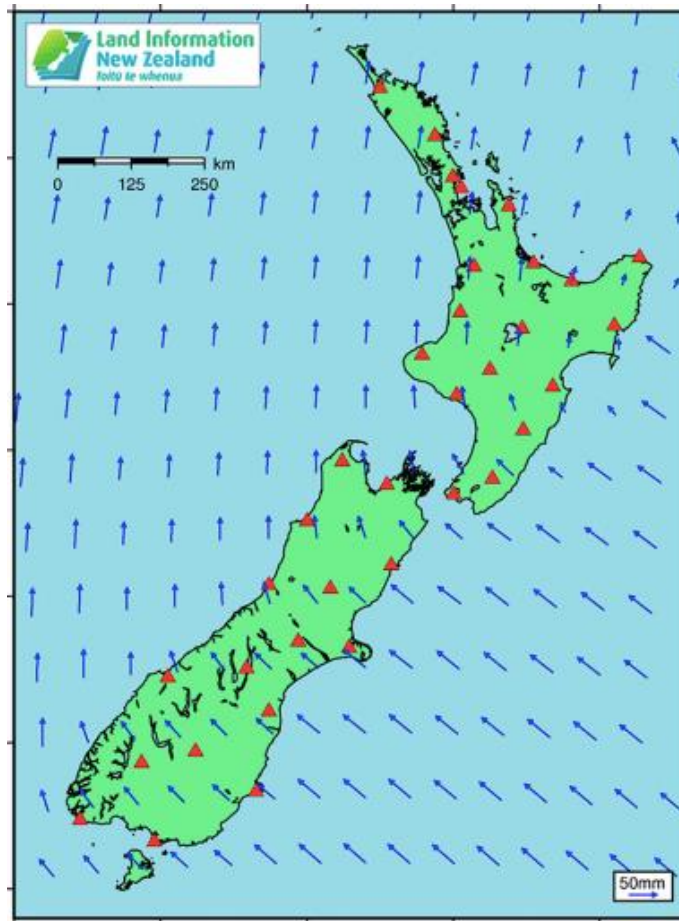


Figure 2-10: Updated deformation model using PositionNZ stations and Nuvel model (Blick and Donnelly 2016).

Further updates to NZGD2000 are expected in the future with the ever-increasing demand for accuracy in modern systems, especially those used by non-specialists that make use of modern technologies that demand accuracy and precision and the greatest possible levels at millimetre scale. (Blick and Donnelly 2016).

2.4.2 Indonesia: Static DGN1995 to Semi-Dynamic IGRS2013

Indonesia is one of many nations that lie at the conjunction of the Eurasian, Pacific, Philippine and Indo-Australian plates, along with several micro-plates and blocks, making it one of the most tectonically complex locations worldwide (see Figure 2-7). Like many other nations along the Pacific Ring of Fire, Indonesia commonly experiences both earthquakes and volcanism due to interaction among these plates, including 2004 Sumatra-Andaman, 2005 Nias and 2007 Bengkulu earthquakes. Secular tectonic motion coupled with earthquake deformation has led to displacements between 31 cm to 6.3 m across various parts of Indonesia (Vigny, et al. 2005, Subarya, Chlieh, et al. 2006).

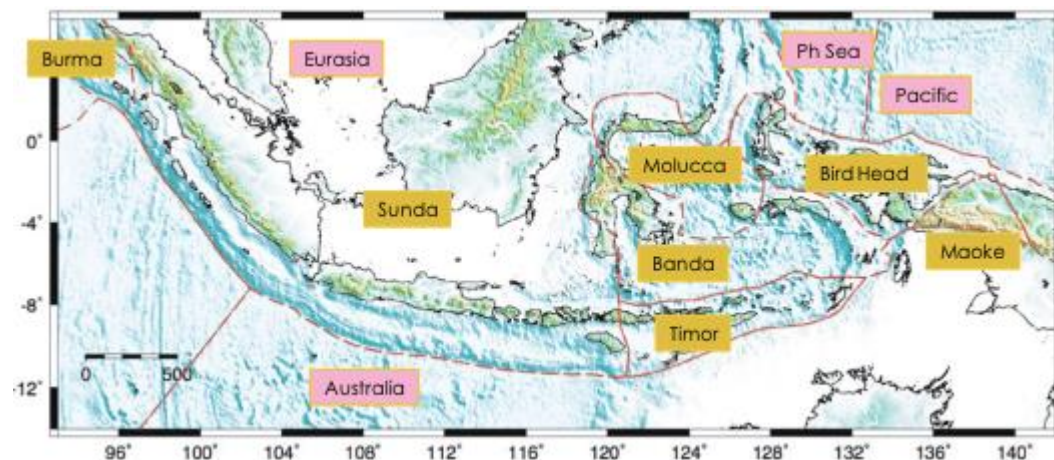


Figure 2-11:Tectonic plates and blocks of Indonesia (Abidin, et al. 2015).

Active tectonics and deformation across Indonesia have distorted all historical static geocentric datums applied across the country. The earliest of these were topocentric geodetic datums developed in the 19th century that were based on the Bessel 1841 reference ellipsoid with varying datum origin points for the islands they were applied to (Scheppers and Schulte 1931). Eventually, these were replaced and unified by a national topocentric datum known as the Indonesian Datum 1974 (ID 1974) which adopted the GRS 1967 reference ellipsoid with a datum origin point set in West Sumatra. ID 1974 was realised using the Navy Navigation Satellite System (NNSS) using Doppler sites and 378 Doppler stations scattered across Indonesia (Rais 1979). The National Geodetic Datum 1995 (DGN 1995) of

Indonesia was then introduced as a modern, although static, geocentric datum realized through precise GPS observation of approximately 460 monuments of the National Geodetic Control Network (NGCN) with WGS 84 as its reference ellipsoid (Subarya and Matindas 1996). Given its static nature and active tectonism, this datum was deemed inadequate for mapping and surveying especially for upcoming applications in navigation and positioning. Additionally, with the advent of space geodesy that provided mm level accuracy there was a need for a more accurate global geocentric datum.

This led to the development of the Indonesia Geospatial Reference System (IGRS 2013) that was developed by Geospatial Agency of Indonesia (BIG) and launched in October 2014 (Abidin, et al. 2015). IGRS 2014 is a semi-dynamic datum based on ITRF2008 reference frame with a reference epoch of January 1st 2012. It employs a relative deformation / velocity model that account for both tectonic motion and earthquake deformation; allowing coordinates to be propagated across time to a common reference epoch. Initial velocity models were estimated and based of modelling of plate motions and earthquakes using MORVEL (DeMets, Gordon and Argus 2010) as seen in Figure 2-8.

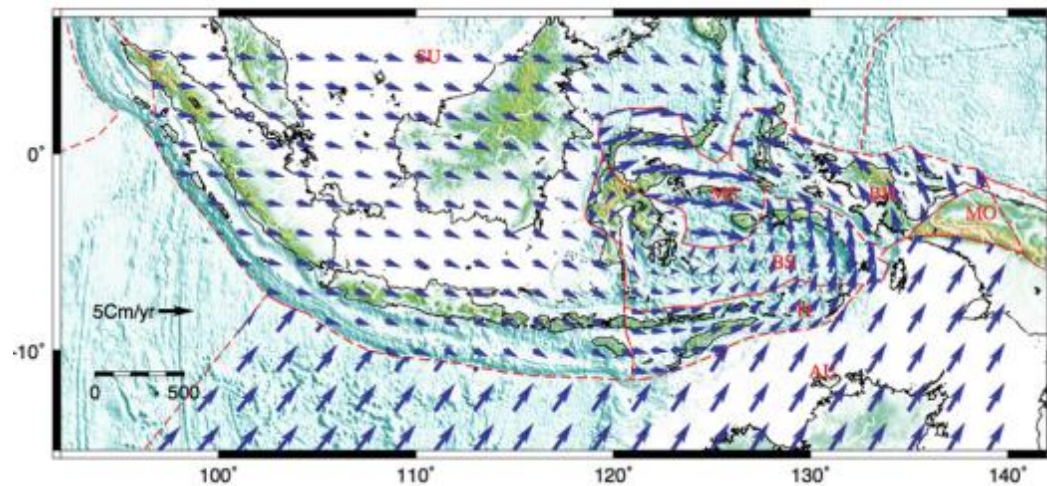


Figure 2-12: Initial velocity model generated by MORVEL (DeMets, Gordon and Argus 2010).

Currently, IGRS 2013 velocity models are based on rates derived from a combination of passive and continuous GPS stations. These include 1350 passive geodetic monuments that make up the Geodetic Horizontal Control Network (Figure 2-9) and 118 GPS CORS sites (Figure 2-10), both maintained by BIG. An additional 183 GPS CORS sites managed by the National Land Agency of Indonesia (BPN) are incorporated into these velocity models (Figure 2-11). GAMIT/GLOBK software was used to process daily coordinate solutions for all sites from which velocities were estimated.

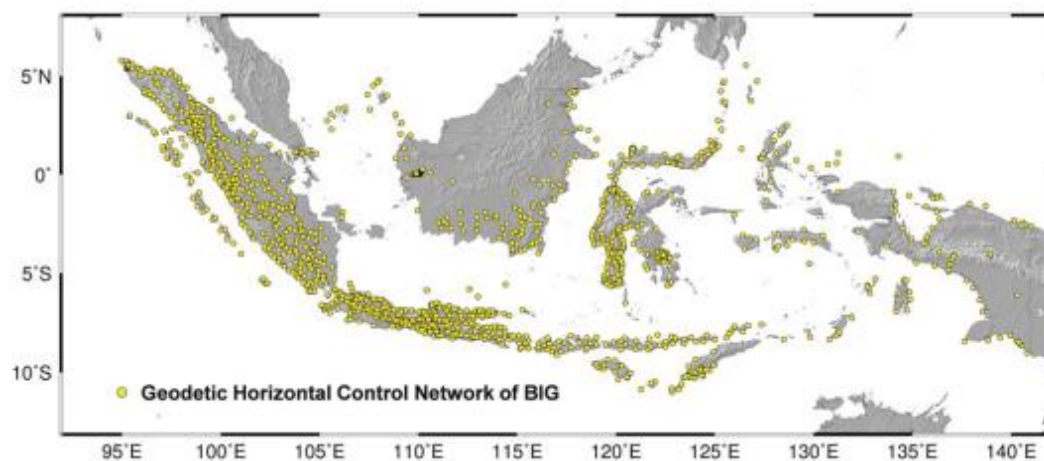


Figure 2-13:Passive geodetic monuments managed by BIG (Abidin, et al. 2015).

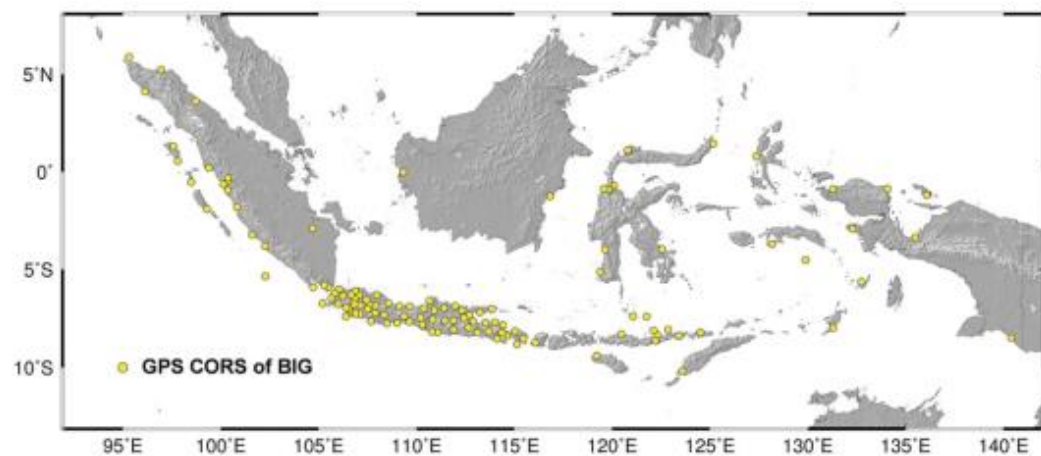


Figure 2-14: Continuous Operating Reference Stations (CORS) operated by BIG (Abidin, et al. 2015).

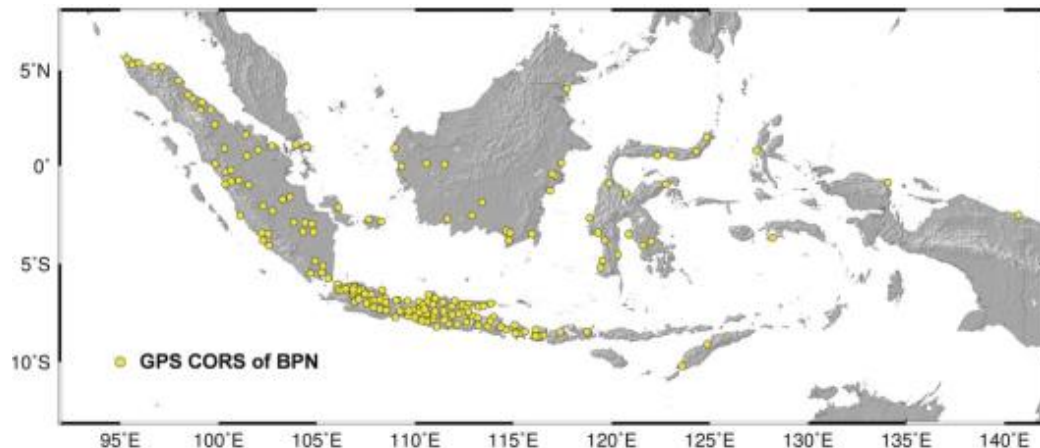


Figure 2-15: Continuous Operating Reference Stations (CORS) operated by BPN (Abidin, et al. 2015).

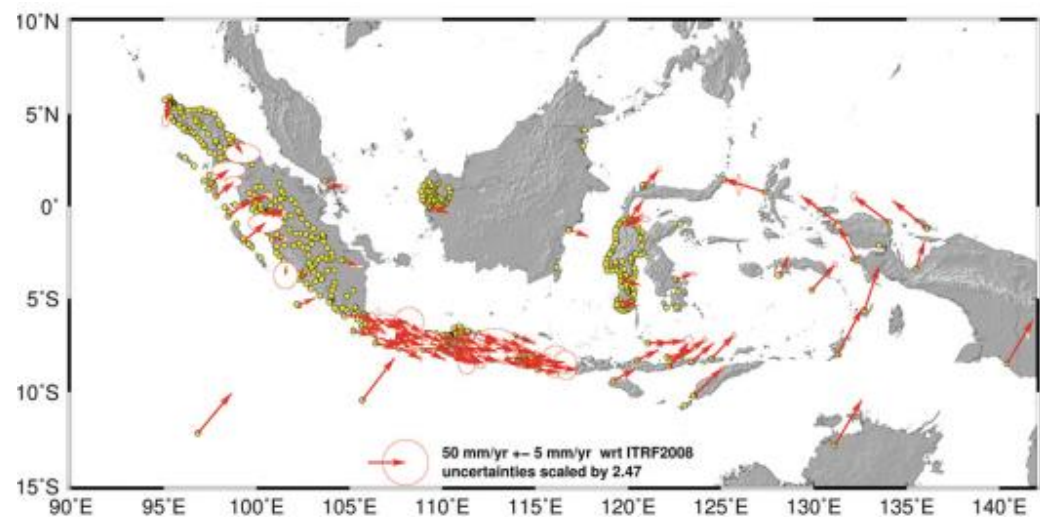


Figure 2-16: ITRF 2008 velocities for most BIG GPS CORS sites (Abidin, et al. 2015).

While velocities models are sufficient for semi-dynamic datum implementation, there is still a need to resolve the MORVEL velocity model with velocities estimated from pGPS and GPS CORS station time series. It is also uncertain whether the current deformation models that consist of multiple blocks accurately models the velocity field of all of Indonesia (Hanifa, et al. 2014). Through densification of the GPS CORS network, deformation estimation across all of Indonesia would be achieved. Successful implementation of IGRS 2013 was achieved through education campaigns and coordination with all mapping and surveying institutions across Indonesia.

2.4.3 Malaysia: Moving away from the Static GDM2000

Also located within the Pacific Ring of Fire is the multi-island nation of Malaysia which lies within the complex tectonic setting with the interaction of the Indo-Australian, Eurasian and Philippines plates. Malaysia lies within the Sundaland block that makes up most of southeast Asia, where significant seismic and volcanic activity takes place (Simons, et al. 2011). Notable earthquakes included the 2004 M 9.2 Sumatra-Andaman earthquake which generate co-seismic displacement up 27 cm in Thailand, 15 cm in parts of Indonesia and 17 cm in Langkawi, Malaysia (Vigny, et al. 2005). Additional major earthquakes which have affected Malaysia include the M 8.6, 2005 Nias-Simeulue earthquake, M 8.5, 2007 Bengkulu earthquake and the M 8.6 2012 Northern Sumatra earthquake.

These events have significantly distorted the geodetic datum currently employed across the nation; the Geocentric Datum of Malaysia 2000 (GDM 2000), that is aligned with ITRF2000 at epoch 2000, but was officially used locally in August 2003 and realized using the Malaysia Active GPS System (MASS). The GDM2000, however, was not continuously updated to align with current realisation of ITRF, making it a static datum that is susceptible to deformation by tectonic forces (Shariff, et al. 2017). Attempts of datum adjustments were made in the past to account deformation from past major earthquake events, however, this was not applied at a national level. Given the tectonic-induced inaccuracies associated with GDM2000, semi-dynamic datums were considered as an optional modern geodetic datum to employ for future use. Prior to semi-dynamic datum implementation, relative deformation models must first be constructed to account for tectonic distortion.

To estimate the rate of tectonic motion and develop deformation models for Malaysia, coordinate solution and velocities were estimated using GPS data acquired by the Malaysia Real-Time Kinetic GNSS network (myRTKnet). This network comprised of 78 stations scattered across the country with distances of 30 – 120 km between. Each station was equipment with a high-precision dual-

frequency GPS receiver that operated continuously across 24 hours. Data from these stations were transferred daily to a central repository and processing centre at the headquarters of the Department of Surveying & Mapping Malaysia (JUPEM) (Jamill and Mohamed 2010). The network was developed to maintain the local geodetic infrastructure, model the ionosphere over Malaysia while also conducting fleet management and tracking for government and private business vehicles.

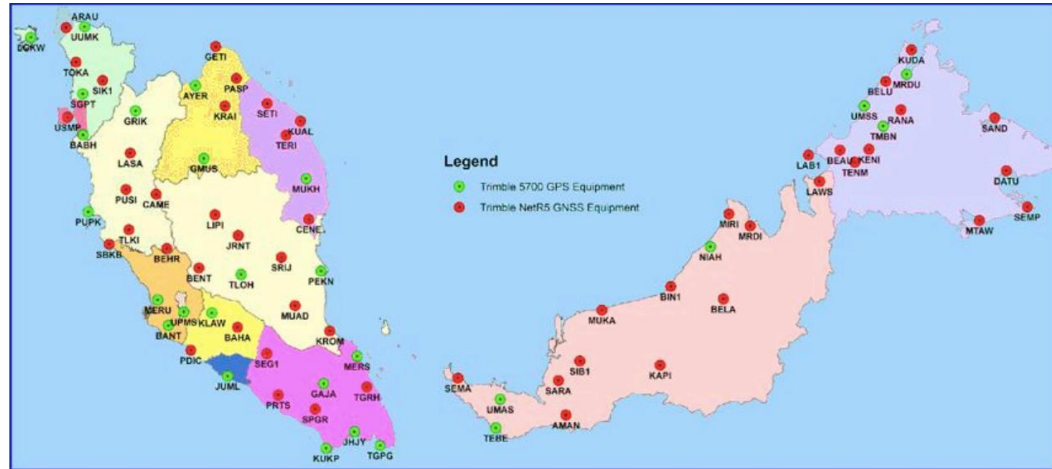


Figure 2-17: Map of the Malaysia Real Time Kinetic GNSS Network (myRTKnet) (Jamill and Mohamed 2010).

Using 65 of these myRTKnet stations, daily coordinate solutions were achieved using Bernese v 5.0 high-precision GNSS processing software (Dach, et al. 2007) for the period of 2004 to 2014. Solutions were estimated using 15 IGS stations as primary control, providing datum definition in ITRF 2008, as they represented relatively stable motion across the 10-year period. Time-series for these selected stations were then plotted using GPS Interactive Time Series Analysis software (GITSA) (Goudarzi, et al. 2013) to estimate station velocity vectors and perform linear least squares regression analysis.

Using velocities, two forms of deformation models were generated: secular and non-secular. Secular deformation models (see Figure 2-14), represent the continuous horizontal velocities experienced as a result of gradual plate motion during aseismic periods. Secular deformation models are generated by the bilinear interpolation of station velocities, creating deformation surfaces.

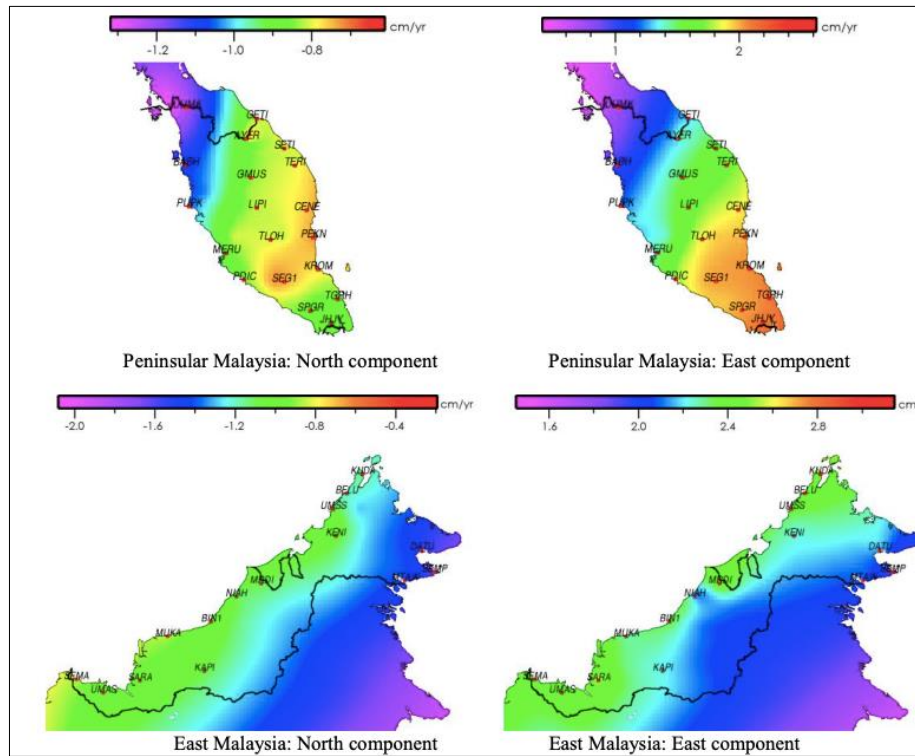


Figure 2-18: Secular Deformation Models showing individual North and East components (Shariff, et al. 2017)

Non-secular deformation models are used to account for the abrupt deformation that occurs with major earthquake events and the post-seismic motion that may be ongoing several years after these events. These deformations are measured using myRTKnet stations and field observations, then used to general non-secular models for four events: the 2004 Sumatran-Andaman, 2005 Nias, 2007 Bengkulu and the 2012 Sumatran earthquakes (Figure 2-15).

Given the ease with which both secular and non-secular deformation models can be constructed for Malaysia semi-dynamic datums were deemed the most useful to act as a modern geodetic datum for the nation. Its implementation was also deemed most appropriate for Malaysia as it would provide a means of acquiring accurate coordinates across time by accounting for secular and non-secular deformation across the nation. It also provides a low-cost and easily achievable way of updating a geodetic datum whenever major deformation events such as earthquakes occur.

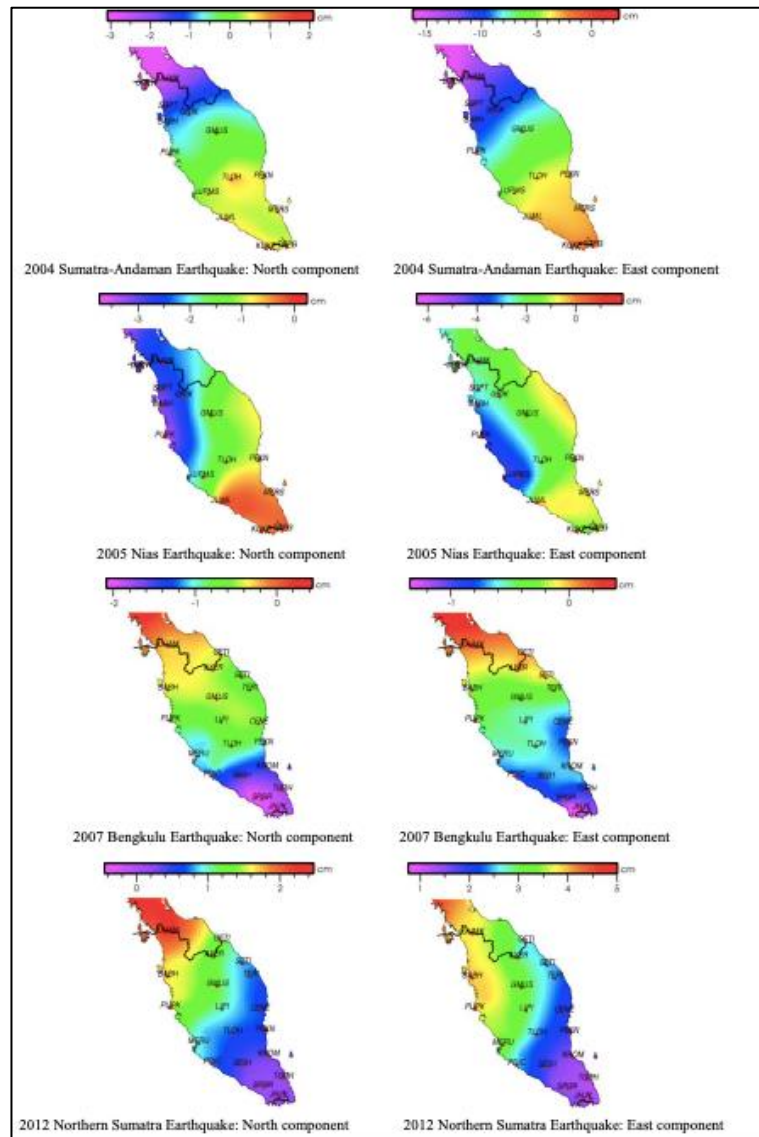


Figure 2-19: Non-secular deformation models for major earthquakes (Shariff, et al. 2017).

As with NZGD2000, there is concern that users may have difficulty understanding the concept of reference epochs and the use of deformation models in propagating coordinates backward and forward. Additionally, the need for both secular and non-secular deformation models further complicates the ease with which these datums can be employed by the surveying community, but are necessary for Malaysia where post-seismic motion may take several years to decay (Paul, et al. 2012).

2.4.4 Philippines Geodetic Datum 2016 (PGD 2016)

The Philippines is currently in the transition to a modern geodetic datum that meets international standards and is in the process of phasing out its traditional static datum; the Philippine Reference System of 1992 (PRS92) that uses Clarke 1866 Spheroid with an origin station at Balanacan (Cayapan 2016). This national datum was established by the Geodetic Survey Component of the Natural Resources Management and Development Project (NRMDP) as a mean of replacing older triangulation network establish by the US Coast and Geodetic Survey in the early 1900's. It was established based on GPS observations of 471 1st to 3rd order survey monuments, some of which were part of this older triangulation network.

The PRS92 static datum is considered outdated and unsuitable for surveying and mapping practices given the accuracy introduced by the active tectonism across the Philippines. These islands lie at the convergence of the Eurasian and Philippine plate where the Eurasian plate is subducted beneath the Philippine in the north-west forming the Manila Trench off the west coast of Luzon. Towards the south-east the Philippine plate is also subducted beneath the Eurasian plate forming the Philippine Trench. The Philippine fault runs through the island nation providing both vertical and strike-slip motion (2-3 cm/year). Abundant volcanic and seismicity occurs across all these islands including the 2013 M 7.2 Bohol earthquake (Kobayashi 2014).

Given deformation within the Philippines, the quality of PRS92 as a geodetic network degraded as its control point coordinates were no longer consistent with their actual positions. The inadequacy of PRS92 meant that a new modern geodetic datum was needed to manage and correlate spatial information, especially with the development of technologies like GPS and the demand of all United Nations member states to adopt and develop systems that use a global geodetic reference frame (GGRF) along the lines of ITRF. Employing such reference frames would provide a means of managing regional, environmental and natural resources data.

The National Mapping and Resource Information Authority (NAMRIA) of the Philippines has proposed the development and maintenance of the Philippine Geocentric Datum of 2016 (PGD2016); a semi-dynamic datum that will make use of a deformation model. PGD2016 will essentially be an upgrade to PRS92 and will be aligned to ITRF, meeting international standards and bringing in a higher level of accuracy and precision desperately needed by the public and private sectors.

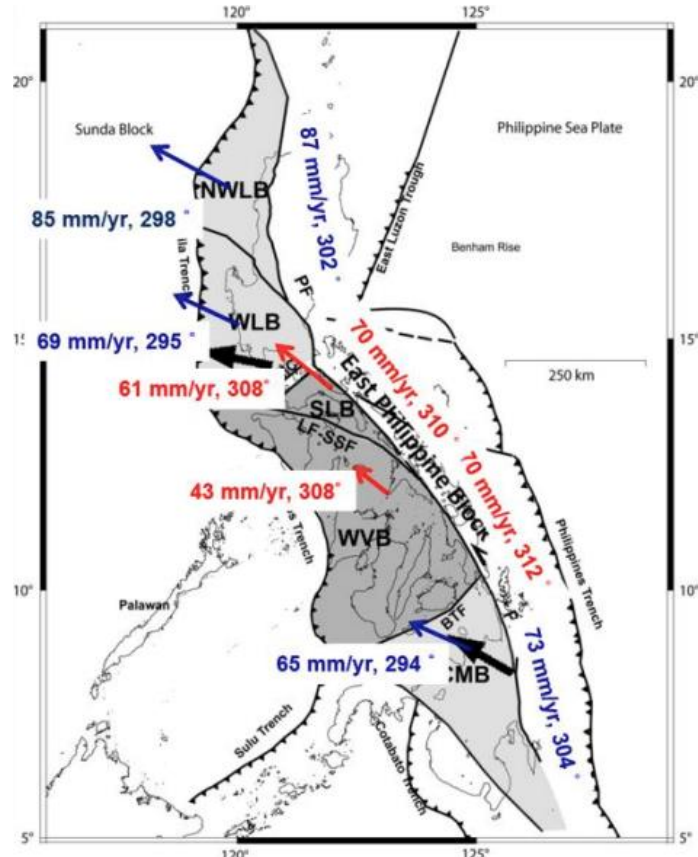


Figure 2-20: Crustal Block zones and estimated velocities across the Philippines (Cayapan 2016).

Semi-dynamic datum development and implementation was chosen given the high expense and complicated nature associated with fully-dynamic datums. Semi-dynamic datum meets the urgent need to align to both geocentric datums and international reference frames, while also providing the nation with time to better discern the complex nature of tectonic deformation occurring. Additionally, NAMRIA is still developing the knowledge based of its human capital to properly execute datum implementation, semi-dynamic datums act as a stepping stone that is

relatively simple to understand before implementing, continuously updating dynamic datums.

To accurately measure and interpret the rate of deformation across the Philippines and develop models to accompany PGD2016, the NAMRIA proposed the densification of the local network of CORS stations known as the Philippine Active Geodetic Network (PageNET). Through this densification project, stations will be less than 70km apart, creating a network with accuracy < 5ppm. Currently, given budgetary restrictions, only 34 stations have been established, however, NAMRIA hope to have 200 stations operational by 2020 (Cayapan 2016).



Figure 2-21: Existing and Proposed Active Geodetic Stations (Cayapan 2016).

2.5 Tectonic Evolution of Trinidad

Trinidad's current geomorphology is best described as ENE striking mountain chains known as the Northern, Central and Southern ranges, between which lie the Caroni (Northern) and Southern basins, along with the poorly exposed Nariva Fold and Thrust belt (Arkle, Owen and Weber 2017). Although these landforms exist contemporaneously with existing transform tectonic regime across the island, they were not formed by forces associated with it, but by other forces (compressive and tensional) that are no longer at play today. Understanding this geological history and evolution is key to understanding the past condition which formed these landscapes.

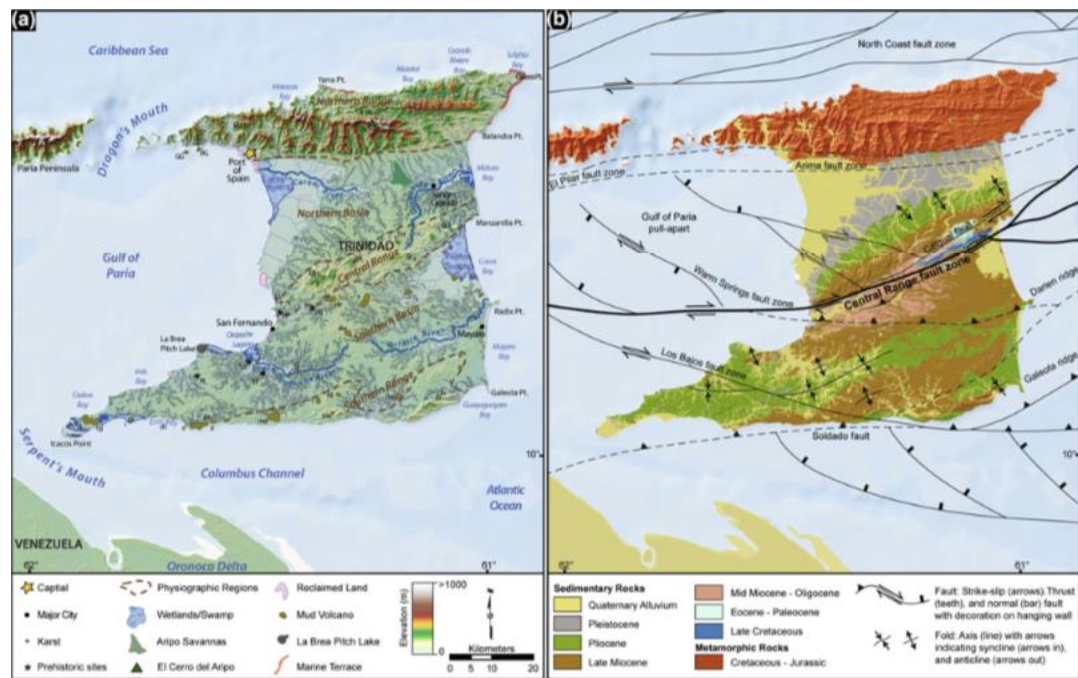


Figure 2-22: (a) Major geomorphic features of Trinidad, (b) Major structural features and geology of Trinidad (Arkle, Owen and Weber 2017).

The tectonic evolution of Trinidad began with the break of Pangea in the Late Triassic to Jurassic when rifting and divergence resulted in the separation of the North American and South American continents. At this time much of Trinidad would have been beneath sea level and along a passive margin marked by extensional normal fault trending east-west as a result of this rifting episode. During the late Eocene to middle Miocene, separation of South America from Antarctica

led to the oblique collision of the South American plate with the Caribbean plate. This collision resulted in the uplift of the Andean chain over northern South American; an exposure of low-grade metamorphic rocks along the El Pilar Fault Zone (EPFZ) that now make up the Paria Peninsula of Venezuela and the Northern Range of Trinidad (Tyson, Babb and Dyer 1991).

Continued collision and compression led to the development of fold and thrust belts across the rest of Trinidad as highlighted by the occurrence of alternating topographic highs and basin lows across the island (Lingrey 2017). Central and southern Trinidad are underlain by Cretaceous to Pleistocene sedimentary rocks that have been folded and faulted by this compression forming the Central and Southern ranges. Both southern and central Trinidad display an obvious ENE structural and topographic trend that is also parallel to the Central Range Fault Zone (CRFZ) as seen in Figure 2-24.

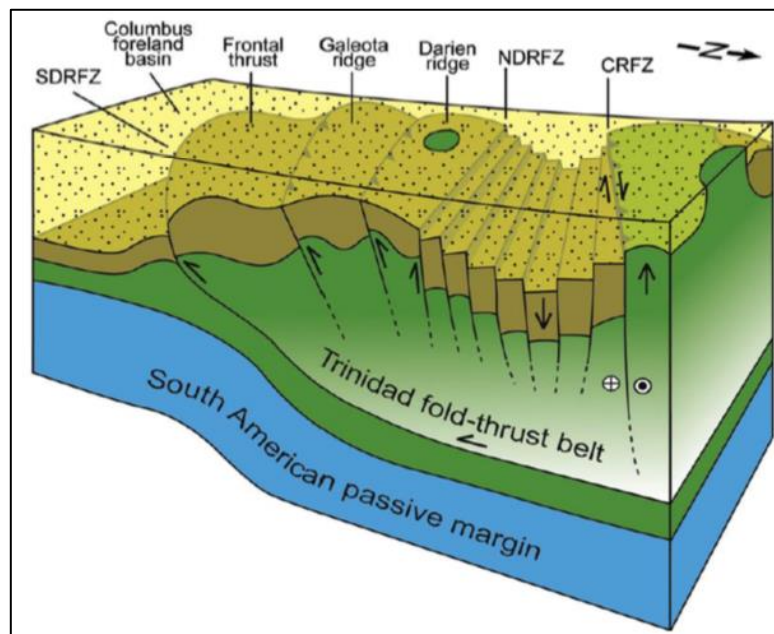


Figure 2-23: North-south cross section of Trinidad, faults and fold & thrust belt formed during a tectonic compression (Soto, Mann and Escalona 2011).

The currently morphology of Trinidad can best be described by models of classic orogenic belts that result from plate collision that a divided into two parts: internal core zones and external foreland zones. Internal core zones are composed of

regionally extensive metamorphosed rocks with basement involved reverse faults, similar to what is observed in the Northern Range. External zones well emulate the morphology scene across Central and Southern Trinidad where foreland basin sediments have been folded and faulted forming fold and thrust belts (Naparima-Nariva and Moruga-Guayaguayare fold belts) with a decline in intensity of deformation towards the craton.

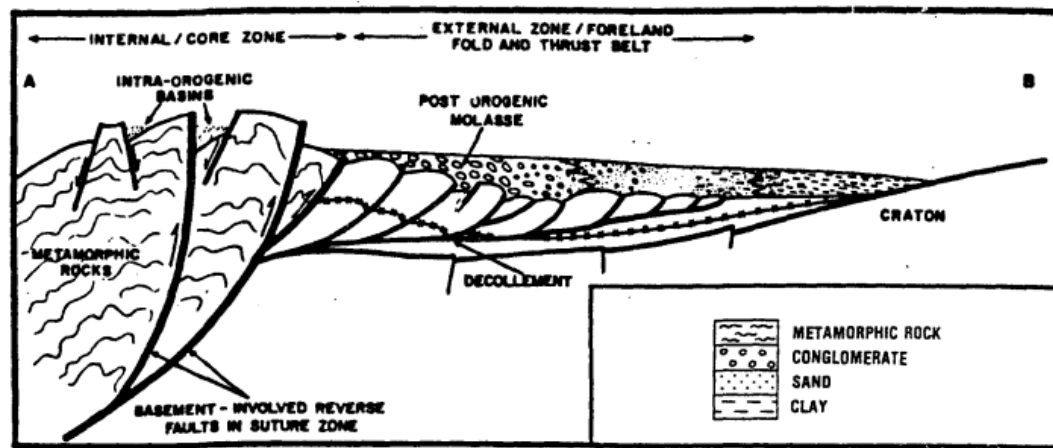


Figure 2-24: Orogenic belt cross-section analogous to Miocene collision that formed Northern Range (internal core) and fold and thrust belts (external zone) (Tyson, Babb and Dyer 1991).

2.6 Neotectonics of Trinidad

Throughout the tectonic evolution of the region, Trinidad currently exists in a period of translational movement which has existed since the late Neogene (Lingrey 2017). The island lies at conjunction and transition from convergence and subduction at the Lesser Antilles volcanic arc and the transform motion at the north section of the South American continent. The island itself lies along the plate boundary that separates the South American plate to the south from the Caribbean plate in the north.

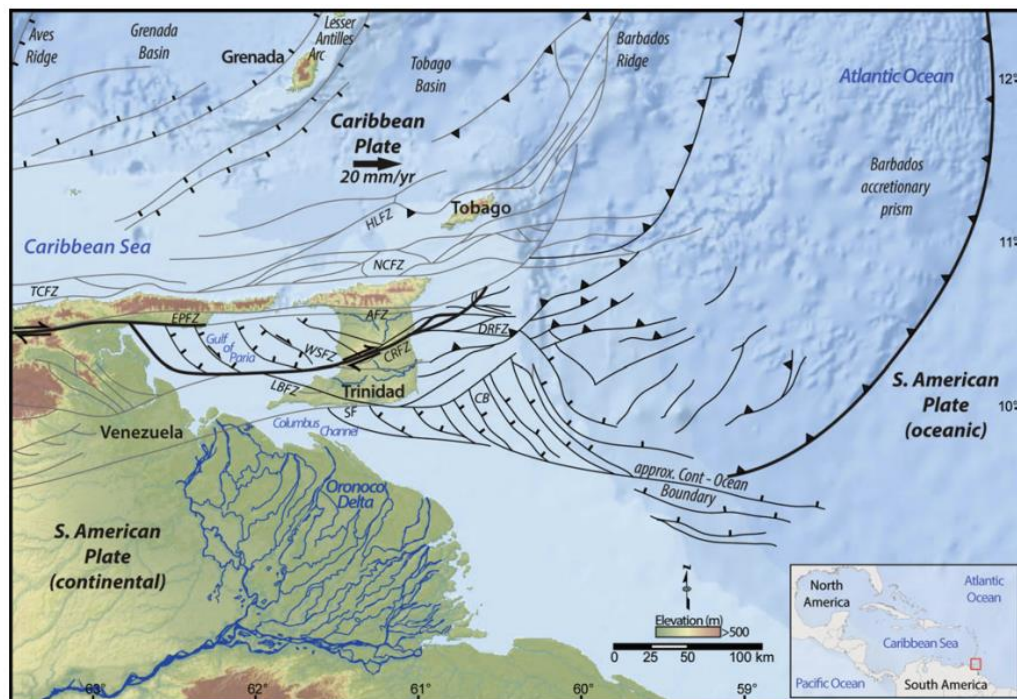


Figure 2-25: Present tectonic regime showing transform motion across NE Venezuela and Trinidad and subduction to the east of the Lesser Antilles (Arkle, Owen and Weber 2017)

Motion along this margin is transform in nature, where the Caribbean plate moves eastward at an average rate of 20 mm/year as estimated by plate models (MORVEL, NUVEL-1) (DeMets, Gordon and Argus 2010) and various GPS campaigns (Pérez, et al. 2001). Evidence of this active tectonism is not only revealed in the deformation of its static geodetic networks, but in natural phenomena including earthquakes and mud diapirism. Studies have shown that most of this motion is taken up across three main fault zones: the Arima, Central Range and Los Bajos fault zones.

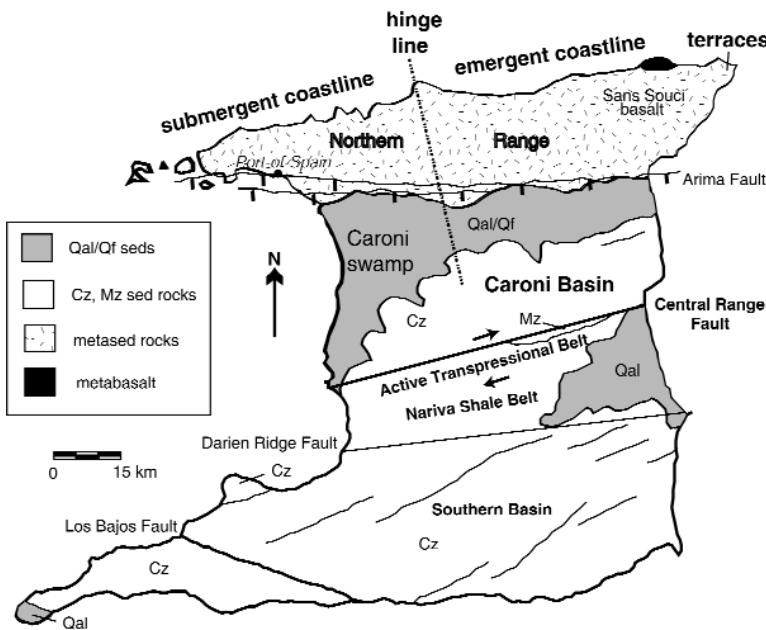


Figure 2-26: Map showing major geomorphic features across Trinidad transected by major fault zones (Weber 2005).

2.6.1 Arima Fault Zone

The El Pilar Fault Zone (EPFZ) is considered to be the prominent plate boundary between the Caribbean and South American plates in north-eastern Venezuela. It is a right-lateral strike slip fault that has a well-recorded history shallow seismicity triggered by motion along this fault zone (Figure 2-25). The Arima Fault Zone is believed to be the eastern extension of this El Pilar – San Sebastian Fault Zones in Trinidad. The AFZ is traverses the southern foothills of the Northern Range and represent the boundary from high relief, low-grade metamorphic rocks to lower relief sedimentary rocks that make up the rest of the island (Algar and Pindell 1993). Geodetic studies have proven that there has been statistically insignificant motion along this fault zone at a rate of 2.2 ± 1.8 mm/year (Weber et al. 2001), despite evidence of fault gouge along its trace. Differing lithologies on either side of this fault may have resulted in differential erosion which exposed this fault trace at the surface. It has been interpreted that motion along the El Pilar fault zone is translated across the Gulf of Paria towards the Warm Springs fault offshore Trinidad and

continues eastward into onshore Central Range Fault Zone which accommodates the majority of plate motion in this area (Babb and Mann 1999).

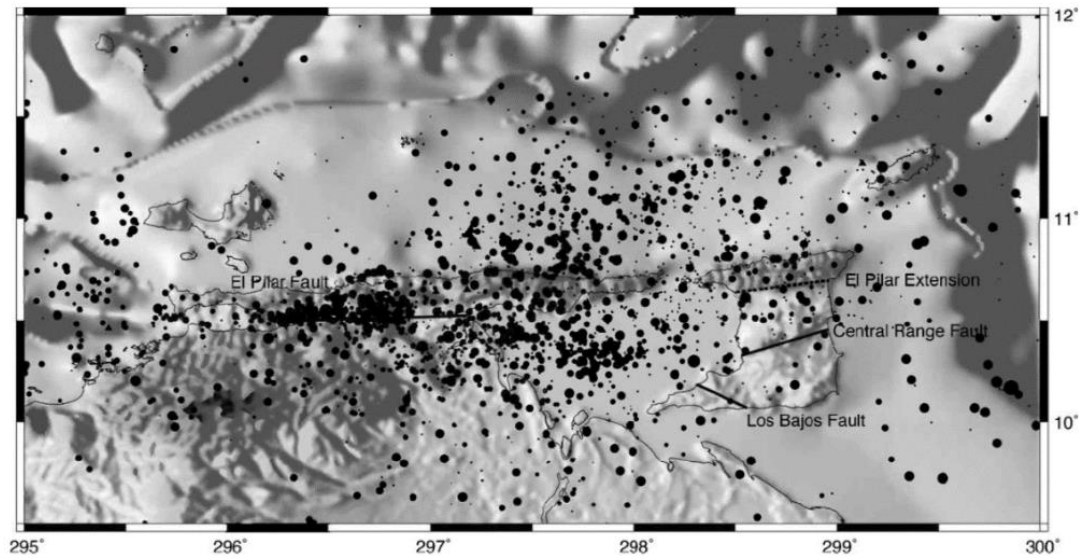


Figure 2-27: Shallow seismic events between 1910 and 2000 across Trinidad and NE Venezuela (Weber et al. 2011).

2.6.2 Central Range Fault Zone

The Central Range Fault is considered unanimously considered to represent the plate boundary between the Caribbean and South American plates across Trinidad. As previously mentioned, this boundary generally strikes eastward across north-eastern Venezuela, just south of the Cordillera de la Costa, steps across the Gulf of Paria, then strikes ENE through central Trinidad as the Central Range Fault Zone (CRFZ). It is a right lateral strike-slip fault across which there is an estimated 12 – 15 mm/year of motion accommodated (Weber et al. 2001, Weber et al. 2011). At this fault, the southern half of Trinidad is moving relatively western with the South American plate, while the north half of Trinidad is moving eastward with the Caribbean plate.

Onshore, the fault crosses the width of the island across an expanse of over 50 km, with an ENE strike of 72° and has left a noticeable scar across the topography of the Central Range (Arkle, Owen and Weber 2017). Occasionally the topographic signature of this fault zone is difficult to identify given the high rates of erosion and

weathering associated with tropical climate, soft shale lithology and significant modifications to the surface due to large-scale agricultural practices (Crosby, et al. 2009). Linear drainage patterns, troughs, shutter ridges and scarps that share a similar trend to the fault are some examples of the faults surface expression.

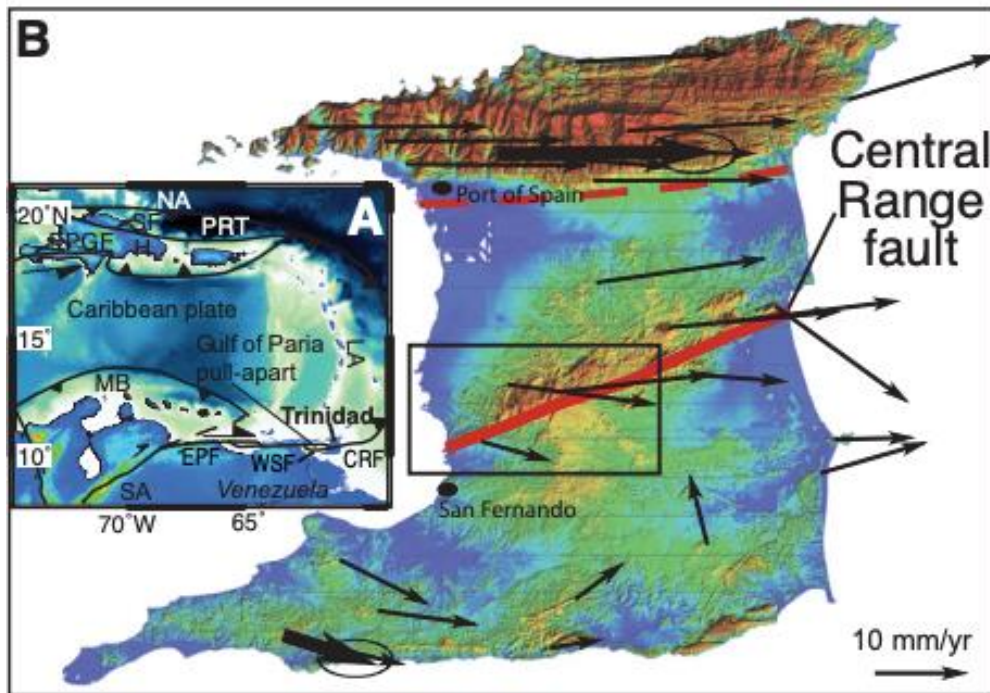


Figure 2-28: Location of Central Range Fault (bold red) and horizontal velocities estimated from GPS campaigns.

While evidence of this fault can be seen from both topography and geodetic studies, where it has been proven to account for 60% of the right-lateral of 20 mm/year movement between plates, its offshore extension was initially less understood. Both 2D and 3D seismic campaigns were conducted in the offshore Block 2ab over an area of 60 km by 30 km to investigate the structural geology and tectonic controls of the CRFZ on stratigraphy in the area. Processed data proved that the Central Range fault extends eastward into the Atlantic Ocean for another 60km (Soto, et al. 2007). Offsets in mapped paleo-fluvial channels and shelf sediments portray a slip rate of 17-19 mm/year along this fault zone (Soto, Mann and Escalona 2011) which is almost comparable with onshore estimates. Eventually the fault merges with other

faults and structures, transitioning into the compressive regime associated with plate convergence and subduction.

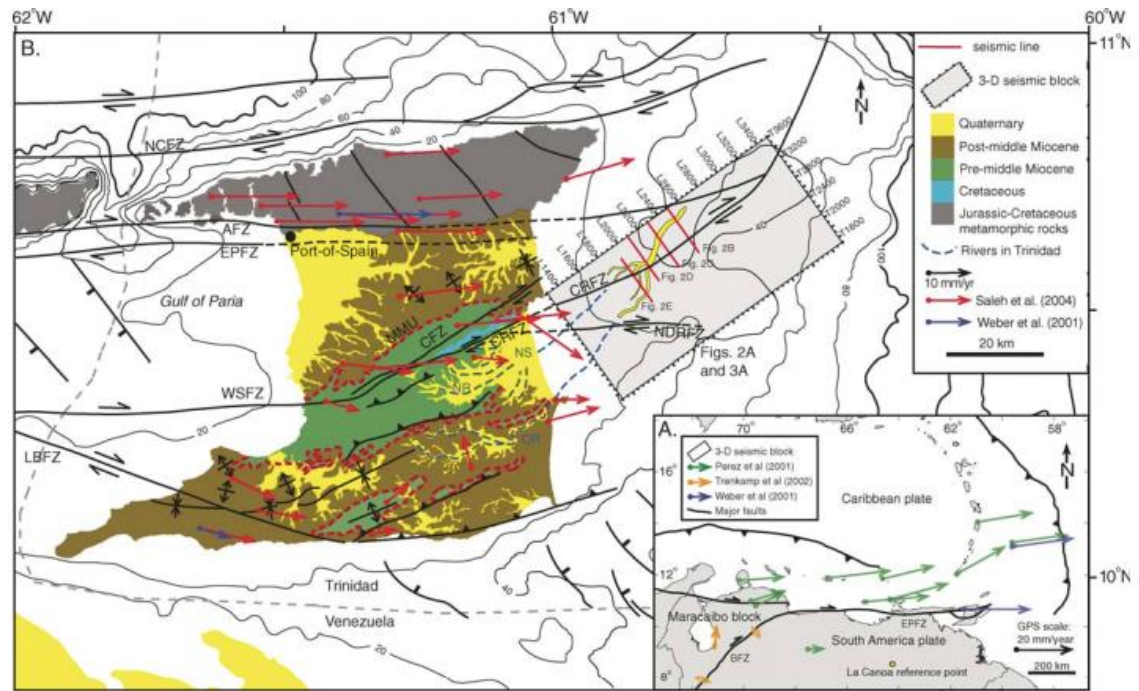


Figure 2-29: Tectonic setting of Trinidad with various estimate horizontal velocities and delineated offshore seismic survey (box) conducted to explore offshore extension of CRFZ (Soto, et al. 2007).

The Central Range fault is also considered to be a potentially seismogenic and hazardous fault system that developed during the Holocene. Paleo-seismic and geomorphic data has provided evidence that at least one major earthquake has occurred along fault zone between 550 and 2710 years ago (Prentice, et al. 2010). Given the estimate slip rates of 12-15 mm/year, if applied across a period of 550 years, strain energy equivalent to a slip of 4.9 m is available for release, the equivalent of a M 7.0 earthquake. However, there has not been any significant earthquake activity along the fault since then and the fault is considered capable of producing large earthquakes in the future (Soto, et al. 2007).

2.6.3 Los Bajos Fault Zone (LBFZ)

The Los Bajos fault is a major fault that transects across south-western Trinidad and whose surface expression can easily be seen in topographic maps. Its onshore expression begins at Point Fortin along the western coastline and terminates 33 km away near Negra Point along the southern coastline. It is a right-lateral strike slip fault along which there has been a total of 10.4 km of displacement (Archie and Gallai-Ragobar 2016), based on separation of lithological formations. The fault zone also acts as a major migration pathway and trapping mechanism for hydrocarbons with the development of multiple oil fields in the area and over 3000 wells drilled. Well logs proximal to the fault zone assist in understanding its structure and potential deformation.

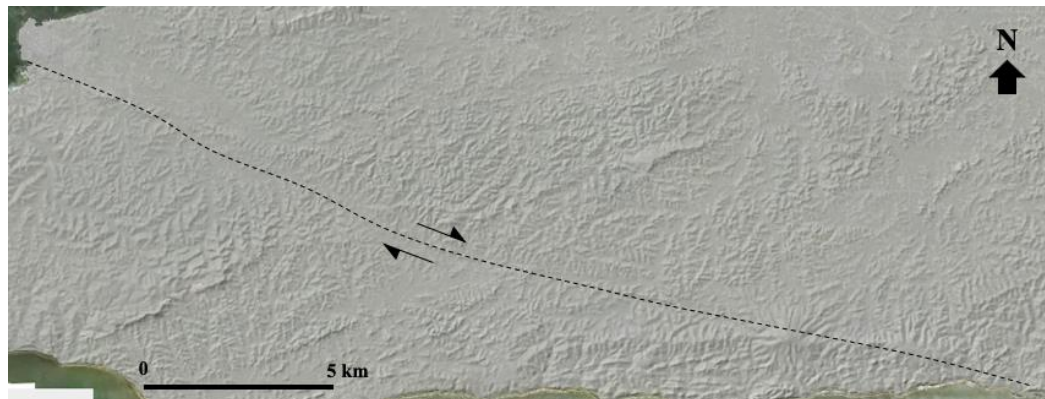


Figure 2-30: Surface trace of Los Bajos fault across topography as depicted in 2014 LIDAR campaign.

Various studies are inconclusive on whether or not the LBFZ is active or not, or if active, unsure at what rates motion is presently occurring. This ambiguity stems from the lack of geodetic monuments across the fault zone from which estimates of horizontal deformation can be executed. Modeled tectonic deformation in the area has suggested that 2 mm/year of slip occurs along Los Bajos, with an additional 6 mm/year occurring along faults in the southern offshore (Koch 1987). Given the 20 mm/year slip rate estimated between the Caribbean and South American plates, studies suggest that 5 mm/year may be accommodated across the LBFZ, if 15 mm/year is already accommodated across the CRFZ, given the additional inactivity of the Arima Fault Zone (Rodriguez, Weber and Shmalzle 2008).

2.7 Halliburton Geophysical Survey

Halliburton Geophysical Services Incorporated (HGS) was contracted by Exxon Mobil Corporation in 1990 to conduct a seismic program across onshore Trinidad for the purpose of oil and gas exploration (HGS 1991). Prior to conducting this program, both horizontal and vertical control was needed for proposed seismic lines. Control points were established across the island of Trinidad, with a greater density across south and central Trinidad where most known oil and gas accumulation existed. Fewer stations were established north of the Central Range where control was not needed. Included in the established 117 control points were:

- 4 Defense Mapping Agency Doppler Stations
- 3 Trigonometric Stations
- 10 Bench Marks
- 100 Seismic Line Control Stations

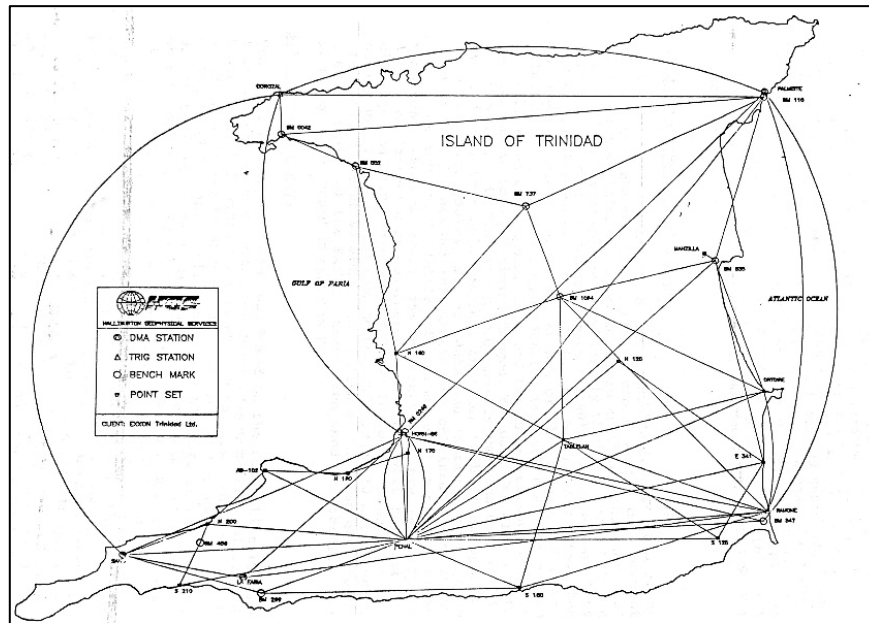


Figure 2-31: Primary network of control stations used to provide survey control for seismic surveys.

Stations were preferentially located in areas with minimal vegetative cover that were also easily accessible. GPS monuments at each station consisted of a 1.5 m long

concrete cylinders that were securely cemented into the ground, at the top of which was a circular aluminium cap that was 8 inches in diameter. Engraved in each cap was its unique identifier number in the form of “TDST-XXXX). Marker posts were installed 2.5 away from these monuments as a means of identifying their general location, especially in forest areas where vegetation overgrowth is common. Several wells were also used as seismic line control stations to tie seismic data to borehole log data obtained from these wells.

Using all these control points a country-wide GPS survey was conducted to obtain coordinates of these control sites and provide geodetic control for these proposed seismic surveys. GPS observation were conducted using Navstar TI-4100 dual-frequency, single channel receivers and associated equipment (HGS 1991).

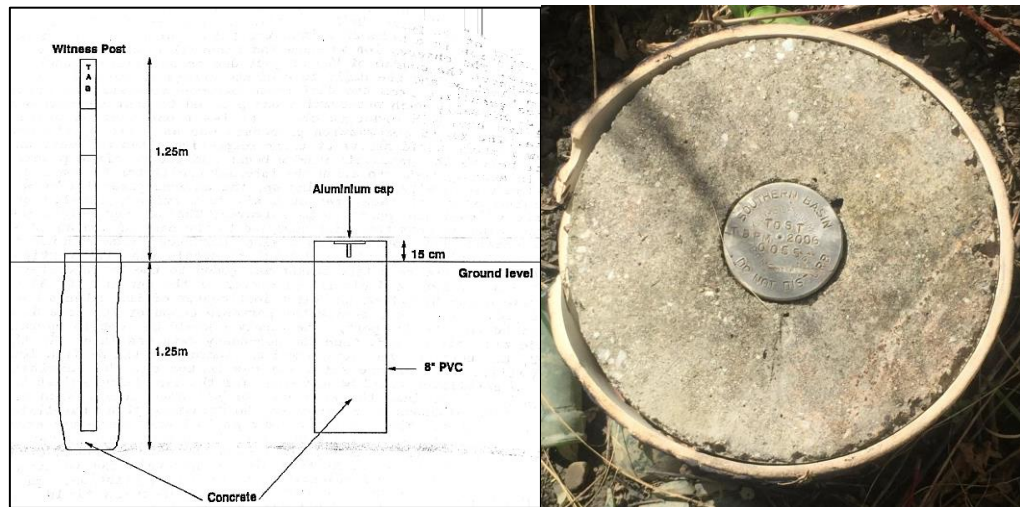


Figure 2-32: (left) Witness post and monument dimensions and (right) Aluminum cap set in concrete for TDST 0055 (Los Iros)

Upon using the GPS constellation in the survey, final coordinates were initially reported in WGS84 then transformed to the Naparima 1955 datum which was widely used across Trinidad at the time. This transformation was accomplished using parameters established from DMA Doppler stations which had known Naparima coordinates at the time. Station coordinates (see Appendix A) and witness diagrams (Figure 2-23) were included in the Final Geodetic Report by Halliburton.

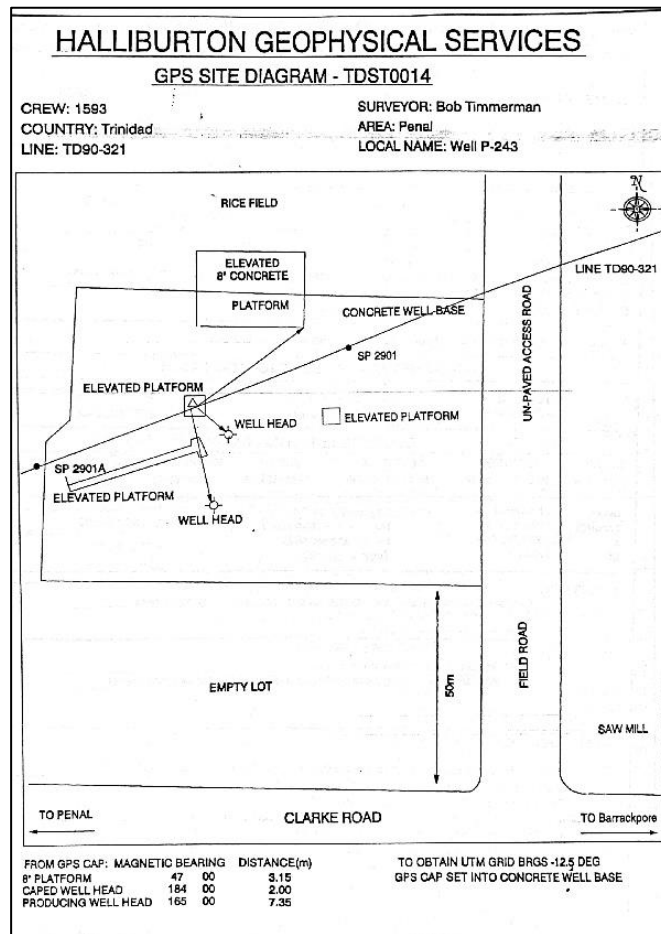


Figure 2-33: Witness diagram for TDST 0014

The deformation models associated with semi-dynamic datums covered in Section 2.4 are all estimated based on continuous or intermittent observation at stations including CORS, geodetic monuments, trigonometric stations, etc. The control stations established by Halliburton provide an ideal means of establishing a local relative deformation model given its distribution across the country and previously estimated coordinates using GPS in 1990. Reobservation of these monuments will shed light on the scale of displacement that has occurred over time due to tectonic deformation, from which relative velocities and a deformation model can be developed.

2.8 Assessment

The dynamic processes associated with plate tectonics are ever present across Trinidad as evidenced by slip along the Central Range fault and geodetically estimated velocities across the island (Saleh, et al. 2004, Weber et al. 2001). With this deformation, traditional, static geodetic datums and reference frames, including the widely used Naparima 1955 datum (Wilson 2000) are affected as well. These datums can no longer provide the accuracy and precision needed by the survey and mapping community, and should be replaced by a modern geodetic datum that accounts for surface deformation.

Semi-dynamic datums may prove to be a suitable candidate as they provide of means of working within a static datum at a single reference epoch while translating spatial data acquired at other epochs through the use of a deformation model (Denys, Winefield and Jordan 2007). In addition to being more realistic to implement, these datums are more user-friendly. Development of a deformation model is completely achievable through repeated or continuous GPS observation of geodetic monuments and GPS stations across a given area (Shariff, et al. 2017, Cayapan 2016, Abidin, et al. 2015, Blick and Donnelly 2016).

Previous studies have conducted GPS observations of old geodetic monuments (Saleh, et al. 2004) and additional observation of newly established points (Weber et al. 2011) to estimate horizontal deformation rates across the island. These studies, however, did not include any of the survey monuments established by Haliburton Geophysical Services; sites which are more widely distributed across Trinidad. GPS re-observation and estimation of site velocities can be accomplished using this network of survey monuments to develop a potential relative deformation model for Trinidad and be used towards semi-dynamic datum implementation for the island.

3 INVESTIGATIVE PROCEDURES

Complementing the research conducted on geodetic datums, the following methodology was employed to best discern the nature of horizontal deformation across the island of Trinidad. This approach required a combination of field work, data processing and an understanding of local tectonics to execute the core objectives identified in Section 1.4; each of which is outlined in the following sections.

3.1 Monument Identification & Selection

Coordinates for each geodetic monument included in a geodetic control survey conducted by Haliburton were recorded and included in the Final Geodetic Report (HGS 1991). With these coordinates referenced to WGS 84 (computed relative to ITRF 89), all 118 monuments were plotted in Google Earth for further observation and scrutiny using the various vintages of satellite imagery available.

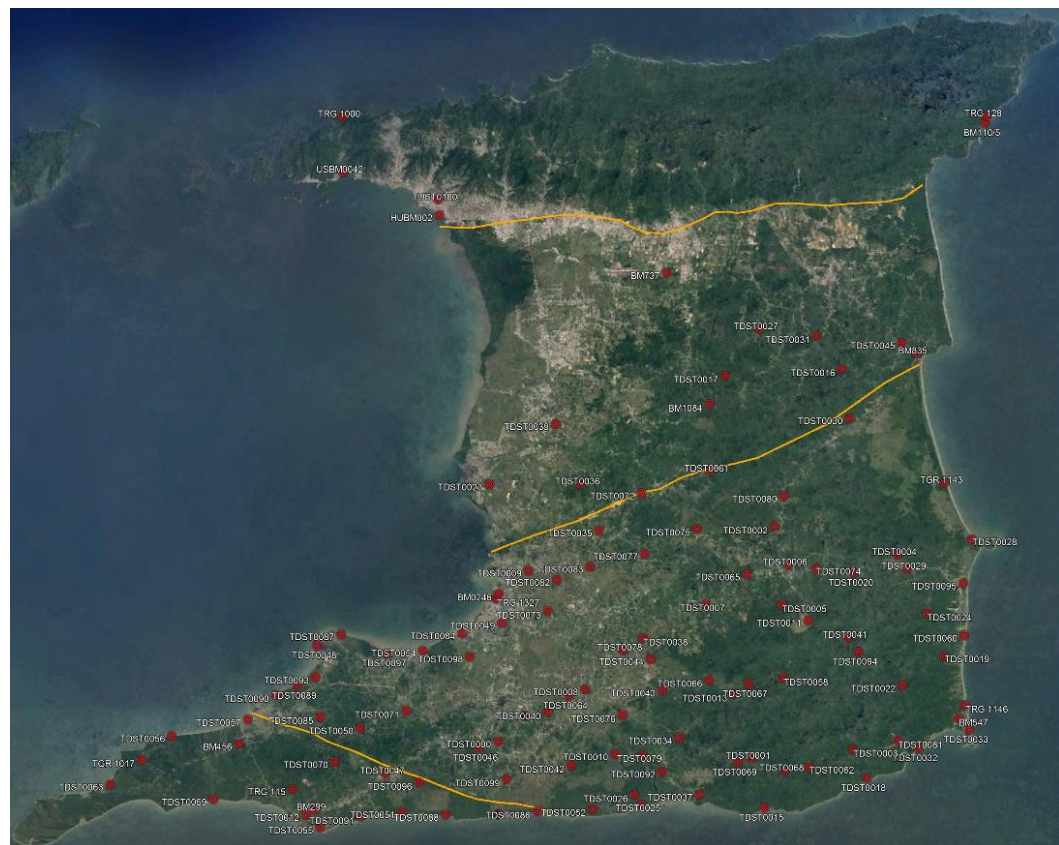


Figure 3-1: Geographic distribution of Haliburton geodetic monuments (red) across Trinidad relative to major fault zones (yellow).

As observed in Figure 4-1, central and southern Trinidad have the highest density of these geodetic monuments. These monuments were established to provide solid geodetic control for seismic surveys; a critical component in oil and gas exploration that is common in these areas. Once plotted, the immediate environments surrounding each monument was observed using Google Earth's satellite imagery. Monuments were deemed unfit for further investigation and omitted based on the following conditions:

- Sea / river reclamation.
- Lack of access road / restricted access.
- Overhead high-tension cables (source of noise).
- Possible destruction or poor satellite visibility introduced by urban sprawl / development.

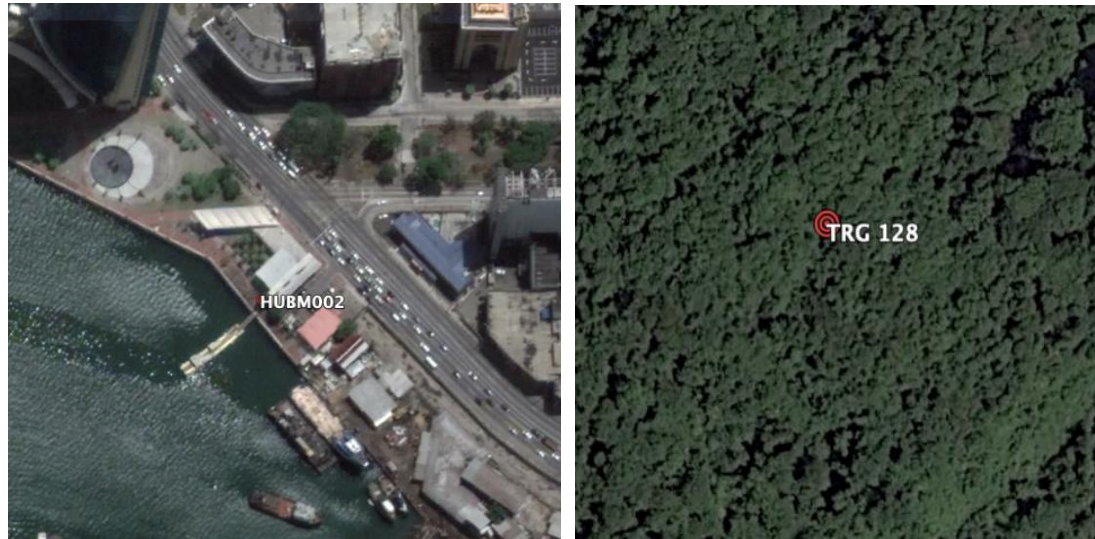


Figure 3-2: Left - Monument HUBM002 likely destroyed my waterfront development in Port of Spain, Right - Monument TRG 128 located deep in forest; inaccessible and proximal to high tension power lines.

From the remaining set, candidate monuments were chosen across the island, with sufficient monuments chosen on either side of the major fault zones. This was done to estimate both the nature of horizontal deformation across the island and the magnitude of displacement that may be occurring across these major faults, using

static GPS observations. Reconnaissance missions were then undertaken with the aid of technical staff from the UWI Department of Geomatics Engineering & Land Management, to physically locate these remaining monuments. These field exercises were conducted in the months preceding GPS observation each year and facilitated using handheld GPS devices and witness diagrams included in the Final Geodetic Report. Once located, the path and site surrounding each geodetic marker was cleared of excess vegetation to allow for ease of access and equipment setup. In some instances, permission was required from land-owners and organisations to access markers as they were established on private property. Despite this, the number of available markers varied among the years in which observations were conducted due to time and manpower restrictions. WGS 84 Coordinates for each listed monument can be found in Appendix A.

Monument #	Label	Location	2014	2015	2016	2017
BM 457	G	Guayaguayare	✓		✓	
TDST 0005	H	Rio Claro	✓			
TDST 0009	E	Gasparillo	✓	✓	✓	✓
TDST 0014	P	Penal	✓	✓	✓	✓
TDST 0029	F	Mayaro	✓	✓	✓	
TDST 0039	B	Freeport	✓	✓	✓	✓
TDST 0045	C	Manzanilla	✓		✓	✓
TDST 0050	M	Forest Reserve	✓			
TDST 0052	K	La Lune				✓
TDST 0055	N	Los Iros	✓	✓	✓	✓
TDST 0061	D	Navet Dam	✓	✓	✓	✓
TDST 0063	O	Cedros	✓			✓
TDST 0066	J	Saunders Trace				✓
TDST 0067	I	Catshill				✓
TDST 0097	L	Rousillac	✓			✓
USMB 0042	A	Chaguaramas	✓	✓		✓
Total # Markers			13	7	8	12

Table 3-1: List of available monuments by year from which GPS observations were conducted.

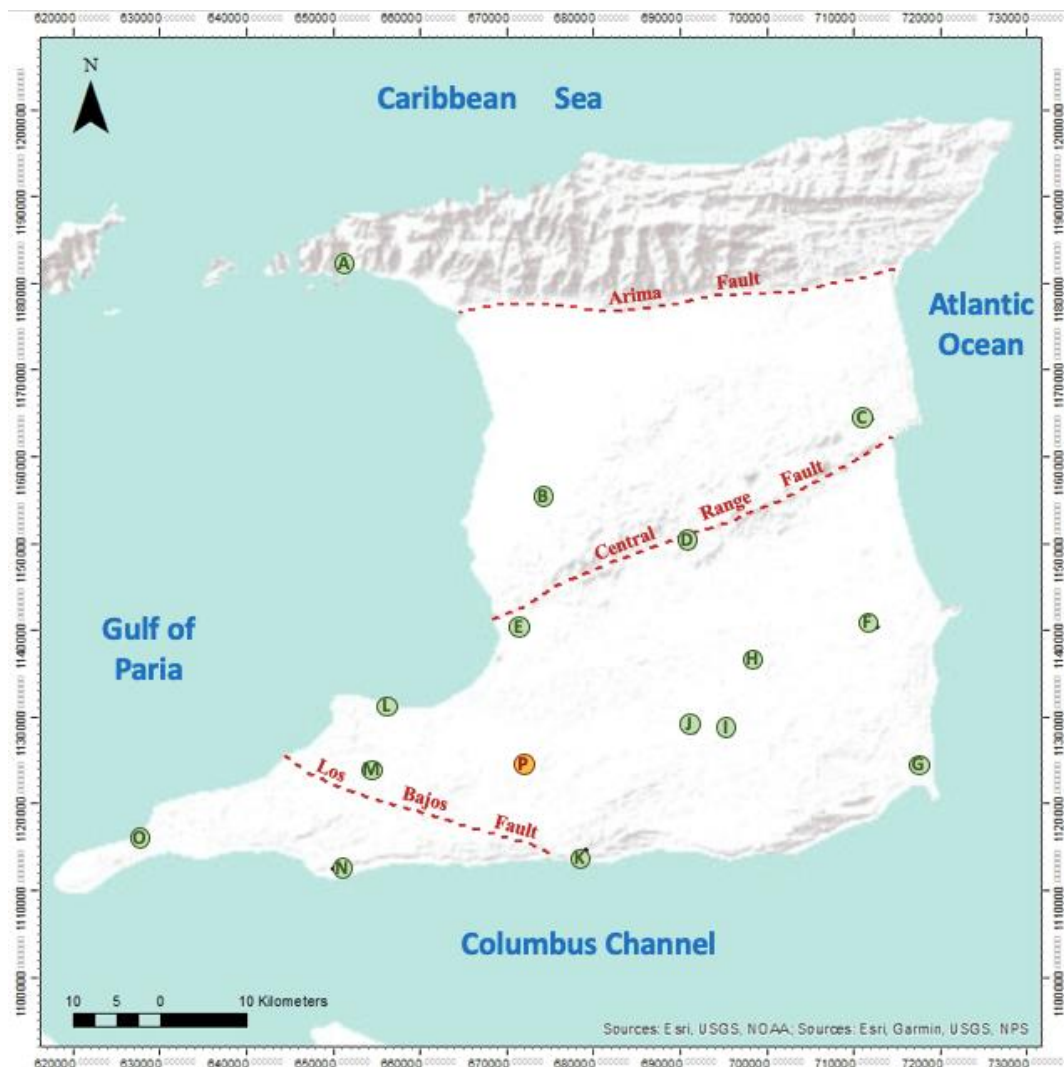


Figure 3-3: Geographic distribution of re-observed sites across Trinidad.

3.2 Data Acquisition via Static GPS Surveying

As the geodetic monument sites were scattered across the island, it was impossible to obtain observations at all sites simultaneously, due to limited equipment and manpower. Consequently, site visits were broken up across multiple days each year and final year Geomatics students assisted in data collection at each monument, making simultaneous observations at all stations possible on a daily basis. The data collected each year was also used towards these students' semester coursework.

Year	Day 1	Day 2	Day 3
2014	October 17th	October 20th	-
2015	October 5th	October 8th	-
2016	October 13th	October 14th	-
2017	October 9th	October 12th	October 16th

Table 3-2: Observation days by year.

Various geodetic grade GPS devices were employed in this study, including a range of Trimble and Leica devices, some of which were on loan from the Lands & Surveys Division. A complete list of devices and antennae used at individual monuments for each year can be found in Appendix B. Once antennae were attached to tripods, they were levelled over the monument caps, following which at least three slope height measurements were taken from the monument cap to the bottom of the antenna or to its centre bumper, depending on the antenna model. At least 4 hours of simultaneous observations were required to accurately obtain monument positions by simultaneous observations using as many points as could be handled with observer and equipment available. This was achieved by having the last group to set up inform all remaining group on when to commence and terminate data logging on each day. Each group was also responsible for sketching witness diagrams of the antenna setup, in addition to making note to any disruption in data logging that may have been caused by equipment or power failure. Heights to antennae were remeasured once logging was completed.



Figure 3-4: Leica GS14 antenna mounted atop tripod over TDST 0014 (Penal).

3.3 Acquiring & Formatting CORS Data

RINEX files from four local Continuously Operating Reference Stations (CORS) were downloaded to establish a primary control framework in which potential monument migration can be estimated. Ten days of 24-hour RINEX data that coincided with the field observation period across each year were downloaded and included data from all 4 stations: Albion (ALBN), Point Fortin (FRTN), Point Galeota (GLTA) and Sangre Grande (GRND). To provide additional control for data acquired in 2016, additional data was downloaded from three newly installed local UNAVCO sites at the University of the West Indies (TTUW), San Fernando (TTSF) and Toco (CN45) shown in Figure 4.4. This compensated for the downtime experienced by FRTN, which was undergoing repairs at this time.



Figure 3-5 Location of TT and UNAVCO CORS across Trinidad

Pre-processing and parsing of data within these RINEX files were accomplished using an executable DOS-based programme called *teqc*, a GNSS toolkit developed by UNAVCO that allows users to manipulate RINEX data and generate outputs that meets the users' particular needs (Estey and Meertens 1999). Such manipulations include the removal of data from satellite constellations of GLONASS, GALLILEO and COMPASS. GLONASS is useful when conducting real time kinetic (RTK) surveys where more satellites offer faster lock and increased redundancy, but do not offer the same benefits in static surveys. They are removed from data files due to previously observed incompatibilities with GPS, resulting in reduced solution accuracy while conducting static observations. These incompatibilities stem from differences in geodetics datums, where GLONASS employs PZ90 and GPS uses WGS84. Final ephemerides are also less precise for GLONASS (5-15 cm) than they are for GPS (2-5 cm) (Wanninger and Wallstab-Frietag 2007). Additionally, recently introduced GPS codes and frequencies including C2 and L5 are omitted as

they are not recognized by the processing software, Total Trimble Control (TTC), which was developed prior to their introduction. Consequently, the following signals are retained for processing GPS data in TTC:

- C1: binary Coarse Acquisition (C/A) code used to uniquely identify satellites.
- L1 & L2: carrier frequencies which transmit ranging codes and navigation data and offer the final carrier phase solutions for geodetic surveys.
- P2: pseudo-range noise (PRN) code that identifies which satellites signals are received from and assists in estimating receiver-satellite distance.

Function	Code
Strip GLONASS Satellites & ephemeris.	teqc -R rinex_in.18o > rinex_out.18o
Decimate to 30 second epochs.	teqc -O.dec 30 rinex_in.18o > rinex_out.18o
Keep specific phases and signals (C1, L1, L2, P2)	teqc -O.obs C1+L1+L2+P2 rinex_in.18o > rinex_out.18o
Catenate multiple obs. and nav. files into one.	teqc rinex1.18o rinex2.18o rinex3.18o > rinex_final.18o
Perform quality check.	teqc +qc rinex_in.18o

Table 3-3: List of teqc commands used to pre-process observation and navigation files.

3.4 Establishing Primary Control in ITRF 2014

Establishing primary control is necessary to assign coordinates to observed monuments across Trinidad and to identify any potential change in these coordinates between the various observation periods. In similar studies, primary control is typically established in an International Terrestrial Reference Frame (ITRF) as most processing software produces coordinates in such a frame. In this project, primary control was established in ITRF2014 and was accomplished using data from the six previously mentioned local CORS sites. RINEX data for each observation day was simultaneously submitted to a free and open-access processing website known as AUSPOS to generate ITRF coordinates for each CORS station.

Created by Geoscience Australia, AUSPOS makes use of a high precision orbit and geodetic parameter determination software known was Bernese Software System. It also makes use of orientation parameters and coordinate solution products provided by the International GPS Service (IGS) (Dawson, Govind and Manning 2001). It makes uses of the 15 closest IGS stations to accurately estimate the ITRF2014 XYZ Coordinates for each CORS site. Generated coordinates for each CORS is then averaged and used as control coordinates for these sites in Trimble Total Control (see Appendix C).

3.5 Establishing Secondary Control in ITRF 2014.

Following establishment of primary control in ITRF 2014 through the use of both TT and UNAVCO CORS, GPS-baselines were processed for observed monuments using Trimble Total Control (TTC). In addition to importing the primary control established by CORS, TTC also makes use of precise ephemerides and clock corrections to estimate real-time satellite position for use in navigation solutions, improving the accuracy of GPS based positioning (Warren and Racquet 2003). Ionospheric models provide an additional level of error reduction by accounting for

the effects of charged particles in the upper atmosphere on GPS signals (McCaffre, et al. 2018).

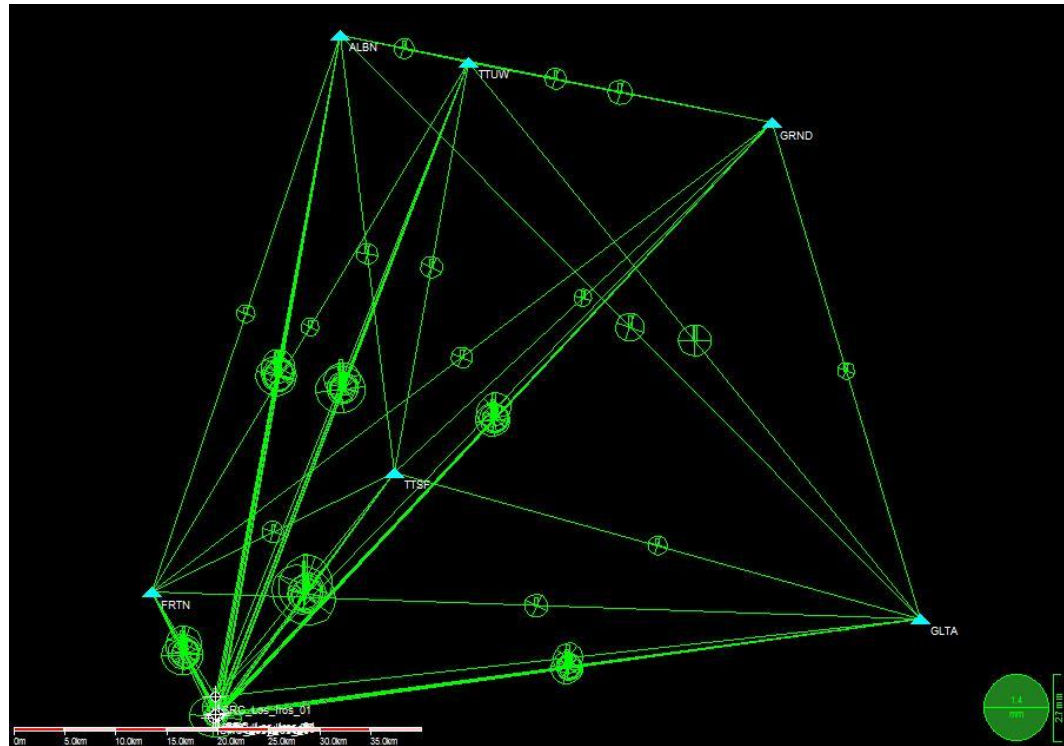


Figure 3-6: Processed baselined in Trimble Total Control

Both CORS and observed monument files were imported into TTC, along with their respective antennae metadata (height and model), prior to processing. Project settings were set to disable GLONASS satellites and register observations as static and captured at 30 second epochs. Once processed, baselines were examined for anomalies and disabled if deemed too anomalous, then least-squares adjusted to achieve consistency and quality control through redundancy to produce ITRF2014 coordinates (95% confidence).

3.6 Transformation to ENU

Adjusted coordinates are reported in ITRF2014, an Earth-Centred, Earth-Fixed (ECEF) coordinate system, however, this coordinate system is not ideal for interpreting motion at the Earth's surface in horizontal and vertical components. A Cartesian coordinate system is employed where the horizontal axes are tangential to

the Earth's surface at the area of interest with directions East and North. This is not a projection, such as Mercator or Lambert, but a translation and rotation of the ECEF as shown in Figure ???. Conversion of the changes in ECEF coordinates to the changes in Cartesian coordinates for each station will provide an estimate of monument displacement across Trinidad horizontally and vertically. This conversion involves a process of three computations (see Figure 4-3), that was executed for the change in monument coordinates for the period of 1990 – 2014, 1990 – 2015, 1990 – 2016 and 1990 – 2017.

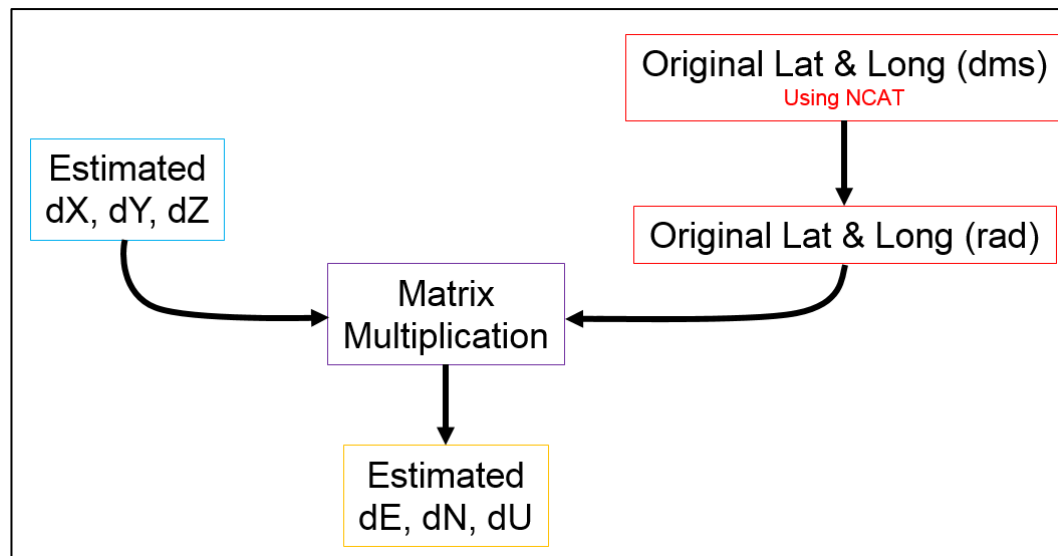


Figure 3-7: Process flowchart for estimating dE , dN , dU .

Where:

- dX, dY, dZ : difference in adjusted coordinates for each monument.
- Station Latitude and Longitude for each day are computed from their XYZ Coordinates using NGS' Coordinate Conversion and Transformation Tool (NCAT).
- Conversion to dE, dN, dU is accomplished using a Matrix Multiplication (see below).

$$\begin{bmatrix} E \\ N \\ U \end{bmatrix} = \begin{bmatrix} -\sin \lambda & \cos \lambda & 0 \\ -\cos \lambda \sin \varphi & -\sin \lambda \sin \varphi & \cos \varphi \\ \cos \lambda \cos \varphi & \sin \lambda \cos \varphi & \sin \varphi \end{bmatrix} \begin{bmatrix} x_p - x_o \\ y_p - y_o \\ z_p - z_o \end{bmatrix}$$

*Figure 3-8: Matrix Multiplication to estimate ENU (Drake 2002) where:
 λ - original latitude in radians, φ - original longitude in radians
 x_p, y_p, z_p - Present ECEF Coordinates, x_o, y_o, z_o - Original ECEF Coordinates
 E, N, U - displacements in Cartesian plane*

3.7 Nominal Reference Station Selection

Semi-dynamic datums employ relative deformation models based on an international frame of reference. These incorporate the relative velocities of monuments across the applicable area, for propagation of coordinate data to a common epoch for observation and decision making (Ogutcu 2018). The relative velocities are estimated by comparing the velocities of all monuments to a site that is preferably a great distance away from any known area of deformation. For horizontal deformation studies across Trinidad, velocities are common compared to a site on the South American continent. Given the limited access to international site data, a local monument from which observations were taken was chosen as an alternate.

This station will act as the nominal reference station and will be considered as being relatively “stable”, with an assigned relative velocity of 0 mm/year. As this station will act as the reference station across all years of observation and comparison, it must exist in a zone that has experience negligible seismicity, at risk of introducing a component of horizontal deformation, resulting in false estimates.

Using earthquake epicentral data provided by the UWI Seismic Research Centre, earthquake events between October 1990 and October 2017 were mapped to observe their distribution and to identify a candidate reference station (see Appendix D). Quick observations of these maps show that there are obvious areas where

seismicity is common including shallow earthquakes along the El Pilar Fault Zone at the Paria Peninsula in Venezuela, in addition to deep earthquakes caused by the subducted South American Plate. Given this, TDST 0014 (Penal) was chosen as the reference station across all observation periods as this area as experienced relatively less seismicity and smaller magnitude earthquakes.

3.8 Vector Computation

Once the change in Easting (dE) and Northing (dN) for each monument is estimated, relative displacements can then be calculated for each time interval. These relative displacements are based on comparing the net displacement of one monument to the net displacement of the nominal reference station, TDST0014 (Penal), using the following formula:

$$\begin{aligned} dE_{stn} - dE_{PENAL} &= \Delta E_{stn} \\ dN_{stn} - dN_{PENAL} &= \Delta N_{stn} \end{aligned}$$

The two components of relative horizontal displacement, ΔE and ΔN , were then resolved into a single estimate of relative velocity using the following equation:

$$\text{Relative Horizontal Velocity (mm/year)} = (\sqrt{\Delta E^2 + \Delta N^2}) / \Delta t$$

Where: Δt is the time difference between observation periods and $\Delta t = 24$ (1990 – 2014), 25 (1990 – 2015), 26 (1990 – 2016), 27 (1990 – 2017)

Azimuth associated with horizontal deformation is also estimated from the resolved vectors. It is measured in degrees relative to cardinal west in an anticlockwise direction and is estimated according to:

$$\text{Azimuth } (^{\circ}) = \text{Arctan } (\Delta N / \Delta E)$$

Direction was then converted to azimuth (relative to cardinal north) and is dependent on which quadrant direction angles fell into (see Table 3-2). A complete list of absolute and relative velocities can be found in Section 4.

ΔE	ΔN	Quadrant	Direction
+ ve	+ ve	1	90 - d
+ ve	- ve	2	90 + d
- ve	- ve	3	270 - d
- ve	+ ve	4	270 + d

Table 3-4: Estimating Direction from Azimuth

4 PROJECT FINDINGS

Deformation models are presented to depict the relative velocities (speed and direction) of geodetic monuments across Trinidad for the periods of 1990 – 2014, 1990 – 2015, 1990 – 2016 and 1990 – 2017. These were constructed using the adjusted ITRF2014 coordinates generated by Trimble Total Control (see Appendix E), from which net and relative displacements across the multi-year periods were estimated. An average relative deformation model was also generated, which represents the overall trends and velocities attained during the various re-observation periods.

In these deformation maps, individual monuments are denoted by letters according to:

A	Chagaramas
B	Freeport
C	Manzanilla
D	Navet
E	Gasparillo
F	Mayaro
G	Guayaguayare
H	Rio Claro
I	Catshill
J	Saunders Trace
K	La Lune
L	Rousillac
M	Forest Reserve
N	Los Iros
O	Cedros
P	Penal *

Table 4-1: Geodetic monument labels for Relative Deformation Models.

Note:

* Penal is designated as the nominal reference station due to constant re-observation between 2014 and 2017 and low seismicity.

4.1 Displacements & Relative Deformation Model: 1990 -2014

Station	dE (m)	dN (m)	ΔE (m)	ΔN (m)	2D Displacement 24 years (m)	Speed (mm/yr)	Accuracy \pm (mm/yr)	Direction (deg)
Chaguaramas	0.206	0.606	0.406	0.007	0.406	16.9	2.1	89
Freeport	0.090	0.748	0.290	0.149	0.326	13.6	2.1	63
Manzanilla	0.114	0.536	0.314	-0.063	0.320	13.3	1.8	101
Navet	-0.075	0.571	0.125	-0.028	0.128	5.3	1.2	103
Gasparillo	-0.118	0.587	0.082	-0.012	0.083	3.5	1.3	98
Rio Claro	-0.107	0.563	0.093	-0.036	0.100	4.2	1.5	111
Guayaguayare	-0.115	0.526	0.085	-0.073	0.112	4.7	1.8	131
Mayaro	0.036	0.571	0.236	-0.028	0.238	9.9	2.2	97
Forest Reserve	-0.116	0.438	0.084	-0.161	0.182	7.6	2.4	152
Rousillac	-0.016	0.659	0.184	0.060	0.194	8.1	2.0	72
Penal	-0.200	0.599	0.000	0.000	0.000	0.0	0.0	0
Los Iros	-0.504	0.463	-0.304	-0.136	0.333	13.9	1.9	246

Table 4-2: Displacements and Annual Relative Velocities for 1990-2014.

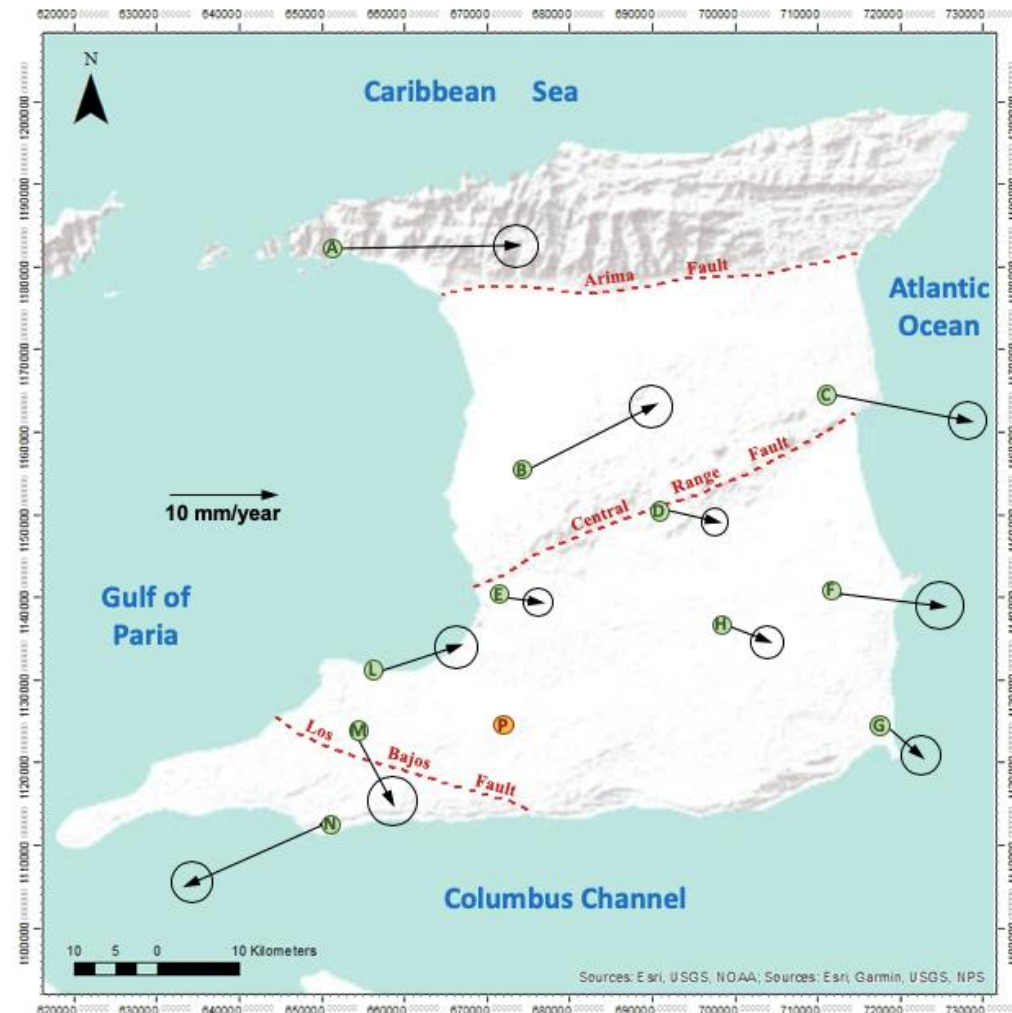


Figure 4-1: Relative Deformation Model for 1990-2014 depicting annual relative velocities and error circles

4.2 Displacements & Relative Deformation Model: 1990 – 2015

Station	dE (m)	dN (m)	ΔE (m)	ΔN (m)	2D Displacement 25 years (m)	Speed (mm/yr)	Accuracy \pm (mm/yr)	Direction (deg)
Chaguaramas	0.225	0.620	0.423	0.012	0.423	16.9	1.9	88
Freeport	0.103	0.752	0.301	0.144	0.334	13.3	2.0	64
Navet	-0.074	0.572	0.124	-0.036	0.129	5.2	1.2	106
Gasparillo	-0.116	0.593	0.082	-0.015	0.083	3.3	1.4	100
Mayaro	0.043	0.575	0.241	-0.033	0.243	9.7	1.9	98
Penal	-0.198	0.608	0.000	0.000	0.000	0.0	0.0	0
Los Iros	-0.498	0.482	-0.300	-0.126	0.325	13.0	1.8	247

Table 4-3: Displacements and Annual Relative Velocities for 1990 - 2015.

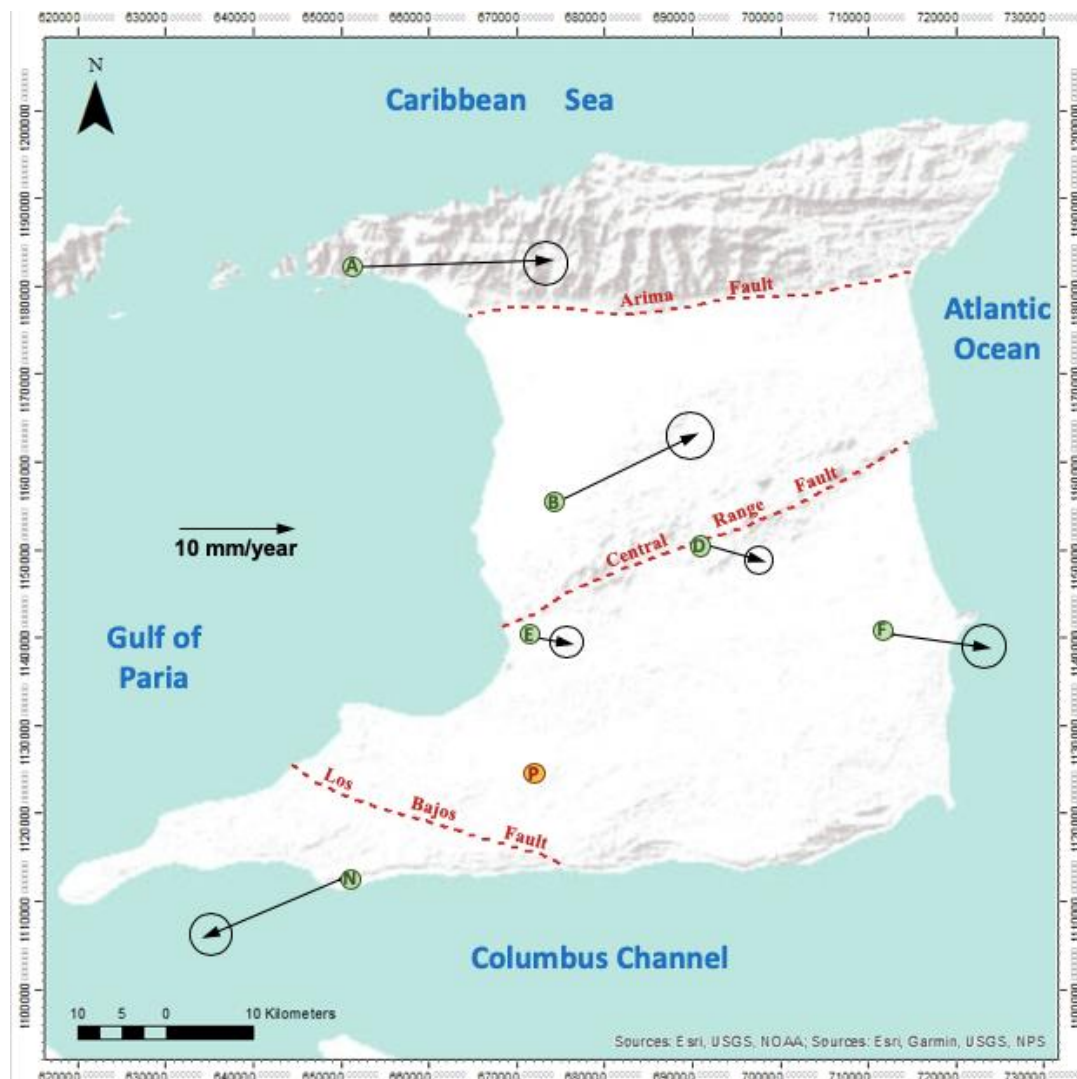


Figure 4-2: Relative Deformation Model for 1990-2015 depicting annual relative velocities and error circles.

4.3 Displacements & Relative Deformation Model: 1990 -2016

Station	dE (m)	dN (m)	ΔE (m)	ΔN (m)	2D Displacement 26 years (m)	Speed (mm/yr)	Accuracy \pm (mm/yr)	Direction (deg)
Freeport	0.127	0.752	0.299	0.155	0.337	13.0	2.2	63
Manzanilla	0.119	0.580	0.291	-0.017	0.292	11.2	2.0	93
Navet	-0.068	0.576	0.104	-0.021	0.106	4.1	1.4	101
Gasparillo	-0.121	0.598	0.051	0.001	0.051	2.0	1.2	89
Guayaguayare	-0.105	0.527	0.067	-0.070	0.097	3.7	2.0	136
Mayaro	0.046	0.572	0.218	-0.025	0.219	8.4	2.1	97
Penal	-0.172	0.597	0.000	0.000	0.000	0.0	0.0	0
Los Iros	-0.492	0.468	-0.320	-0.129	0.345	13.3	1.9	248

Table 4-4: Displacements and Annual Relative Velocities for 1990 - 2016.

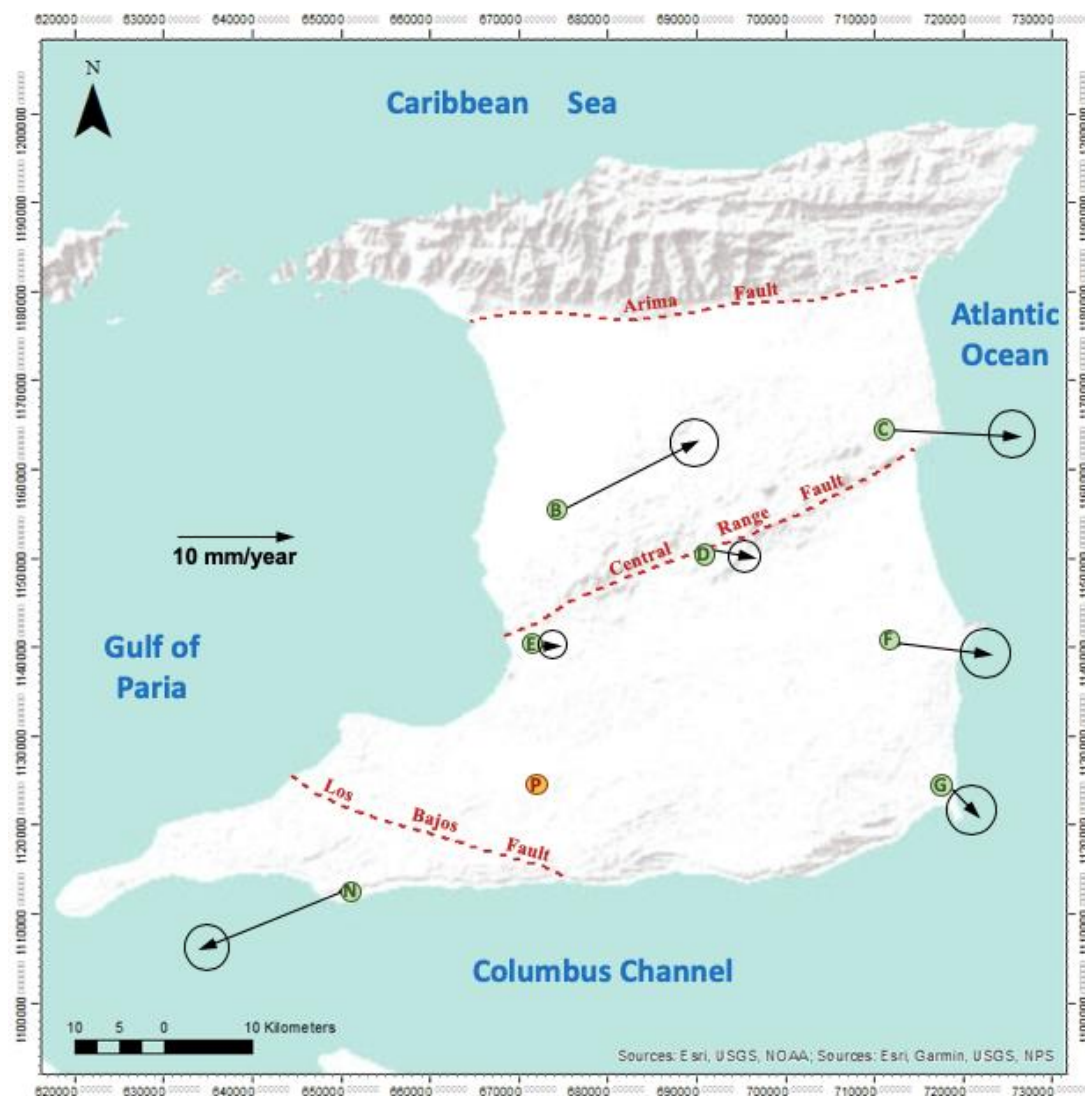


Figure 4-3: Relative Deformation Model for 1990-2016 depicting annual relative velocities and error circles.

4.4 Displacements & Relative Deformation Model: 1990 -2017

Station	dE (m)	dN (m)	ΔE (m)	ΔN (m)	2D Displacement 27 years (m)	Speed (mm/yr)	Accuracy \pm (mm/yr)	Direction (deg)
Chagaramas	0.296	0.604	0.492	-0.025	0.493	18.2	1.8	93
Freeport	0.139	0.779	0.335	0.150	0.367	13.6	2.1	66
Manzanilla	0.139	0.579	0.335	-0.050	0.339	12.5	2.1	99
Navet	-0.071	0.574	0.125	-0.055	0.137	5.1	1.3	114
Gasparillo	-0.125	0.614	0.071	-0.015	0.073	2.7	1.3	102
La Lune	-0.177	0.670	0.019	0.041	0.045	1.7	1.5	25
Catshill	-0.161	0.553	0.035	-0.076	0.084	3.1	1.4	155
Saunders Tr.	-0.207	0.466	-0.011	-0.163	0.163	6.1	1.5	184
Rousillac	-0.048	0.675	0.148	0.046	0.155	5.7	1.9	73
Penal	-0.196	0.629	0.000	0.000	0.000	0.0	0.0	0
Los Iros	-0.513	0.482	-0.317	-0.147	0.349	12.9	1.7	245
Cedros	*	*	0.039	0.091	0.099	3.7	2.5	23

Table 4-5: Displacements and Annual Relative Velocities for 1990 - 2017.

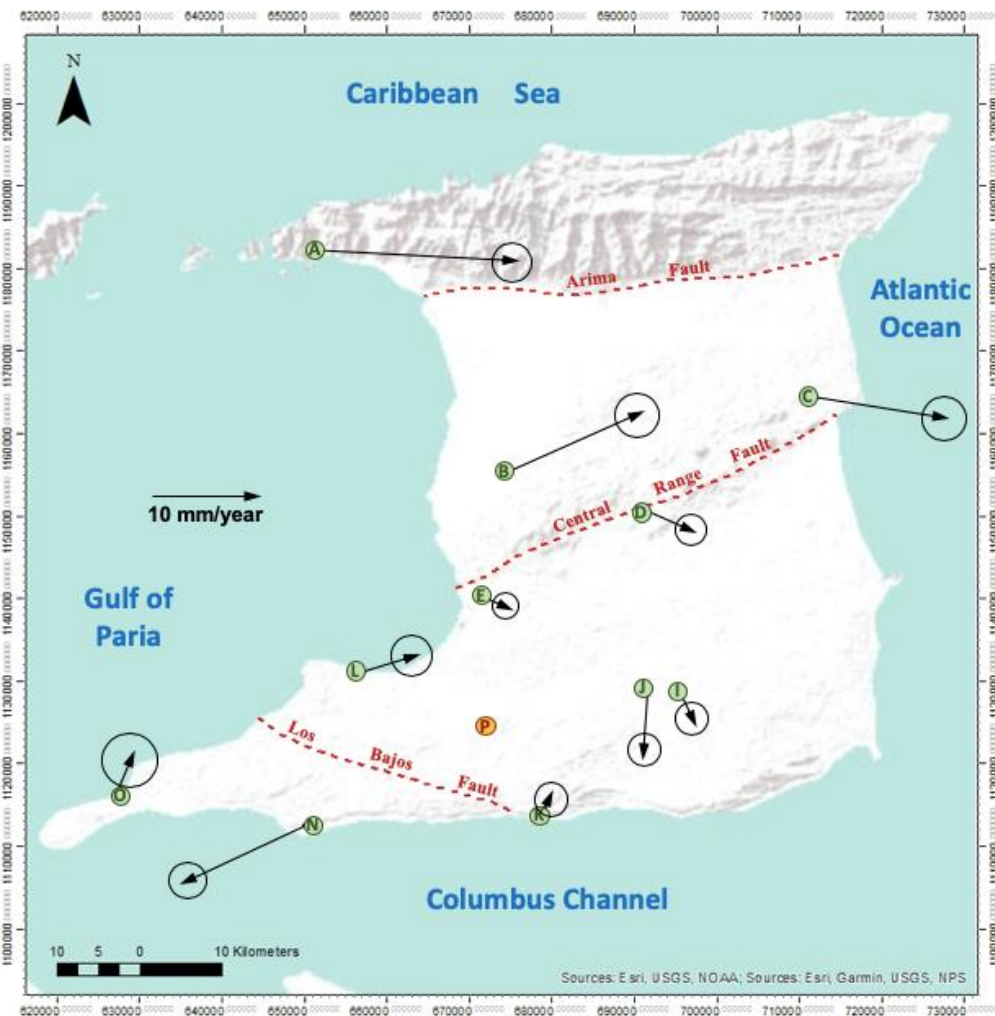


Figure 4-4: Relative Deformation Model for 1990-2017 depicting annual relative velocities and error circles

4.5 Average Relative Deformation Model

Using these various estimates of relative velocities, an average relative deformation model was generated for Trinidad, which compiled the average relative velocities for all monuments that have been re-observed between 2014 to 2017. This model can be used to complement semi-dynamic datums for Trinidad; providing a means of propagating spatial data to a common reference epoch for data correlation and decision-making purposes. This average relative deformation model also provides both a quantitative and qualitative look at the scale of horizontal deformation occurring across the island.

Station	Average ΔE (m)	Average ΔN (m)	Avg Speed (mm/yr)	Accuracy \pm (mm/yr)	Average Direction
Chaguaramas	0.440	-0.002	17.4	1.9	90
Freeport	0.306	0.150	13.4	2.1	64
Manzanilla	0.313	-0.043	12.4	2.0	98
Navet	0.120	-0.035	4.9	1.3	106
Gasparillo	0.072	-0.010	2.9	1.3	97
Rio Claro	0.093	-0.036	4.2	1.5	111
Guayaguayare	0.076	-0.072	4.2	1.9	133
Mayaro	0.232	-0.029	9.4	2.1	97
La Lune	0.019	0.041	1.7	1.5	25
Catshill	0.035	-0.076	3.1	1.4	155
Saunders Tr.	-0.011	-0.163	6.1	1.5	184
Forest Reserve	0.084	-0.161	7.6	2.4	152
Rousillac	0.166	0.053	6.9	2.0	73
Los Iros	-0.310	-0.135	13.3	1.8	247
Cedros	0.039	0.091	3.7	2.5	23

Table 4-6: Average relative displacements in E and N and average relative velocities (speed and direction).

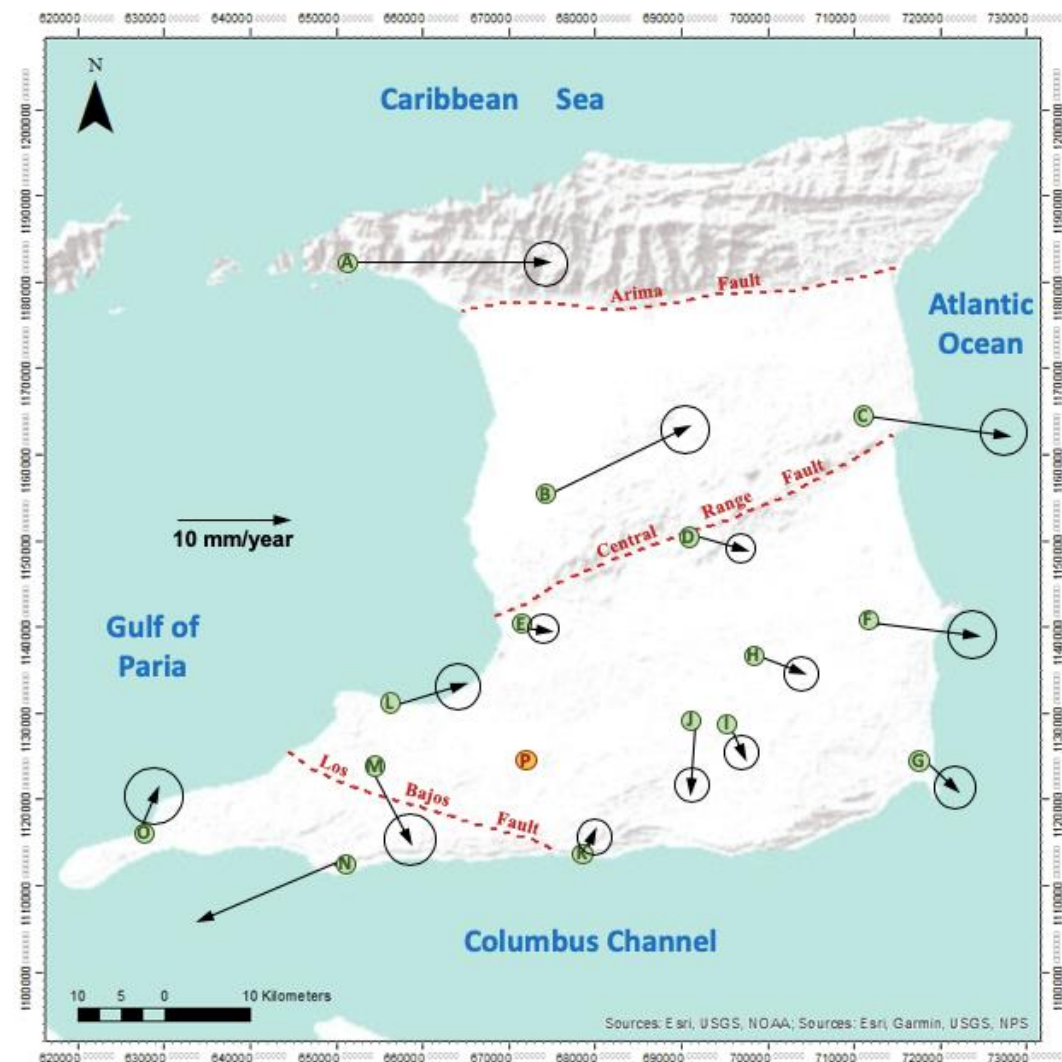


Figure 4-5: Average Relative Deformation model depicting average annual relative velocities and error circles.

4.6 Observed Trends

Results between different epochs are assimilated through a series of graphs towards identification of trends in the speed and direction. Monuments are grouped according to the fault blocks they fall into shown in Figure 4-6:

- Block 1: North of Arima Fault Zone.
- Block 2: Bounded by the Arima Fault Zone and the Central Range Fault Zone.
- Block 3: Bounded by the Central Range Fault Zone and Los Bajos Fault Zone.
- Block 4: South of Los Bajos Fault Zone.

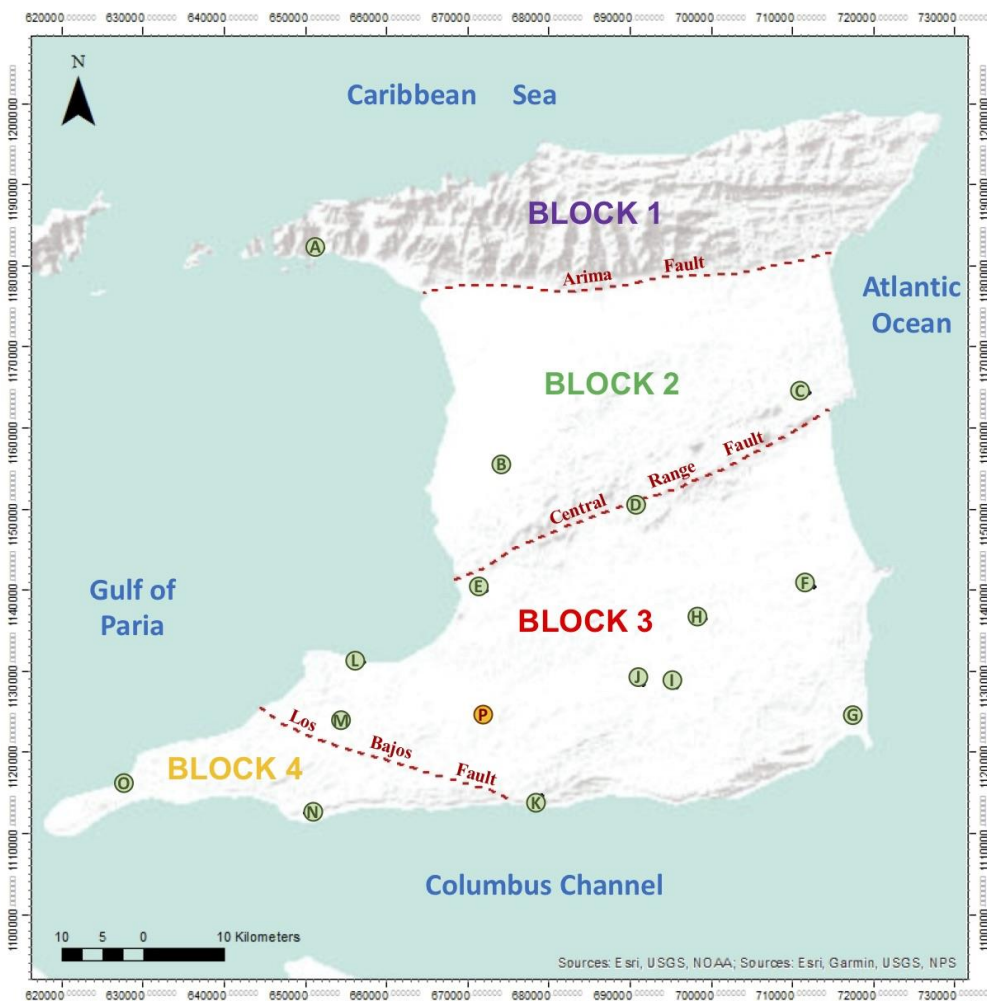


Figure 4-6: Map showing location of monuments within respective fault blocks.

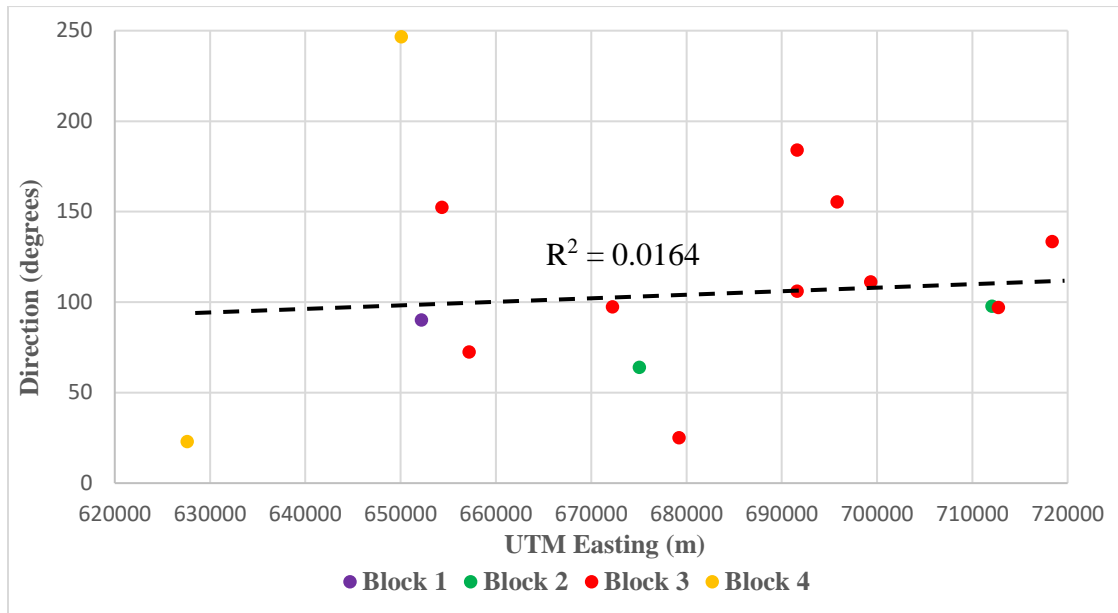


Figure 4-7: Plot of monument direction vs UTM Easting for 15 sites across Trinidad.

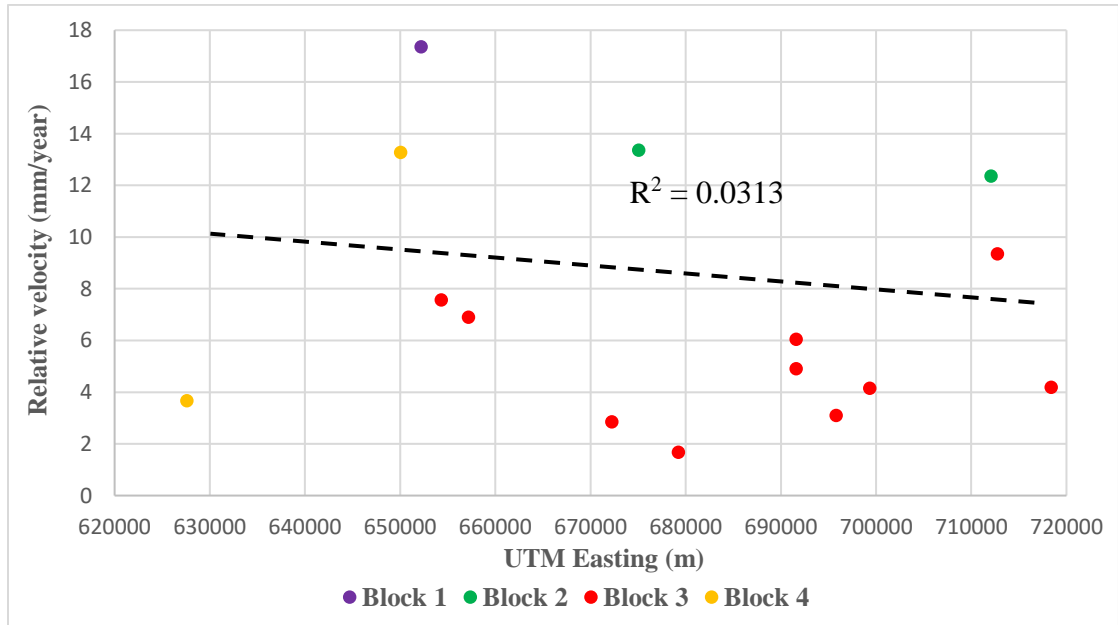


Figure 4-8: Plot of monument relative velocity vs UTM Easting for 15 sites across Trinidad.

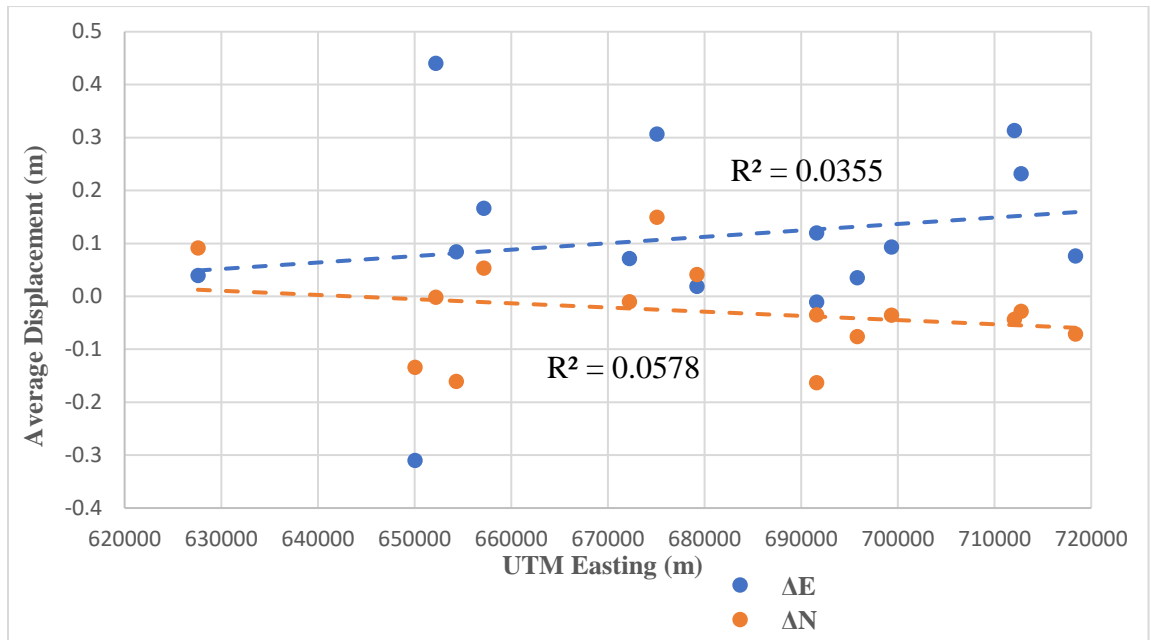


Figure 4-9: Plot of average relative displacements in Easting and North vs UTM Easting.

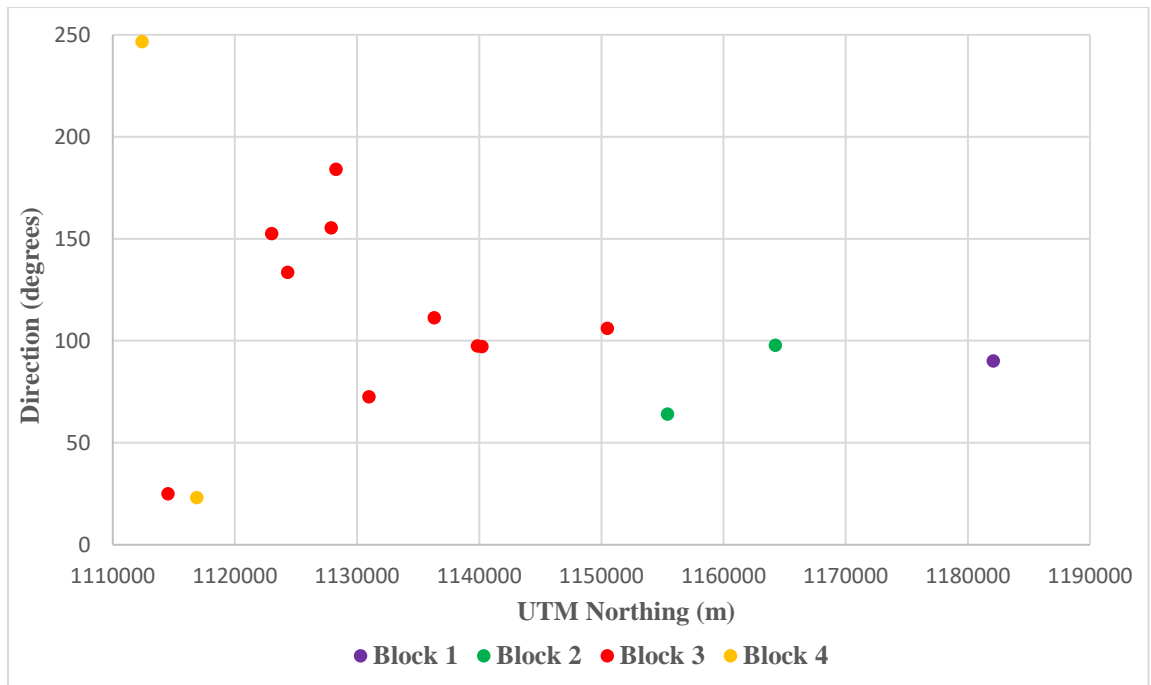


Figure 4-10: Plot of monument direction vs UTM Northing for 15 sites across Trinidad

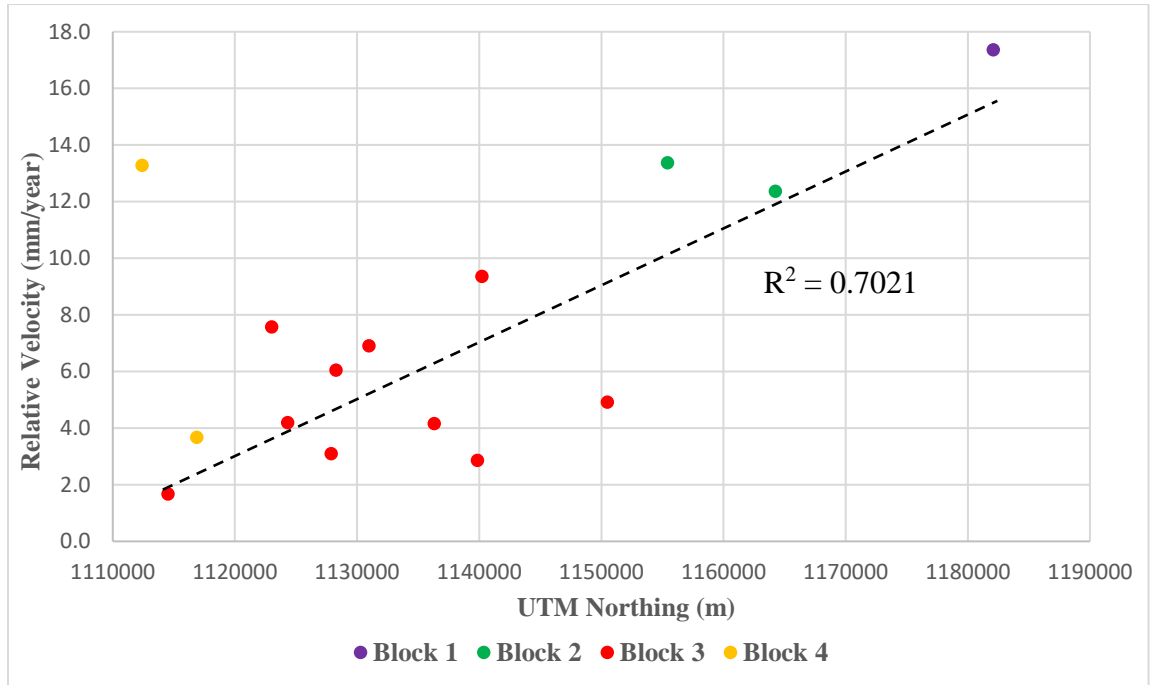


Figure 4-11: Plot of monument relative velocity vs UTM Northing for 15 sites across Trinidad.

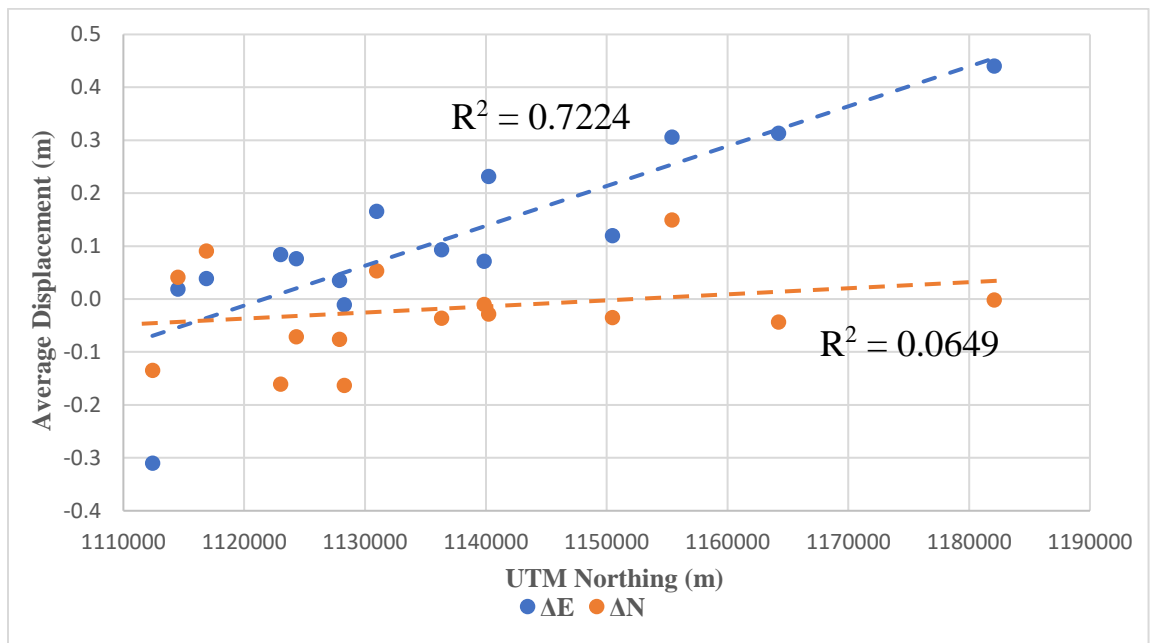


Figure 4-12: Plot of average relative displacements in Easting and North vs Northing.

5 DISCUSSION

Estimating rates of horizontal deformation across a given area can be hindered by the various steps taken in achieving them including errors in data acquisition, processing, etc. However, careful and meticulous procedures followed in conducting these geodetic investigations have successfully yielded estimates of both speed and direction (velocity) for all 17 sites across onshore Trinidad. Analysis of these results and identification of key trends provide a means of both verifying past studies and proving the need for a modern geodetic datum in Trinidad.

5.1 Distortion of Traditional Datums

A new modern datum must consider the on-going horizontal deformation occurring across the island. Across 27 years (1990 to 2017) stations have changed position by as little as 4.5 cm at La Lune in southern Trinidad to as much as 49 cm at Chaguaramas in the northern parts of the island relative to Penal. These sites also show wide disparities in velocities of 1.7 ± 1.5 mm/year at La Lune and 17.4 ± 1.9 mm/year at Chaguaramas. Compounding this are the varying directions of motion estimated at these stations including:

- Purely eastern motion (90°) at Chaguaramas
- South-eastern motion for many stations south of the Central Range Fault including Navet Dam (106°), Rio Claro (111°) and Guayaguayare (133°).
- South-westerly motion at Los Iros (247°).

From these variations in offsets, velocities and directions, one can now confidently assume that coordinated points used to realise traditional geodetic datums in Trinidad including Naparima 1955 and the 1901-1903 triangulation network, have since changed position and these datums are no longer considered to be realised. Datums have distorted since their initial realization due to this horizontal deformation and their use as geodetic control can no longer be applied in surveying at national level with confidence.

5.2 Deformation Speed

As seen in Table 4-6, the site at Chaguramas has the fastest average relative velocity of 17.4 ± 1.9 mm/year in northern Trinidad while the slowest site is at La Lune in the extreme south of the island with a velocity of 1.7 ± 1.5 mm/year. There appears to be a directly proportional relationship between average relative velocity and UTM Northing ($R^2 = 0.7021$); velocity increases northward across the island, as seen in Figure 4-11. This is consistent with past studies (Saleh, et al. 2004, Weber et al. 2001, Weber et al. 2011) that show similar trends.

Increase in speed towards the north of the island is largely attributed to a northward increase in the magnitude of eastern displacement (ΔE) as seen in Figure 4-12. This northward increase in both speed and eastward displacement can be attributed to the increasing influence of Caribbean plate motion which moves at a rate of 20 mm/year in a relatively easterly direction (85°). Meanwhile, there is no correlation between site velocity and UTM Easting as seen in Figure 4-8 ($R^2 = 0.0313$) nor ΔE component ($R^2 = 0.0355$) and ΔN component ($R^2 = 0.0578$). Additionally, there exists no direct relationship between monument velocity and UTM Easting ($R^2 = 0.0313$) as seen in Figure 4-8.

Los Iros is the only site that does not follow this trend and moves at an average relative velocity of 13.3 ± 1.8 mm/year in a south westerly direction. This outlier in both speed and direction is a direct result of comparing this site's velocity to that of the nominal reference site, Penal. While considered to be "stationary", Penal is located on the northern half of the Los Bajos Fault, while Los Iros is located on the southern half. The large velocity and difference in direction at Los Iros reveals the expected right-lateral movement expected at the Los Bajos Fault, although 13.3 ± 1.8 mm/year this magnitude is much larger than 5 mm/year previously estimated (Rodriguez, Weber and Shmalzle 2008). Further and more detailed investigations are required to determine the true slip rates along this fault.

5.3 Deformation Direction

With the exception of a few sites (La Lune, Mayaro and Forest Reserve) the direction of movement of GPS sites become less easterly and more southerly when moving from north to south across the island. The direction of motion can be subdivided by fault blocks as seen in Figure 4-6:

Block 1: Motion is purely with the Chagaramas site moving in direction of 90°.

Block 2: Motion is still largely easterly but Freeport moves along strike with the CRFZ (64°), while Manzanilla moves in an ESE direction.

Block 3: Crossing the Central Range Fault the direction of motion becomes largely ESE (Gasparillo, Navet Dam, Mayaro, Rio Claro) and transitions into south-easterly motion at Guayaguayare and almost southern at Catshill and Saunders Trace.

Block 4: With the exception of Cedros, motion in this block would be dictated by Los Iros which moves in a south-westerly direction (247°). This is a result of the right-lateral nature of the Los Bajos fault where a station in the southern block would move westward relative to a station in the northern block (Penal).

As seen in Figure 4-5, there appears to be a clockwise rotation in the direction of motion across Trinidad for most sites north of the Los Bajos Fault, with the except of La Luna and Forest Reserve. This rotation is a result in the decrease in the magnitude of ΔE southwards ($R^2 = 0.7244$) while ΔN stays relatively constant ($R^2 = 0.0649$) as seen Figure 4-12. The decrease in ΔE towards the south of the island is a result of decreasing influence of Caribbean Plate motion relative to South America (Lingrey 2017).

5.4 Regional Tectonics

Stations located north of the Central Range Fault Zone move significantly faster ($12.4 - 17.4$ mm/year) than those located south of it ($1.7 - 7.6$ mm/year), with the exception of the Los Iros station that is located south of the Los Bajos Fault Zone. This drastic change in velocities across the CRFZ support its nomination as the surface expression of the plate boundary across onshore Trinidad. This also suggests that there is increased influence by the Caribbean Plate in northern Trinidad, especially in Chaguanas where its speed and direction (17.4 ± 1.9 mm/year at 90°) is closest to the Caribbean Plate's estimates of 20mm/year at 85° (DeMets, Gordon and Argus 2010). Together, these observations have confirmed that horizontal deformation and tectonism across Trinidad is a direct result of interaction between Caribbean and South American plates.

5.5 Neotectonics

Results derived from this investigation support the idea that northward compression that contributed towards the creation of present-day Trinidad has since ceased and that horizontal deformation across the island is accommodated by three major fault zones: the Arima Fault, the Central Range Fault and the Los Bajos Fault in confirmation of previous studies Weber et al 2011, Saleh et al. 2004. All three fault zones exhibit some sense of dextral (right-lateral) strike-slip motion.

At the Arima Fault, block 1 moves at an average rate of 17.4 ± 1.9 mm/year while velocities within Block 2 move at an average relative velocity of 13 mm/year, giving an estimated difference of 3 mm/year across the fault zone. This is corroborated by estimate slip rates of 2.2 ± 1.8 mm/year in previous studies (Weber et al. 2001), although these estimates are considered statistically insignificant and the fault itself may be inactive.

The Central Range Fault exhibits right lateral motion with relative velocities of 13 mm/year in Block 2 and average relative velocities of 3.9 mm/year directly across

the fault in Block (average of Gasparillo and Navet Dam). This suggest a calculated difference of 9 mm/year across the fault zone, a rate that is smaller than past estimates of 12 ± 3 mm/year (Weber et al. 2001, Weber et al. 2011). While regular strike-slip motion seems to be occurring at the western end of this fault zone (based on differences in motion between Freeport and Gasparillo), transpression may be occurring towards its eastern end where the direction of motion of the Manzanilla site is south-easterly and not parallel with the trend of the fault zone.

It is also possible that the Los Bajos Fault also exhibits right-lateral motion as it has in the past (Archie and Gallai-Ragobar 2016) when comparing both the speed and direction of motion of the Los Iros site located on the southern half of the fault zone (Block 4) relative to that of Penal (Block 3). The estimate average velocity of Los Iros relative to Penal is 13.3 ± 1.8 mm/year, suggesting a larger than expected velocity difference across the fault zone when compared to previous studies (Koch 1987, Rodriguez, Weber and Shmalzle 2008).

Given these variations in velocities and direction of motion, it is obvious that Trinidad does not experience uniform deformation across its landmass. This non-uniform deformation surely distorts static geodetic datums and their networks including the Old Trinidad datum and the widely used Naparima 1955 datum. Coordinates estimated using these datums will carry with them significant innaccuracies that do not meet surveying and mapping standards and pose a threat to decision-making. There is a need for a modern geodetic datum that accounts for the active tectonism and deformation across the island, an aspect that can feasibly be executed through semi-dynamic datum implementation. The relative velocities estimated at sites across the island have laid the necessary groundwork for Relative Deformation Model (RDM) development that can be used to complement a future semi-dynamic datum.

6 CONCLUSION

The aim of this research project was to investigate the nature and degree of horizontal deformation that the island of Trinidad experienced, using GPS and satellite-based geodetic methods, across a 24 to 27-year period (1990 vs 2014-2017). Sites used by Halliburton in their own geodetic survey conducted in 1990 were located and re-observed using these GPS methods. Prior to processing this new data, primary control was established in an international frame of reference using data acquired at local CORS sites with connection to reputable international stations. Data was processed in Trimble Total Control to establish updated current coordinates. Old (1990) and new (2014 – 2017) datasets were then compared to estimate relative horizontal velocities for individual sites. Using these findings, estimates from previous deformation surveys conducted locally were used for comparison and were either corroborated or disproven. Furthermore, deformation estimates were used to highlight the shortcomings associated with the local use of traditional static datums and promote the implementation of a semi-dynamic datum through the development of a relative deformation model.

6.1 Key Achievements

Relative velocities were estimated for 15 sites out of the many listed in Halliburton's Final Geodetic report, as many of the original markers have been destroyed. The following conclusions were derived for the extent of Trinidad covered by the sites used:

- I. Site offsets ranging between 0.099 m (La Lune) and 0.493 m (Chagaramas) across the 24 to 27-year period have proven that static geodetic datums, including Old Trinidad 1901/2 and Naparima 1955 datums are inadequate for use as national survey control. Control points used to coordinate and realise these traditional datums have since moved from their original positions, distorting the entire datum.
-

- II. Horizontal deformation across Trinidad is not uniform as exhibited by large variations in both velocity and direction. Relative velocities range from 1.7 ± 1.5 mm/year (La Lune) to 17.4 ± 1.9 mm/year (Chaguaramas), while direction of motion ranges from 23° (Cedros) to 247° (Los Iros). While these variations are somewhat consistent with previous studies (Saleh et al. 2004, Weber et al. 2011), they also prove that deformation models are necessary to capture these variations to support potential future semi-dynamic datum implementation.

- III. Deformation speed increases northerly across the island and is believed to represent the increasing influence of Caribbean plate motion north of the Central Range Fault Zone. Simultaneously, this influence by the Caribbean plate is responsible for change in direction of motion from predominantly easterly north of the Central Range Fault Zone, to south-easterly south of it.

- IV. Dextral slip is evident across all three major fault zones with a difference of approximately 3 mm/year observed across the Arima Fault Zone and 9-10 mm/year across the Central Range Fault Zone, estimated that are consistent with those estimated by Weber et al. 2009. Conversely, Los Iros, located south of both the Los Bajos Fault Zone and the Penal reference point, has a velocity of 13.3 ± 1.8 mm/year, suggesting that Los Bajos is still an active, right-lateral strike-slip fault. It also suggests that this area must be further studied to accurately discern the nature of deformational across this fault zone.

- V. Relative velocities estimated for the 15 GPS sites across the country are inadequate to develop a standard relative deformation model. Variation between markers means that more sites must be located or constructed in an

attempt to densify the network and provide a more detailed concept of horizontal deformation that can be used for semi-dynamic datum implementation.

6.2 Future Investigative Needs

Given the findings of this research, the development of a semi-dynamic datum for Trinidad requires the following:

I. CORS & UNAVCO Stations

Zeroth order control is defined by national CORS stations that have been established by the Government of Trinidad and Tobago and additional UNAVCO stations. All such stations need to be incorporated into a regular adjustment so that velocities within some defined ITRF are available at high accuracy. Such an approach will require several years of data. CORS have been operating for 12 years and its data is available and could be processed at daily epochs, while more recent installations made by UNAVCO are much shorter in duration. This network would provide the foundation for geodetic control at national level.

II. Network Densification

While the 16 re-observed GPS sites provided a sense of the variation in both magnitude and direction of horizontal motion across the island, they are not sufficient to provide a complete sense of ongoing deformation. Although Halliburton's geodetic survey included over 100 sites, several of these sites have been destroyed by urban development, inaccessible due to dense vegetation or located in unsafe communities. Survey monuments and sites that make up other networks, once stable and accessible, can be used to densify the model. Additional sites can be constructed and observed overtime to discern horizontal motion, although this may require significant coordination amongst the surveying community, geologists and relevant

spatial agencies. A denser network of sites is necessary to detect displacement among the several minor faults that exist across Trinidad. It is possible that displacement among these minor faults may, together with the major faults mentioned in this study.

III. Processing Software

Trimble Total Control (TTC) was chosen as the processing software for this project due to its accessibility, ease of use and compatibility with GPS receivers used and data acquired. However, adjusted coordinate reports generated by the software do not provide the necessary covariances to estimate error ellipses for site velocities. Alternate software such as GAMIT and GLOBK, while not as user friendly, provides a means of analysing GNSS data and provided positional errors from which error ellipses can be estimated.

IV. ITRF Translation

In the future, as ITRF is updated, a means of moving from newer variants to that in which the datum is defined will need to be developed. This is typically achieved using a 7-parameter similarity transformation with time variant parameters. The determination of such parameters is dependent on the national zeroth order control being well connected to primary ITRF stations with regular (daily) adjustment.

7 REFERENCES

- Abidin, Hasanuddin Z, Susilo Susilo, Irwan Meilano, Cecep Subarya, Kosasih Prijanta, M. Arief Syafi'i, Edwin Hendrayana, Joni Effendi, and Doni Sukmayadi. 2015. "On the Development and Implementation of a Semi-Dynamic Datum for Indonesia ." *IGA 150 Years* 91-99.
- Algar, S. T., and Tim Pindell. 1993. "Structure and deformation history of the Northern Range of Trinidad and adjacent areas." *Tectonics* 12 (4): 814-829.
- Altamimi, Zuheir, Laurent Metivier, Paul Rebischung, Helene Rouby, and Xavier Collileux. 2017. "ITRF2014 Plate motion model." *Geophysical Journal International* 209 (3): 1906-1912.
- Altamimi, Zuheir, Paul Rebischung, Laurent Metivier, and Xavier Collileux. 2016. "ITRF2014: A new release of the International Terrestrial Reference Frame modeling nonlinear station motions." *Journal of Geophysical Research* 121 (8): 6109-6131.
- Altamimi, Zuheir, Xavier Collileux, J Legrand, B. Garayat, and C. Boucher. 2007. "ITRF2005: A new release of the International Terrestrial Reference Frame based on time series of station positions and Earth Orientation Parameters." *Journal of Geophysical Research: Solid Earth* 112 (B9).
- ANZLIC, Australian New Zealand Spatial Information Council. 2016. *ANZLIC Intergovernmental Committee on Surveying and Mapping (ICSM)*. Accessed March 20, 2019. <http://icsm.gov.au/education/fundamentals-mapping/datums>.
- Archie, Curtis, and Nancy Gallai-Ragobar. 2016. "Structural and Stratigraphic Evolution of the North Marine Area, Gulf of Paria, Trinidad, Since the Pliocene." *AAPG Databases Inc.* Petroleum Company of Trinidad and Tobago. Accessed March 20, 2019. http://www.searchanddiscovery.com/pdfz/documents/2016/30447archie/ndx_archie.pdf.html.

- Arkle, Jeanette C., Lewis A. Owen, and John C. Weber. 2017. "Trinidad and Tobago." In *Lanforms and Landscape of the Lesser Antilles*, by Casey D. Allen, 267-291. Springer International Publishing.
- Babb, Stephen, and Paul Mann. 1999. *Structural and sedimentary development of a Neogene transpressional plate boundary between the Caribbean and South America plates in Trinidad and the Gulf of Paria*. Vol. 4, in *Sedimentary basins of the world.*, 495-557. Elsevier.
- Baratin Wachten, Laura-May. 2018. *Using low-frequency earthquakes to monitor slow tectonic deformation in the central Southern Alps, New Zealand*. PhD Thesis, Wellington: University of Wellington.
- Beavan, J., and J. Haines. 2001. "Contemporary horizontal velocity and strain rate fields of the Pacific-Australia plate boundary zone through New Zealand." *Journal of Geophysical Research* 106: 741-770.
- Blick, G. 2003. "Implementation and development of NZGD2000." *New Zealand Surveyor* 15-19.
- Blick, G., and G. Rowe. 1997. "Progress Towards A New Geodetic Datum for New Zealand." *New Zealand Surveyor* (New Zealand Institute of Surveyors) 287: 25-29.
- Blick, G., and N. Donnelly. 2016. "From static to dynamic datums: 150 years of geodetic datums in New Zealand." *New Zealand Journal of Geology and Geophysics* 59 (1): 15-21.
- Blick, G., N. Donnelly, and A. Jordan. 2009. *The Practical Implications and Limitations of the Introduction of a Semi-Dynamic Datum – A New Zealand Case Study*. Berlin: Geodetic Reference Frames, 115-120.
- Cayapan, Victoria D. Charisma. 2016. *Modernization of the Philippine Geodetic Reference System*. Strategic Plan 2016-2020, Manila: National Mapping and Resource Information Authority.
- Chapman, Arthur D. 2005. *Principles of Data Quality*. GBIF.

- Chatzinikos, M., and C. Kotsakis. 2016. "Appraisal of the Hellenic Geodetic Reference System 1987 based on backward-transformed ITRF coordinates using a national velocity model." *Survey Review* 49 (356): 1-13.
- Ching, Kuo-en, and Kwo-hwa Chen. 2015. "Tectonic effect for establishing a semi-dynamic datum in Southwest Taiwan." *Earth, Planets and Space* 67 (207): 1-14.
- Crook, C., N. Donnelly, J. Beavan, and C. Pearson. 2016. "From geophysics to geodetic datum: updating the NZGD2000 deformation model." *New Zealand Journal of Geology and Geophysics* 59 (1): 22-31.
- Crosby, C. J., Carol S. Prentice, John C. Weber, and D. Ragona D. 2009. *Logs of paleoseismic excavations across the Central Range fault, Trinidad*. Open File Report, US Geological Survey, 1228.
- Dach, R., U. Hugentobler, P. Fridez, and M. Meindl. 2007. *Bernese GPS Software Version 5.0*. Switzerland: Astronomical Institute, University of Bern.
- Dawson, John, Ramesh Govind, and John Manning. 2001. "Application of the AUSLIG online GPS processing system (AUSPOS) to Antarctica." *Proceeding of Satnav*. he Australian Surveying and Land Information Group (AUSLIG).
- DeMets, C, R. G. Gordon, and D. F. Argus. 2010. "Geologically current plate motions." *Geophysical Journal International* (Ge) 181: 1-80.
- Denys, Paul, Rachelle Winefield, and Aaron Jordan. 2007. "Incorporating localised deformation events in dynamic datums." *Presentation at XXX FIG General Assembly and Working Week*. Hong Kong. 1-15.
- Donnelly, Nic, Graeme Blick, and Richard Stanaway. 2013. *Going Geocentric - Deformation models for Dynamic (and semidynamic) Datums*. Presentation, Manila: Land Information New Zealand.
- Drake, Simon Picton. 2002. *Converting GPS Coordinates ($\phi\lambda h$) to Navigation Coordinates (ENU)*. Edinburgh: DSTO Electronics and Surveillance Research Laboratory.

- Estey, Louise H., and Charles M Meertens. 1999. "TEQC: The Multi-Purpose Toolkit for GPS/GLONASS Data." *GPS Solutions* 3 (1): 42-49.
- Fazilova, Dilbarkhon. 2017. "The review and development of a modern GNSS network and datum in Uzbekistan." *Geodesy and Geodynamics* 8 (3): 187-192.
- Gentle, P., G. Blick, and K. Gledhill. 2016. "The development and evolution of the GeoNet and PositioNZ GNSS continuously operating network in New Zealand." *New Zealand Journal of Geology and Geophysics* 59 (1): 33-42.
- Goudarzi, M. A., M. Cocard, R. Santerre, and T. Woldai. 2013. "GPS interactive time series analysis software." *GPS Solutions* 17 (4): 595-603.
- Haasdyk, Joel, Nic Donnelly, Chris Harrison, Craig Roberts, and Richard Stanaway. 2014a. "Options for Modernising the Geocentric Datum of Australia." *Proceedings of Research @ Locate'14 Conference*. Canberra, Australia: CEUR Workshop Proceedings. 72-85.
- Hanifa, N. R., T. Sagiya, F. Kimata, J. Efendi, and H. Z. Abidin. 2014. "Interplate coupling model off the southwestern coast of Java, Indonesia, based on continuous GPS data in 2008–2010." *Earth & Planetary Science Letters* 401: 159-171.
- HGS. 1991. *Final Geodetic Report*. Halliburton Geophysical Services.
- Jamill, Hansan, and Azhari Mohamed. 2010. "The Malaysia Real Time Kinetic GNSS Network in 2010 and Beyond." *FIG Congres 2010*. Sydney, Australia. 1-15.
- Kobayashi, Tomokazu. 2014. "Remarkable ground uplift and reverse fault ruptures for the 2013 Bohol earthquake (Mw 7.1), Philippines, revealed by SAR pixel offset analysis." *Geoscience letters* 1 (1): 1-7.
- Koch, K. R. 1987. *Parameter Estimation and Hypothesis Testing in Linear Models*. Springer Science & Business Media.
- Lee, L. P. 1978. *First-order geodetic triangulation of New Zealand 1909–49 and 1973–74*. Technical Series No. 1, Wellington: Department of Lands and Survey.

- Li, Xiong, and Hans-Jurgen Gotze. 2001. "Ellipsoid, geoid, gravity, geodesy and geophysics." *Geophysics* 66 (6): 1660-1668.
- Lingrey, Steven. 2017. "Plate Tectonic Setting and Cenozoic Deformation of Trinidad: Foldbelt Restoration in a Region of Significant Strike-Slip." In *Thrust Belts and Foreland Basins*, 163-177. Berlin: Springer.
- Malys, Stephen, Robert Wong, and Scott A. True. 2016. "The WGS 84 Terrestrial Reference Frame in 2016." *IG-11*. Sochi, Russia. 1-33.
- McCaffre, Anthony M., P.T. Jayachandran, Richard B. Langley, and Jean-Marie Sleewaegen. 2018. "On the accuracy of the GPS L2 observable for ionospheric monitoring." *GPS Solutions* 22-23.
- Mugnier, Clifford J. 2000. "The Republic of Trinidad and Tobago." *Photogrammetric Engineering & Remote Sensing* 66 (11): 1307-1308.
- Ogutcu, Sermet. 2018. "Deformation of static datum: Turkish CORS network (TUSAGA-Aktif)." *Geodetica et Geophysica* 53 (3): 543-553.
- Paul, J., C. Rajendra, A. R. Lowry, V. Andrade, and K. Rajendran. 2012. "Andaman postseismic deformation observations: Still slipping after all these years?" *Bulletin of the Seismological Society of America* 102 (1): 343-351.
- Pérez, Omar J., Roger Bilham, Rebecca Bendick, Jose R. Velandia, Napoleon Hernández, Carlos Moncayo, Melvin Hoyer, and Mike Kozuch. 2001. "Velocity field across the southern Caribbean plate boundary and estimates of Caribbean/South-American plate motion using GPS geodesy 1994–2000." *Geophysical Research Letters* 28 (15): 2987-2990.
- Petit, Gerard, and Brian Luzum. 2010. *IERS Technical Note No. 36*. IERS Conventions, Frankfurt: Verlag des Bundesamts für Kartographie und Geodäsie.
- Prentice, Carol S., John C. Weber, Christopher J. Crosby, and Daniel Ragona. 2010. "Prehistoric earthquakes on the Caribbean-South American plate boundary, Central Range fault, Trinidad." *Geology* 38 (8): 675-678.
- Rais, J. 1979. "Doppler surveying in Indonesia (1974–1979)." *IAG Symposium General Assembly XVII*. Canberra, Australia: IUGG.

- Rodriguez, Anthony, John C. Weber, and G. Shmalzle. 2008. "Global Positioning System (GPS) determination of motions, neotectonics, and seismic hazard in Trinidad and Tobago." *American Geophysical Union Annual Meeting*.
- Saleh, Jarir, K. Edwards, J. Barbaste, S. Balkaransingh, D. Grant, John C. Weber, and T. Leong. 2004. "On some improvements in the geodetic framework of Trinidad and Tobago." *Survey Review* 37 (294): 604-625.
- Scheppers, JHG, and FCA Schulte. 1931. *Geodetic Survey in the Netherlands East Indies*. IUGG.
- Shariff, N. S., J. Gill, Z. M. Amin, and K. M. Omar. 2017. "Towards the Implementation of a Semi-Dynamic Datum for Malaysia." *The International Archives of Photogrammetry, Remote Sensing and Spatial Information Sciences* 42 (4): 185-199.
- Simons, M., S. E. Minson, A. Sladen, F. Ortega, J. Jiang, S. E. Owen, L. Meng, and J. Ampuero. 2011. "The 2011 magnitude 9.0 Tohoku-Oki earthquake: Mosaicking the megathrust from seconds to centuries." *Science* 332 (6036): 1421-1425.
- Soto, David Manuel, Paul Mann, Alejandro Escalona, and Leslie J. Wood. 2007. "Late Holocene strike-slip offset of a subsurface channel interpreted from three-dimensional seismic data, eastern offshore Trinidad." *Geology* 35 (9): 859-862.
- Soto, David, Paul Mann, and Alejandro Escalona. 2011. "Miocene-to-recent structure and basinal architecture along the central range strike-slip fault zone, eastern offshore Trinidad." *Marine and Petroleum Geology* 28 (1): 212-234.
- Stanaway, Richard, C. Roberts, and Graeme Blick. 2014. "Realisation of a Geodetic Datum Using a Gridded Absolute Deformation Model (ADM)." In *Earth on the Edge: Science for a Sustainable Planet*, 259-265. Berlin, Heidelberg: Springer.
- Subarya, C., and RWM Matindas. 1996. *Geocentric Indonesian Datum 1995*. Bakosurtanal, Indonesia: National Agency of Surveying and Mapping.

- Subarya, C., M. Chlieh, L. Prawirodirdjo, and J. P. Avouac. 2006. "Plate-boundary deformation associated with the great Sumatra–Andaman earth- quake." *Nature* 440: 46-51.
- Torge, Wolfgang, and Jurgen Muller. 2012. *Geodesy*. Hanover: Walter de Gruyter.
- Tregoning, Paul, and Russel Jackson. 1999. "The Need for Dynamic Datums." *Geomatics Research Australasia* 87-102.
- Tyson, Llewellyn, Stephen Babb, and Bryan Dyer. 1991. "Middle Miocene Tectonics and its effects on Late Miocene Sedimentation in Trinidad." *2nd Geological Conference of Trinidad & Tobago*. Port of Spain: GSTT. 26-40.
- United Nations. 2006. "Arbitration between Barbados and the Republic Arbitration between Barbados and the Republic of Trinidad and Tobago, relating to the delimitation of the exclusive economic zone and the continental shelf between them, decision of 11 April 2006." The Hague, 147-251.
- Uruski, Chris. 2014. "The contribution of offshore seismic data to understanding the evolution of the New Zealand continent." *Geological Society of London: Special Publications* 413: 35-51.
- Vigny, C., W. J. Simons, S. Abu, and R. Bamphenyu. 2005. "Insight into the 2004 Sumatra–Andaman earthquake from GPS measurements in Southeast Asia." *Nature* 436 (7048): 201-206.
- Wang, Jiang, Jingling Wang, and Craig Roberts. 2009. "Investigations into a Dynamic Geocentric Datum." In *Observing our Changing Earth*, 11-19. Berlin, Heidelberg: Springer-Verlag.
- Wanninger, Lambert, and Stephan Wallstab-Frietag. 2007. "Combined Processing of GPS, GLONASS, and SBAS Code Phase and Carrier Phase Measurements." *Proceedings of ION GNSS*. Germany: Geodetic Institute, Dresden University. 866-875.
- Warren, David L.M. , and John F. Racquet. 2003. "Broadcast vs. precise GPS ephemerides: a historical perspective." *GPS Solutions* 151-156.

- Weber, John C. 2005. "Neotectonics in the Trinidad and Tobago, West Indies segment of the Caribbean-South American plate boundary." *Occasional Papers of the Geological Institute of Hungary* 204: 21-29.
- Weber, John C., Jarir Saleh, S. Balkaransingh, T. Dixon, W. Ambeh, T. Leong, A. Rodriguez, and Keith Miller. 2011. "Triangulation-to-GPS and GPS-to- GPS geodesy in Trinidad, West Indies: Neotectonics, seismic risk, and geologic implications." *Marine and Petroleum Geology* 28 (1): 200-211.
- Weber, John C., Timothy H. Dixon, Charles DeMets, William B. Ambeh, Pamela Jansma, Glen Mattioli, Jarir Saleh, Giovanni Sella, Roger Bilham, and Omar Perez. 2001. "GPS estimate of relative motion between the Caribbean and South American plates, and geologic implications for Trinidad and Venezuela." *Geology* 29 (1): 75-78.
- Weber, John, Jarir Saleh, S. Balkaransingh, and Timothy Hugh Dixon. 2011. "Triangulation-to-GPS and GPS-to-GPS geodesy in Trinidad, West Indies: Neotectonics, seismic risk, and geologic implications." *Marine and Petroleum Geology* 28 (1): 200-211.
- Wilson, Ian. 2000. *Geodesy Category Report (Draft)*. Geodesy Category Report, Madison: Land Tenure Centre - University of Wisconsin, 1-30.

8 APPENDICES

8.1 APPENDIX A – Haliburton Site Coordinates (Final Geodetic Report)

Site ID#	Station	Easting - WGS84 (m)	Northing - WGS84 (m)
BM 457	Guayaguayare	718376.64	1124311.99
TDST 0005	Rio Claro	699320.92	1136318.91
TDST 0009	Gasparillo	672223.68	1139840.57
TDST 0014	Penal	671971.68	1124373.09
TDST 0029	Mayaro	712732.63	1140217.27
TDST 0039	Freeport	675050.71	1155411.58
TDST 0045	Manzanilla	712059.62	1164224.90
TDST 0050	Forest Reserve	654316.06	1123005.15
TDST 0052	La Lune	679215.22	1114504.71
TDST 0055	Los Iros	650051.69	1112403.06
TDST 0061	Navet Dam	691589.26	1150482.64
TDST 0063	Cedros	627582.37	1116875.03
TDST 0066	Saunders Tr.	691595.57	1128272.84
TDST 0067	Catshill	695806.17	1127888.11
TDST 0097	Rousillac	657168.73	1130964.83
USBM 0042	Chagaramas	652184.28	1182066.67

Table 8-1: WGS84 UTM Coordinates for re-observed sites.

8.2 APPENDIX B – Device & Antenna Metadata

Date	Point ID #	Location	Antenna Height (m)	Position	Instrument
10/17/2014	USBM 0042	Chaguarmas	1.589	Bottom of Notch	Trm 5700 with Zephyr Geodetic Antenna
	TDST 0045	Manzanilla	1.793	Centre of Bumper	Trimble R6-4
	TDST 0029	Mayaro	1.373	Bottom of Notch	Trm 5700 with Zephyr Geodetic Antenna
	BM 547	Guayaguayare	1.415	Centre of Bumper	Trimble R6-4
	TDST 0005	Rio Claro	1.546	Centre of Bumper	Trimble R6-4
	TDST 0039	Freeport	1.871	Centre of Bumper	Trimble R6-4
	TDST 0061	Navet Dam	1.466	Bottom of Notch	Trm 5700 with Zephyr Geodetic Antenna
10/20/2014	TDST 0009	Gasparillo	1.550	Centre of Bumper	Trimble R6-4
	TDST 0014	Penal	1.584	Bottom of Notch	Trm 5700 with Zephyr Geodetic Antenna
	TDST 0097	Rousillac	1.563	Bottom of Notch	Trm 5700 with Zephyr Geodetic Antenna
	TDST 0050	Forest Reserve	1.526	Centre of Bumper	Trimble R6-4
	TDST 0063	Cedros	1.676	Bottom of Notch	Trm 5700 with Zephyr Geodetic Antenna
	TDST 0055	Los Iros	1.536	Centre of Bumper	Trimble R6-4

Table 8-2: Antennae height and receiver metadata for stations re-observed in 2014.

Date	Point ID #	Location	Antenna Height (m)	Position	Instrument
2015-10-05	TDST 0050	Forest Reserve	1.978	Centre of Bumper	Trimble R8-3 Internal
	TDST 0055	Los Iros	1.932	Centre of Bumper	Trimble R6 Internal
	TDST 0039	Freeport	1.567	Centre of Bumper	Trimble R6 Internal
	TDST 0063	Cedros	1.966	Centre of Bumper	Trimble R6-4 Internal
	TDST 0097	Rousillac	1.877	Centre of Bumper	Trimble R6-4 Internal
	TDST 0014	Penal	1.907	Bottom of Notch	Trm 5700 with Zephyr Geodetic Antenna
	TDST 0009	Gasparillo	1.762	Bottom of Notch	Trm 5700 with Zephyr Geodetic Antenna
2015-10-08	TDST 0039	Freeport	2.014	Centre of Bumper	Trimble R6 Internal
	TDST 0061	Navet Dam	1.880	Centre of Bumper	Trimble R8-3 Internal
	TDST 0045	Manzanilla	2.102	Centre of Bumper	Trimble R6-4 Internal
	TDST 0029	Mayaro	1.830	Bottom of Notch	Trm 5700 with Zephyr Geodetic Antenna
	USBM 0042	Chaguaramas	1.890	Centre of Bumper	Trimble R6 Internal

Table 8-3: Antennae height and receiver metadata for stations re-observed in 2015.

Date	Point ID #	Location	Antenna Height (m)	Position	Instrument
2016-10-13	TDST 0029	Mayaro	1.489	Center of Bumper	Trimble R6 Internal
	TDST 0045	Manzanilla	2.134	Center of Bumper	Trimble R6 (L&S Rover)
	TDST 0061	Navet Dam	1.879	Center of Bumper	Trimble R6 (L&S Rover)
	BM 547	Guayaguayare	1.412	Center of Bumper	Trimble R6-4 Internal
	TDST 0014	Penal	2.528	Bottom of Antenna Mount	Leica GS14
	TDST 0009	Gasparillo	2.160	Center of Bumper	Trimble R6 Internal
	TDST 0055	Los Iros	1.417	Bottom of Antenna Mount	Leica GS14
	TDST 0039	Freeport	1.851	Center of Bumper	Trimble R6-4 Internal
2016-10-14	TDST 0029	Mayaro	1.759	Center of Bumper	Trimble R6 (L&S Rover)
	TDST 0045	Manzanilla	1.770	Center of Bumper	Trimble R6-4 Internal
	TDST 0061	Navet Dam	1.838	Center of Bumper	Trimble R6 Internal
	BM 547	Guayaguayare	1.697	Center of Bumper	Trimble R6-4 Internal
	TDST 0039	Freeport	2.179	Center of Bumper	Trimble R6 (L&S Rover)
	TDST 0097	Rousillac	2.058	Bottom of Antenna Mount	Leica GS14
	TDST 0063	Cedros	1.854	Bottom of Antenna Mount	Leica GS14

Table 8-4: Antennae height and receiver metadata for stations re-observed in 2016.

Date	Point ID #	Location	Antenna Height (m)	Position	Instrument
10/09/2017	TDST 0052	La Lune	1.709	Center of Bumper	Trimble R6-4 Internal
	TDST 0014	Penal	1.814	Bottom of Antenna Mount	Leica GS14
	TDST 0009	Gasparillo	1.962	Bottom of Antenna Mount	Leica GS14
	TDST 0066	Sauders Trace	1.834	Center of Bumper	Trimble R6 Internal
	TDST 0067	Catshill	1.692	Center of Bumper	Trimble R6 Internal
10/12/2017	TDST 0039	Freeport	1.802	Center of Bumper	Trimble R6 Internal
	TDST 0014	Penal	1.704	Bottom of Antenna Mount	Leica GS14
	TDST 0009	Gasparillo	1.964	Bottom of Antenna Mount	Leica GS14
	TDST 0063A	Cedros	1.920	Center of Bumper	Trimble R6-4 Internal
	TDST 0063B	Cedros	1.895	Center of Bumper	Trimble R6 Internal
	TDST 0063	Cedros	1.582	Center of Bumper	Trimble M3
	TDST 0097	Rousillac	1.788	Center of Bumper	Trimble R6 Internal
10/16/2017	TDST 0039	Freeport	1.827	Center of Bumper	Trimble R6 Internal
	TDST 0061	Navet Dam	1.816	Center of Bumper	Trimble R6 Internal
	TDST 0045	Manzanilla	2.110	Bottom of Antenna Mount	Leica GS14
	TDST 0055	Los Iros	1.497	Bottom of Antenna Mount	Leica GS14
	TDST 0009	Gasparillo	1.468	Center of Bumper	Trimble R6 Internal
	USBM 0042	Chaguaramas	1.711	Center of Bumper	Trimble R6-4 Internal

Table 8-5: Antennae height and receiver metadata for stations re-observed in 2017.

8.3 APPENDIX C – CORS ITRF2014 Coordinates

ALBN 2014				FRTN 2014			
DATE	X (m)	Y (m)	Z (m)	DATE	X (m)	Y (m)	Z (m)
2014-10-14	2989768.766	-5509832.323	1172450.878	2014-10-14	2978246.261	-5527208.424	1118828.888
2014-10-15	2989768.771	-5509832.33	1172450.884	2014-10-15	2978246.262	-5527208.424	1118828.888
2014-10-16	2989768.757	-5509832.314	1172450.88	2014-10-16	2978246.262	-5527208.425	1118828.887
2014-10-17	2989768.767	-5509832.316	1172450.88	2014-10-17	2978246.269	-5527208.43	1118828.887
2014-10-18	2989768.767	-5509832.326	1172450.881	2014-10-18	2978246.257	-5527208.411	1118828.884
2014-10-19	2989768.774	-5509832.329	1172450.882	2014-10-19	2978246.269	-5527208.432	1118828.887
2014-10-20	2989768.773	-5509832.32	1172450.883	2014-10-20	2978246.267	-5527208.424	1118828.888
2014-10-21	2989768.764	-5509832.32	1172450.887	2014-10-21	2978246.263	-5527208.428	1118828.898
2014-10-22	2989768.771	-5509832.331	1172450.883	2014-10-22	2978246.264	-5527208.419	1118828.89
2014-10-23	2989768.762	-5509832.306	1172450.877	2014-10-23	2978246.265	-5527208.425	1118828.893
\bar{x}	2989768.767	-5509832.322	1172450.882	\bar{x}	2978246.264	-5527208.424	1118828.889
σ	0.005	0.008	0.003	σ	0.004	0.006	0.004
GLT 2014				GRND 2014			
DATE	X (m)	Y (m)	Z (m)	DATE	X (m)	Y (m)	Z (m)
2014-10-14	3044620.754	-5491473.618	1116234.703	2014-10-14	3027676.395	-5490873.632	1163994.742
2014-10-15	3044620.755	-5491473.617	1116234.703	2014-10-15	3027676.393	-5490873.626	1163994.743
2014-10-16	3044620.757	-5491473.622	1116234.708	2014-10-16	3027676.392	-5490873.622	1163994.741
2014-10-17	3044620.754	-5491473.616	1116234.702	2014-10-17	3027676.393	-5490873.626	1163994.742
2014-10-18	3044620.758	-5491473.61	1116234.701	2014-10-18	3027676.4	-5490873.627	1163994.742
2014-10-19	3044620.759	-5491473.617	1116234.706	2014-10-19	3027676.398	-5490873.628	1163994.744
2014-10-20	3044620.757	-5491473.621	1116234.706	2014-10-20	3027676.396	-5490873.632	1163994.746
2014-10-21	3044620.754	-5491473.609	1116234.704	2014-10-21	3027676.391	-5490873.618	1163994.74
2014-10-22	3044620.757	-5491473.618	1116234.703	2014-10-22	3027676.394	-5490873.628	1163994.742
2014-10-23	3044620.752	-5491473.604	1116234.701	2014-10-23	3027676.395	-5490873.632	1163994.741
\bar{x}	3044620.756	-5491473.615	1116234.704	\bar{x}	3027676.395	-5490873.627	1163994.742
σ	0.002	0.006	0.002	σ	0.003	0.005	0.002

Table 8-6: ITRF2014 Coordinates for TT Cors for period October 14th – 23rd, 2014
(Generated by AUSPOS).

ALBN 2015				FRTN 2015			
DATE	X (m)	Y (m)	Z (m)	DATE	X (m)	Y (m)	Z (m)
2015-10-02	2989768.780	-5509832.311	1172450.896	2015-10-02	2978246.264	-5527208.424	1118828.904
2015-10-03	2989768.785	-5509832.315	1172450.895	2015-10-03	2978246.266	-5527208.428	1118828.905
2015-10-04	2989768.780	-5509832.315	1172450.897	2015-10-04	2978246.261	-5527208.423	1118828.901
2015-10-05	2989768.780	-5509832.315	1172450.899	2015-10-05	2978246.269	-5527208.433	1118828.905
2015-10-06	2989768.782	-5509832.319	1172450.9	2015-10-06	2978246.273	-5527208.444	1118828.911
2015-10-07	2989768.774	-5509832.308	1172450.897	2015-10-07	2978246.257	-5527208.421	1118828.907
2015-10-08	2989768.789	-5509832.331	1172450.893	2015-10-08	2978246.279	-5527208.464	1118828.91
2015-10-09				2015-10-09	2978246.269	-5527208.434	1118828.906
2015-10-10				2015-10-10	2978246.263	-5527208.426	1118828.902
2015-10-11				2015-10-11	2978246.269	-5527208.434	1118828.906
\bar{x}	2989768.783	-5509832.316	1172450.897	\bar{x}	2978246.267	-5527208.433	1118828.906
σ	0.004	0.007	0.002	σ	0.006	0.013	0.003
GLTA 2015				GRND 2015			
DATE	X (m)	Y (m)	Z (m)	DATE	X (m)	Y (m)	Z (m)
2015-10-02	3044620.754	-5491473.613	1116234.714	2015-10-02	3027676.405	-5490873.62	1163994.757
2015-10-03	3044620.759	-5491473.62	1116234.714	2015-10-03	3027676.404	-5490873.619	1163994.757
2015-10-04	3044620.754	-5491473.613	1116234.712	2015-10-04	3027676.406	-5490873.619	1163994.758
2015-10-05	3044620.757	-5491473.62	1116234.714	2015-10-05	3027676.411	-5490873.631	1163994.759
2015-10-06	3044620.759	-5491473.623	1116234.718	2015-10-06	3027676.416	-5490873.641	1163994.763
2015-10-07	3044620.751	-5491473.612	1116234.715	2015-10-07	3027676.396	-5490873.611	1163994.761
2015-10-08	3044620.760	-5491473.632	1116234.714	2015-10-08	3027676.423	-5490873.655	1163994.762
2015-10-09	3044620.764	-5491473.624	1116234.714	2015-10-09	3027676.411	-5490873.625	1163994.756
2015-10-10	3044620.760	-5491473.623	1116234.715	2015-10-10	3027676.408	-5490873.626	1163994.761
2015-10-11	3044620.764	-5491473.624	1116234.714	2015-10-11	3027676.411	-5490873.625	1163994.756
\bar{x}	3044620.758	-5491473.62	1116234.714	\bar{x}	3027676.409	-5490873.627	1163994.759
σ	0.004	0.006	0.002	σ	0.007	0.013	0.003

Table 8-7: ITRF2014 Coordinates for TTCORS for period October 2nd – 11th, 2015
(Generated by AUSPOS).

CN45 2016			
DATE	X (m)	Y (m)	Z (m)
2016-10-09	3043289.990	-5476327.736	1191308.743
2016-10-10	3043289.990	-5476327.732	1191308.746
2016-10-11	3043289.996	-5476327.742	1191308.742
2016-10-12	3043289.992	-5476327.732	1191308.744
2016-10-13	3043289.989	-5476327.729	1191308.745
2016-10-14	3043289.990	-5476327.728	1191308.745
2016-10-15	3043289.992	-5476327.728	1191308.743
2016-10-16	3043289.987	-5476327.723	1191308.741
2016-10-17	3043289.989	-5476327.724	1191308.743
2016-10-18	3043289.988	-5476327.726	1191308.741
\bar{x}	3043289.990	-5476327.730	1191308.743
σ	0.003	0.006	0.002
TTSF 2016			
DATE	X (m)	Y (m)	Z (m)
2016-10-09	2998199.016	-5514075.903	1130376.083
2016-10-10	2998199.016	-5514075.907	1130376.086
2016-10-11	2998199.019	-5514075.905	1130376.086
2016-10-12	2998199.017	-5514075.903	1130376.085
2016-10-13	2998199.016	-5514075.901	1130376.087
2016-10-14	2998199.019	-5514075.909	1130376.087
2016-10-15	2998199.009	-5514075.891	1130376.084
2016-10-16	2998199.018	-5514075.906	1130376.083
2016-10-17	2998199.013	-5514075.899	1130376.085
2016-10-18	2998199.013	-5514075.896	1130376.084
\bar{x}	2998199.016	-5514075.902	1130376.085
σ	0.003	0.005	0.001
TTUW 2016			
DATE	X (m)	Y (m)	Z (m)
2016-10-09	3001099.635	-5504196.941	1169841.706
2016-10-10	3001099.634	-5504196.938	1169841.706
2016-10-11	3001099.636	-5504196.941	1169841.704
2016-10-12	3001099.634	-5504196.936	1169841.706
2016-10-13	3001099.634	-5504196.931	1169841.704
2016-10-14	3001099.635	-5504196.936	1169841.708
2016-10-15	3001099.63	-5504196.928	1169841.703
2016-10-16	3001099.638	-5504196.93	1169841.706
2016-10-17	3001099.636	-5504196.941	1169841.707
2016-10-18	3001099.632	-5504196.933	1169841.706
\bar{x}	3001099.634	-5504196.936	1169841.706
σ	0.002	0.005	0.002

Table 8-8: ITRF2014 Coordinates for UNAVCO CORS for period October 9th – 18th, 2016 (Generated by AUSPOS).

ALBN 2017			
DATE	X (m)	Y (m)	Z (m)
2017-10-08	2989768.795	-5509832.299	1172450.924
2017-10-09	2989768.800	-5509832.299	1172450.923
2017-10-10	2989768.798	-5509832.29	1172450.925
2017-10-11	2989768.798	-5509832.291	1172450.92
2017-10-12	2989768.807	-5509832.313	1172450.925
2017-10-13	2989768.806	-5509832.313	1172450.926
2017-10-14	2989768.803	-5509832.302	1172450.925
2017-10-15	2989768.801	-5509832.296	1172450.926
2017-10-16	2989768.796	-5509832.282	1172450.921
2017-10-17	2989768.799	-5509832.289	1172450.92
\bar{x}	2989768.800	-5509832.297	1172450.924
σ	0.004	0.010	0.002
GLTA 2017			
DATE	X (m)	Y (m)	Z (m)
2017-10-08	3044620.75	-5491473.616	1116234.73
2017-10-09	3044620.753	-5491473.61	1116234.728
2017-10-10	3044620.746	-5491473.617	1116234.732
2017-10-11	3044620.754	-5491473.615	1116234.73
2017-10-12	3044620.755	-5491473.62	1116234.731
2017-10-13	3044620.751	-5491473.614	1116234.732
2017-10-14	3044620.754	-5491473.617	1116234.732
2017-10-15	3044620.749	-5491473.612	1116234.731
2017-10-16	3044620.749	-5491473.609	1116234.73
2017-10-17	3044620.75	-5491473.61	1116234.733
\bar{x}	3044620.751	-5491473.614	1116234.731
σ	0.003	0.004	0.001
GRND 2017			
DATE	X (m)	Y (m)	Z (m)
2017-10-08	3027676.423	-5490873.599	1163994.781
2017-10-09	3027676.424	-5490873.606	1163994.781
2017-10-10	3027676.413	-5490873.598	1163994.782
2017-10-11	3027676.428	-5490873.611	1163994.784
2017-10-12	3027676.431	-5490873.619	1163994.785
2017-10-13	3027676.421	-5490873.607	1163994.786
2017-10-14	3027676.424	-5490873.606	1163994.782
2017-10-15	3027676.425	-5490873.607	1163994.789
2017-10-16	3027676.425	-5490873.607	1163994.785
2017-10-17	3027676.418	-5490873.596	1163994.784
\bar{x}	3027676.423	-5490873.606	1163994.784
σ	0.005	0.007	0.003

Table 8-9: ITRF2014 Coordinates for TT Cors for period October 8th – 17th, 2017
 (Generated by AUSPOS)

8.4 APPENDIX D - Historical Earthquake Maps

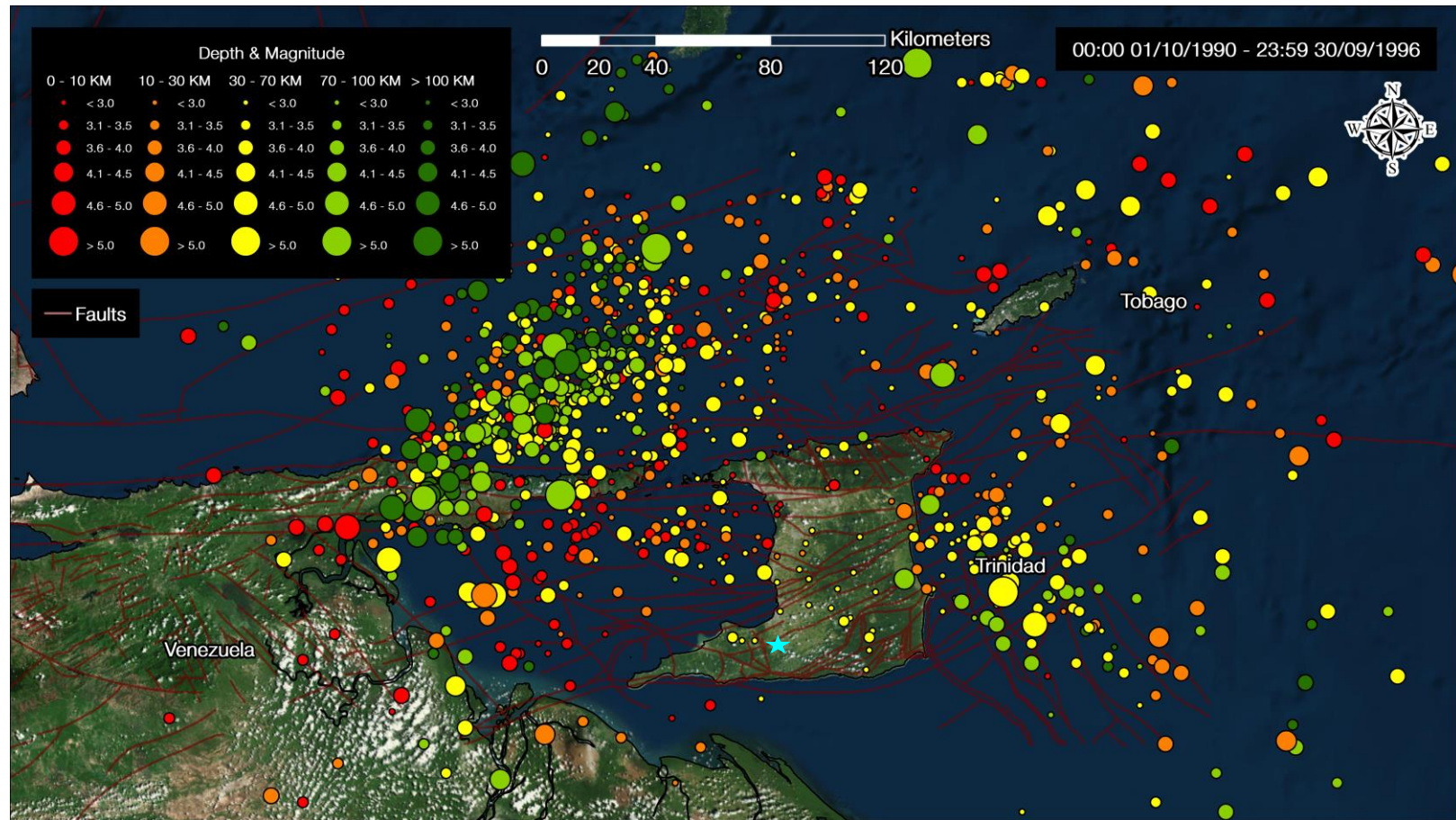


Figure 8-1: Map showing distribution of earthquakes by magnitude and depth in and surrounding Trinidad relative to the Penal reference site (blue star) for the period October 1990 - September 1996.

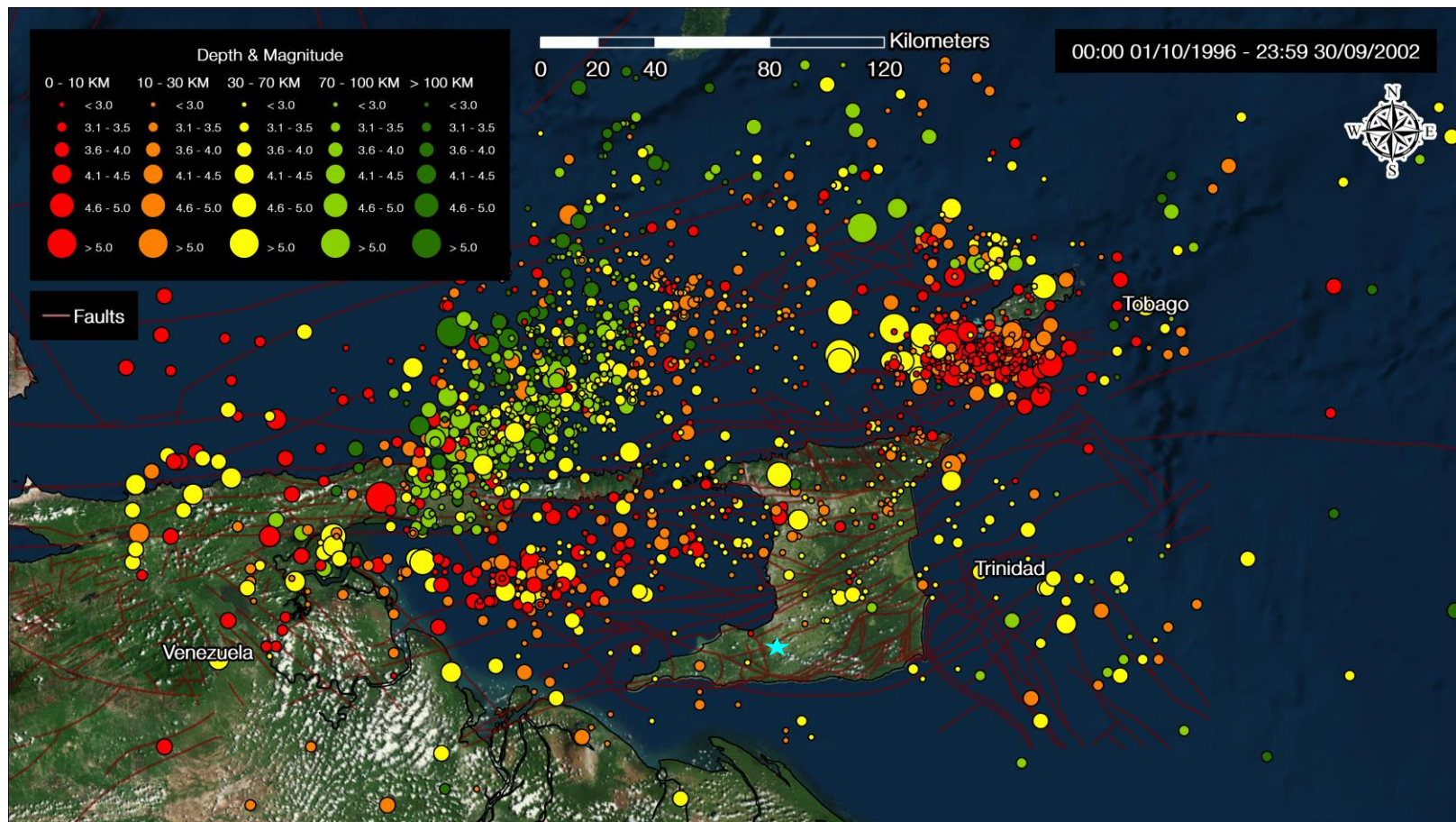


Figure 8-2: Map showing distribution of earthquakes by magnitude and depth in and surrounding Trinidad relative to the Penal reference site (blue star) for the period October 1996 - September 2002.

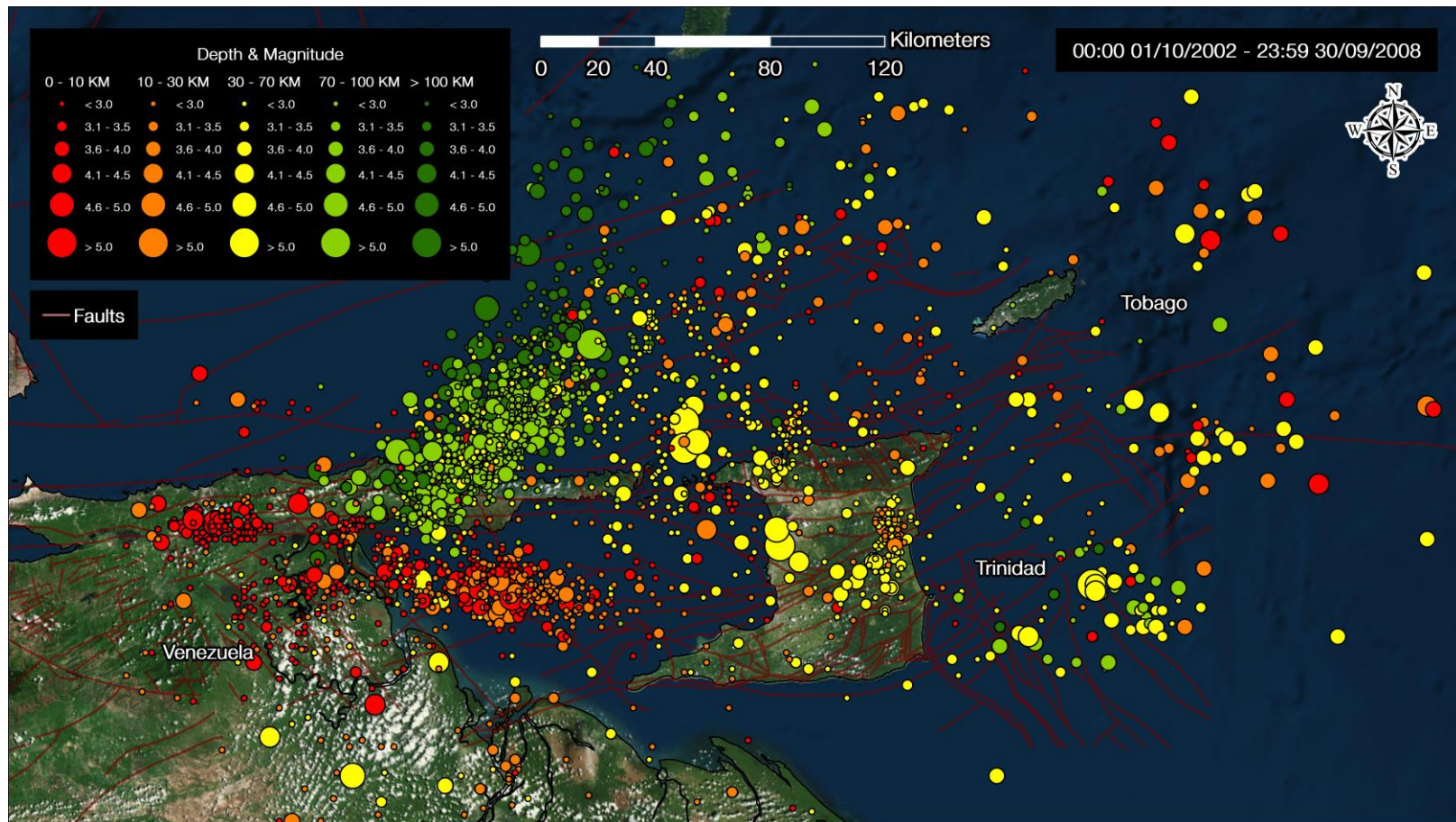


Figure 8-3: Map showing distribution of earthquakes by magnitude and depth in and surrounding Trinidad relative to the Penal reference site (blue star) for the period October 2002 - September 2008.

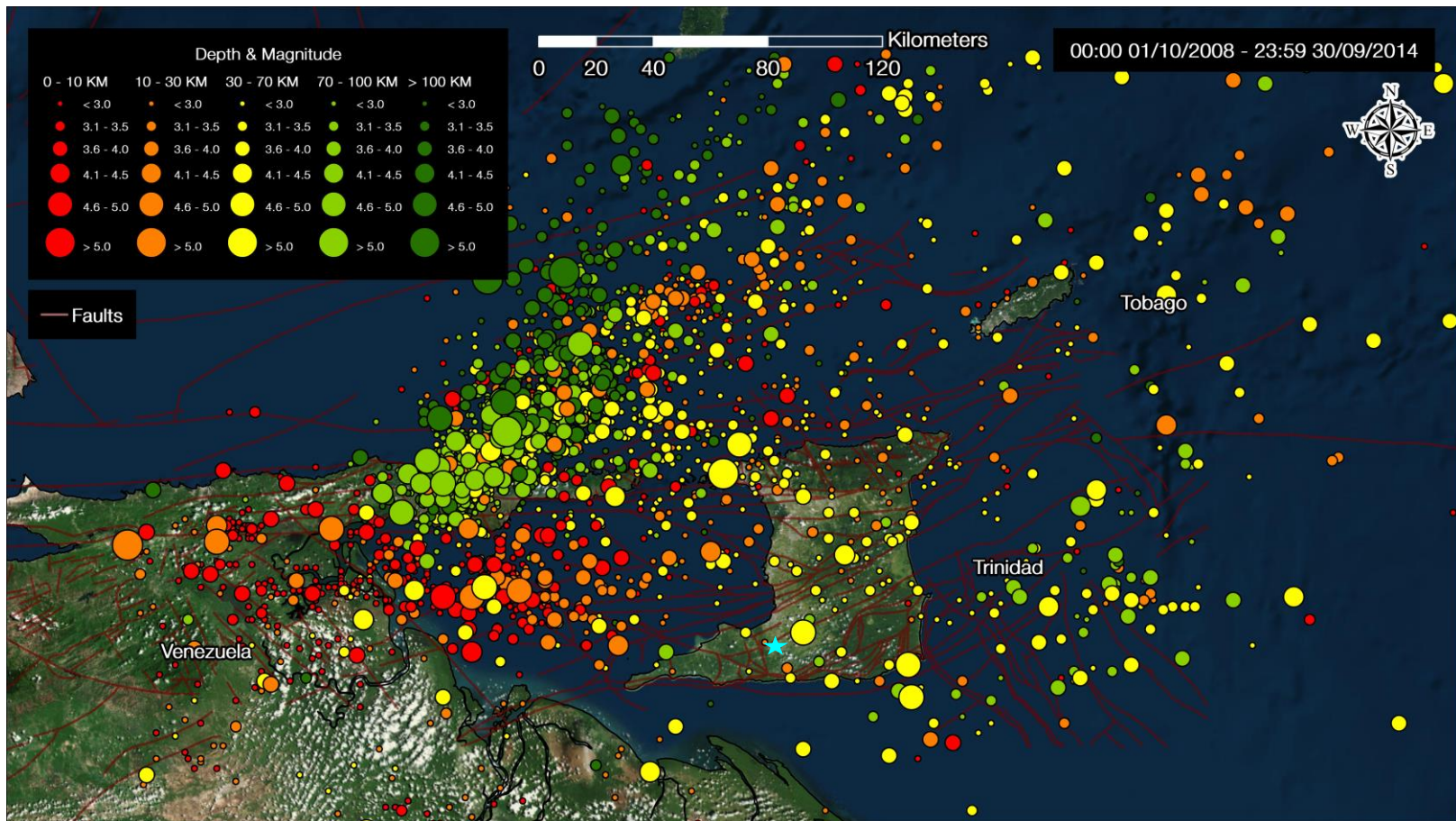


Figure 8-4: Map showing distribution of earthquakes by magnitude and depth in and surrounding Trinidad relative to the Penal reference site (blue star) for the period October 2008 - September 2014.

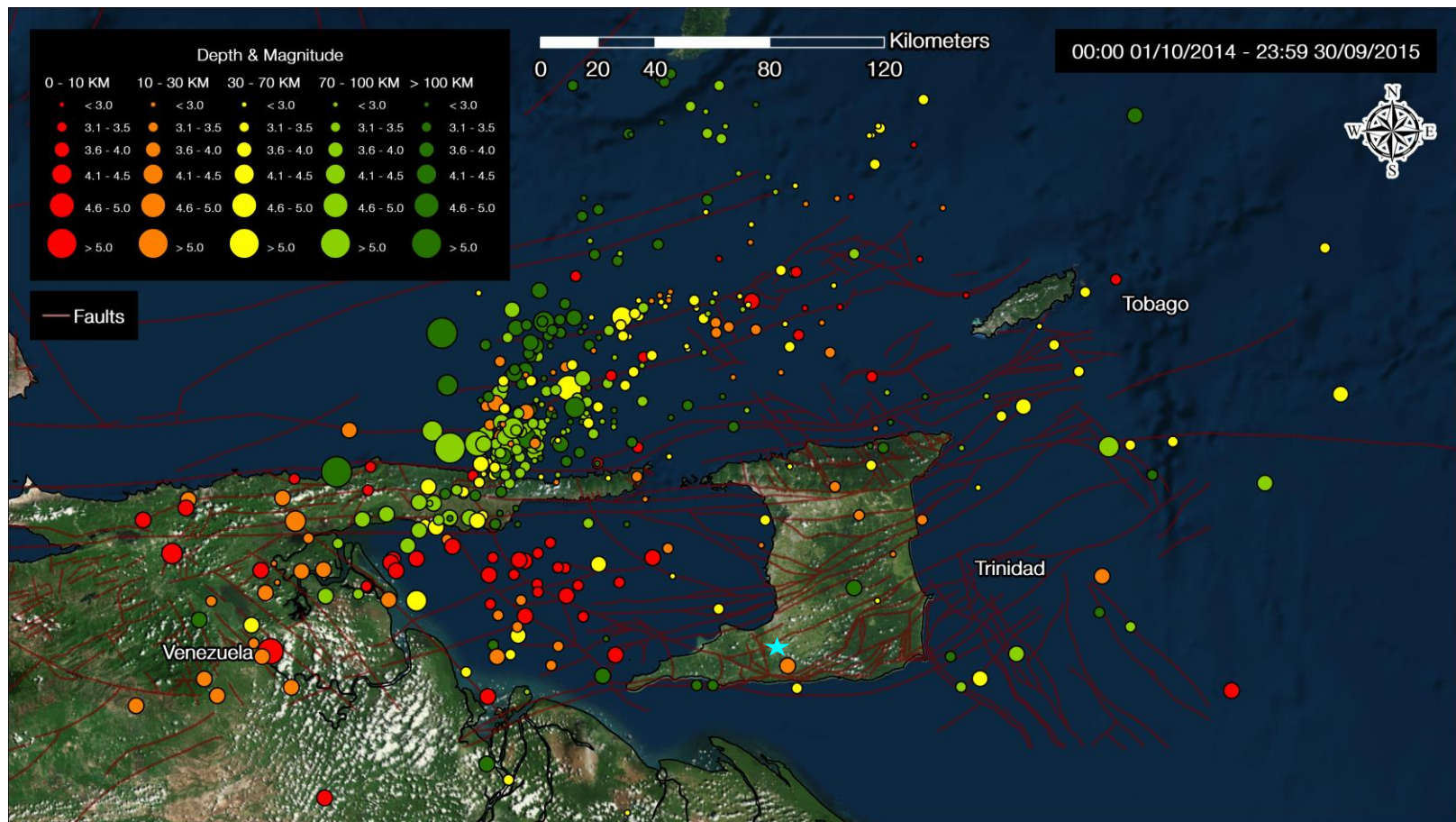


Figure 8-5: Map showing distribution of earthquakes by magnitude and depth in and surrounding Trinidad relative to the Penal reference site (blue star) for the period October 2014 - September 2015.

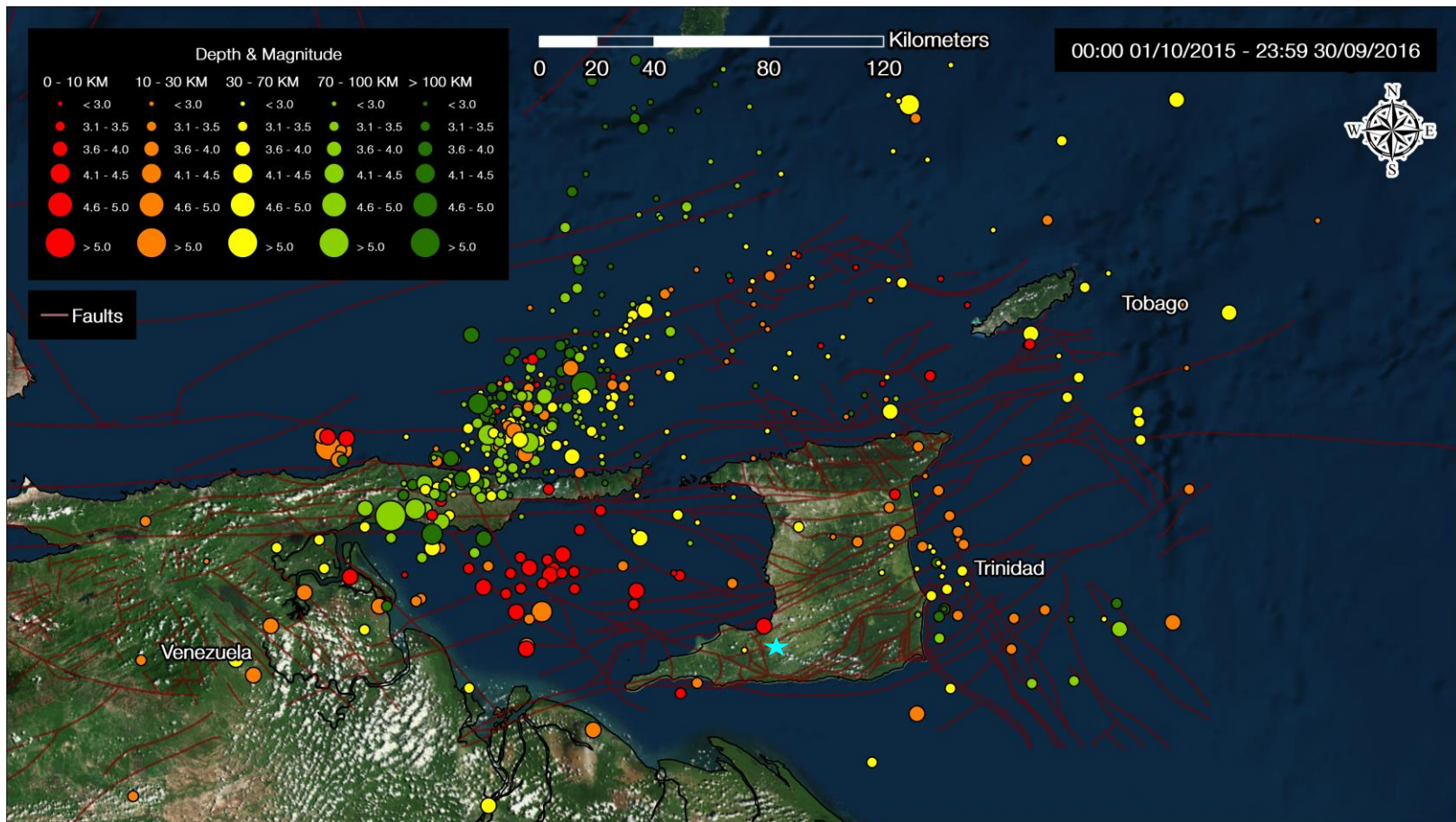


Figure 8-6: Map showing distribution of earthquakes by magnitude and depth in and surrounding Trinidad relative to the Penal reference site (blue star) for the period October 2015 - September 2016.

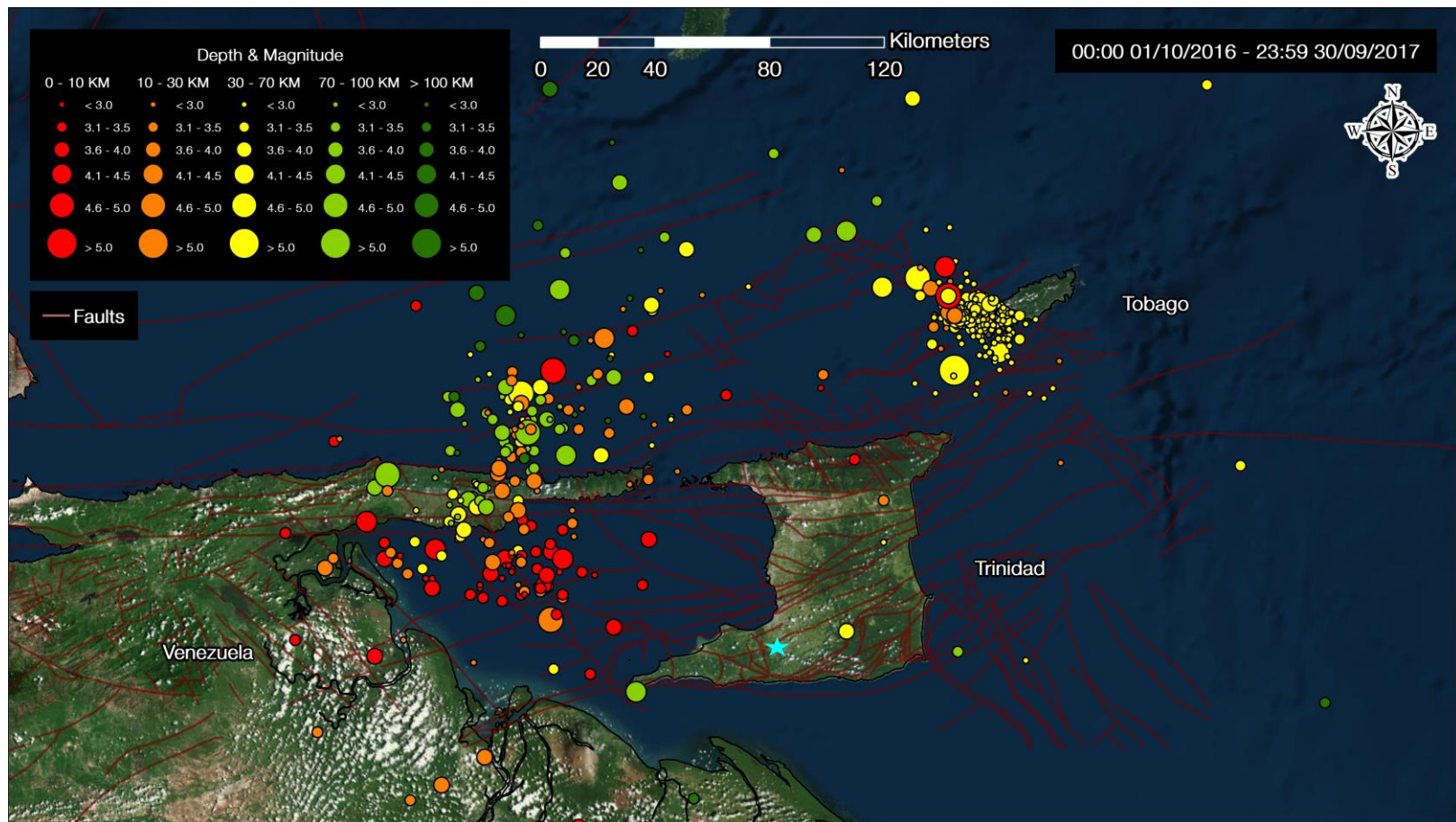


Figure 8-7: Map showing distribution of earthquakes by magnitude and depth in and surrounding Trinidad relative to the Penal reference site (blue star) for the period October 2016 - September 2017.

8.5 APPENDIX E – Adjusted ITRF2014 Coordinates

SITE	DATE			ITRF 2014 Coordinates					
	Day	Month	Year	X (m)	σX	Y (m)	σY	Z (m)	σZ
USBM 0042 Chaguramas	1	10	1990	2980456.1933		-5514191.3095		1175342.1382	
	17	10	2014	2980455.6844	5.3	-5514189.9340	6.6	1175342.4812	4.6
	8	10	2015	2980455.7600	10.0	-5514190.0346	10.7	1175342.5182	6.2
	16	10	2017	2980455.8216	7.8	-5514189.9988	17.9	1175342.5020	9.0
TDST 0039 Freeport	1	10	1990	3002800.0322		-5507671.6537		1149033.2734	
	17	10	2014	3002799.3459	6.9	-5507670.2065	8.5	1149033.7390	5.1
	5	10	2015	3002799.2268	6.1	-5507669.9646	7.4	1149033.6833	4.8
	8	10	2015	3002799.4135	8.6	-5507670.3037	10.0	1149033.7654	6.2
	13	10	2016	3002799.4103	4.8	-5507670.2484	7.3	1149033.7558	4.3
	12	10	2017	3002799.4268	5.9	-5507670.2527	10.8	1149033.7854	5.7
	16	10	2017	3002799.4094	7.0	-5507670.2506	13.3	1149033.7770	7.4
TDST 0045 Manzanilla	1	10	1990	3034517.9796		-5488450.0816		1157488.4791	
	17	10	2014	3034517.3033	10.0	-5488448.6238	9.7	1157488.7261	7.8
	13	10	2016	3034517.3378	4.1	-5488448.6742	6.5	1157488.7821	4.0
	16	10	2017	3034517.3384	5.7	-5488448.6336	13.2	1157488.7748	6.4
TDST 0061 Navet Dam	1	10	1990	3017736.4696		-5500586.4853		1144108.7391	
	17	10	2014	3017735.7190	6.1	-5500585.2740	8.1	1144109.0579	5.6
	8	10	2015	3017735.7229	8.8	-5500585.2771	9.6	1144109.0603	5.8
	13	10	2016	3017735.7381	4.1	-5500585.2942	6.0	1144109.0682	3.6
	16	10	2017	3017735.7358	7.1	-5500585.2946	16.9	1144109.0663	8.3
TDST 0009 Gasparillo	1	10	1990	3001577.2489		-5511514.2285		1133729.0393	
	20	10	2014	3001576.4239	4.5	-5511512.9601	6.5	1133729.3618	4.1
	5	10	2015	3001576.4546	5.2	-5511513.0117	5.9	1133729.3784	3.8
	13	10	2016	3001576.4686	3.6	-5511513.0497	5.4	1133729.3909	3.3
	9	10	2017	3001576.4830	3.5	-5511513.0842	8.2	1133729.4140	3.9
	12	10	2017	3001576.4609	4.9	-5511513.0393	9.2	1133729.4238	5.0
	16	10	2017	3001576.4391	6.3	-5511513.0226	13.3	1133729.3959	6.8
TDST 0029 Mayaro	1	10	1990	3037073.7797		-5491998.6510		1133880.3834	
	17	10	2014	3037073.0890	4.5	-5491997.3276	6.3	1133880.6921	4.1
	10	10	2015	3037073.0672	8.0	-5491997.2730	9.6	1133880.6862	5.5
	13	10	2016	3037073.0852	4.5	-5491997.3004	6.9	1133880.6887	4.1
BM 547 Guayaguayare	1	10	1990	3043297.9245		-5491791.1276		1118197.4030	
	17	10	2014	3043297.0827	5.0	-5491789.8454	5.6	1118197.6636	3.9
	13	10	2016	3043297.0889	5.1	-5491789.8361	7.3	1118197.6631	4.1
TDST 0005 Rio Claro	1	10	1990	3025650.4333		-5499099.8076		1130125.9853	
	17	10	2014	3025649.7214	10.1	-5499098.7367	13.4	1130126.3255	8.8
TDST 0067 Catshill	1	10	1990	3023257.9925		-5502141.1923		1121852.5639	
	9	10	2017	3023257.1303	5.8	-5502139.9568	11.3	1121852.8561	5.3

Table 8-10: ITRF2014 Adjusted Coordinates for re-observed sites (generated by TTC).

SITE	DATE			ITRF 2014 Coordinates					
	Day	Month	Year	X (m)	σX	Y (m)	σY	Z (m)	σZ
TDST 0066 Saunders Trace	1	10	1990	3019532.6931		-5504099.4993		1122253.2920	
	9	10	2017	3019531.7770	6.6	-5504098.2588	15.2	1122253.4906	6.9
TDST 0052 La Lune	1	10	1990	3009775.4081		-5512206.9706		1108769.8869	
	9	10	2017	3009774.5380	3.5	-5512205.7458	8.4	1108770.3021	4.0
TDST 0097 Rousillac	1	10	1990	2989054.3125		-5520089.2489		1125062.5323	
	20	10	2014	2989052.5000	4.2	-5520087.8347	6.0	1125062.8779	3.9
	12	10	2017	2989053.5842	5.6	-5520088.0053	10.8	1125062.9588	5.7
TDST 0050 Forest Reserve	1	10	1990	2987200.4840		-5522731.6773		1117246.6523	
	20	10	2014	2987199.6073	4.8	-5522730.2998	6.0	1117246.8052	4.2
TDST 0055 Los Iros	1	10	1990	2984289.3320		-5526414.5407		1106825.4815	
	20	10	2014	2984288.1764	6.6	-5526413.4622	7.2	1106825.6861	5.5
	5	10	2015	2984288.2404	5.9	-5526413.5678	6.6	1106825.7267	4.3
	13	10	2016	2984288.2474	4.8	-5526413.5685	7.8	1106825.7133	4.3
	16	10	2017	2984288.3110	5.7	-5526413.7298	13.3	1106825.7579	6.5
TDST 0063 Cedros	1	10	1990	2964129.4282		-5536333.4080		1111312.2259	
	12	10	2017A	2964134.1862	6.3	-5536324.9978	12.4	1111331.3002	6.3
	12	10	2017 B	2964270.1594	6.4	-5536238.0901	12.5	1111381.1288	6.3
TDST 0014 Penal	1	10	1990	3002600.3500		-5514078.8550		1118513.7335	
	20	10	2014	3002599.3997	4.7	-5514077.5289	6.6	1118514.0521	4.2
	5	10	2015	3002599.4260	5.0	-5514077.5715	5.8	1118514.0698	3.8
	13	10	2016	3002599.3028	4.1	-5514077.2921	6.2	1118514.0041	3.7
	9	10	2017	3002599.4554	3.5	-5514077.6229	8.7	1118514.1021	4.0
	12	10	2017	3002599.4440	5.3	-5514077.6259	10.5	1118514.1137	5.4

Table 8-11: ITRF2014 Adjusted Coordinates for re-observed site, continued (generated by TTC).